ISSN 1949-8462 (online)

World Journal of *Cardiology*

World J Cardiol 2020 July 26; 12(7): 303-361

Published by Baishideng Publishing Group Inc

World Journal of Cardiology

Contents

Monthly Volume 12 Number 7 July 26, 2020

World Journal of Cardiology

Monthly Volume 12 Number 7 July 26, 2020

Contents

ABOUT COVER

Editorial board member of *World Journal of Cardiology*, Dr. Anan is the Director of Institute for Clinical Research in National Hospital Organization (NHO) Miyakonojo Medical Center, Japan. Having received his MD degree from Kagoshima University, Japan, in 1982. He spent 3.5 years as a postdoctoral research fellow at Department of Genetics, Harvard Medical School, and the Cardiovascular Division, Brigham and Women´s Hospital, Boston, Massachusetts, USA. He carried out researches on molecular genetic analyses of cardiomyopathies, and published papers in Journal of Clinical Investigation and New England Journal of Medicine, *etc*. His ongoing research interests are molecular genetics of inherited cardiovascular diseases (particularly hypertrophic cardiomyopathy) and cancer therapy induced cardiomyopathy. He is a reviewer of several scientific journals and has published more than 50 peer-reviewed articles.

AIMS AND SCOPE

The primary aim of *World Journal of Cardiology* (*WJC*, *World J Cardiol*) is to provide scholars and readers from various fields of cardiology with a platform to publish high-quality basic and clinical research articles and communicate their research findings online.

WJC mainly publishes articles reporting research results and findings obtained in the field of cardiology and covering a wide range of topics including acute coronary syndromes, aneurysm, angina, arrhythmias, atherosclerosis, atrial fibrillation, cardiomyopathy, congenital heart disease, coronary artery disease, heart failure, hypertension, imaging, infection, myocardial infarction, pathology, peripheral vessels, public health, Raynaud's syndrome, stroke, thrombosis, and valvular disease.

INDEXING/ABSTRACTING

The *WJC* is now abstracted and indexed in Emerging Sources Citation Index (Web of Science), PubMed, PubMed Central, Scopus, China National Knowledge Infrastructure (CNKI), China Science and Technology Journal Database (CSTJ), and Superstar Journals Database.

NAME OF JOURNAL
World Journal of Cardiology

ISSN
ISSN 1949-8462 (online)

LAUNCH DATE
December 31, 2009

FREQUENCY
Monthly

EDITORS-IN-CHIEF
Ramdas G Pai, Dimitrios Tousoulis, Marco Matteo Ciccone

EDITORIAL BOARD MEMBERS
https://www.wjgnet.com/1949-8462/editorialboard.htm

PUBLICATION DATE
July 26, 2020

INSTRUCTIONS TO AUTHORS
https://www.wjgnet.com/bpg/gerinfo/204

GUIDELINES FOR ETHICS DOCUMENTS
https://www.wjgnet.com/bpg/GerInfo/287

GUIDELINES FOR NON-NATIVE SPEAKERS OF ENGLISH
https://www.wjgnet.com/bpg/gerinfo/240

PUBLICATION ETHICS
https://www.wjgnet.com/bpg/GerInfo/288

PUBLICATION MISCONDUCT
https://www.wjgnet.com/bpg/gerinfo/208

ARTICLE PROCESSING CHARGE
https://www.wjgnet.com/bpg/gerinfo/242

STEPS FOR SUBMITTING MANUSCRIPTS
https://www.wjgnet.com/bpg/GerInfo/239

ONLINE SUBMISSION
https://www.f6publishing.com

E-mail: bpgoffice@wjgnet.com https://www.wjgnet.com

World Journal of Cardiology

Submit a Manuscript: https://www.f6publishing.com

World J Cardiol 2020 July 26; 12(7): 303-333

DOI: 10.4330/wjc.v12.i7.303

ISSN 1949-8462 (online)

REVIEW

MicroRNA sequences modulating inflammation and lipid accumulation in macrophage "foam" cells: Implications for atherosclerosis

Richard James Lightbody, Janice Marie Walsh Taylor, Yvonne Dempsie, Annette Graham

ORCID number: Richard James Lightbody 0000-0003-1603-7310; Janice Marie Walsh Taylor 0000-0002-3646-4726; Yvonne Dempsie 0000-0003-3516-4067; Annette Graham 0000-0002-1323-1962.

Author contributions: Taylor JMW, Dempsie Y and Graham A were involved in the study conceptualisation; Dempsie Y and Graham A were involved in the funding acquisition; all authors were involved in the writing, review and editing of the manuscript, and read and approved the final manuscript.

Supported by Heart Research UK, No. RG2651.

Conflict-of-interest statement: Prof. Graham A and Dr. Dempsie Y have received research funding from Heart Research UK (RG2651) in support of PhD research student, Mr Lightbody RJ; Prof. Graham A, Dr. Dempsie Y and Dr. Taylor JMW are employees of Glasgow Caledonian University.

Richard James Lightbody, Janice Marie Walsh Taylor, Yvonne Dempsie, Annette Graham, Department of Biological and Biomedical Sciences, School of Health and Life Sciences, Glasgow Caledonian University, Glasgow G4 0BA, United Kingdom

Corresponding author: Annette Graham, BSc, MA, PhD, Professor, Department of Biological and Biomedical Sciences, School of Health and Life Sciences, Glasgow Caledonian University, 70 Cowcaddens Road, Glasgow G4 0BA, United Kingdom. ann.graham@gcu.ac.uk

Abstract

Accumulation of macrophage "foam" cells, laden with cholesterol and cholesteryl ester, within the intima of large arteries, is a hallmark of early "fatty streak" lesions which can progress to complex, multicellular atheromatous plaques, involving lipoproteins from the bloodstream and cells of the innate and adaptive immune response. Sterol accumulation triggers induction of genes encoding proteins mediating the atheroprotective cholesterol efflux pathway. Within the arterial intima, however, this mechanism is overwhelmed, leading to distinct changes in macrophage phenotype and inflammatory status. Over the last decade marked gains have been made in understanding of the epigenetic landscape which influence macrophage function, and in particular the importance of small non-coding micro-RNA (miRNA) sequences in this context. This review identifies some of the miRNA sequences which play a key role in regulating "foam" cell formation and atherogenesis, highlighting sequences involved in cholesterol accumulation, those influencing inflammation in sterol-loaded cells, and novel sequences and pathways which may offer new strategies to influence macrophage function within atherosclerotic lesions.

Key words: Coronary heart disease; Atherosclerosis; Macrophage "foam" cell; Cholesterol; Inflammation; MicroRNA

Core tip: Micro-RNA (miRNA) sequences are short non-coding RNAs which play a key role in epigenetic regulation of gene transcription and translation. Significant changes in

Manuscript source: Unsolicited manuscript

Received: January 30, 2020
Peer-review started: January 30, 2020
First decision: April 18, 2020
Revised: June 3, 2020
Accepted: June 10, 2020
Article in press: June 10, 2020
Published online: July 26, 2020

P-Reviewer: Barik R, S Berezin AE, Kharlamov AN
S-Editor: Yan JP
L-Editor: A
E-Editor: Zhang YL

miRNA expression occur in macrophage "foam" cells, laden with cholesterol and cholesteryl ester, which contribute not only to macrophage phenotype and inflammatory status, but also to novel pathways which may influence the development of atherosclerotic lesions, the principal underlying cause of coronary heart disease. The rapid expansion of this field of research is leading to new therapeutic targets and strategies for treatment of this progressive and highly complex global disease.

Citation: Lightbody RJ, Taylor JMW, Dempsie Y, Graham A. MicroRNA sequences modulating inflammation and lipid accumulation in macrophage "foam" cells: Implications for atherosclerosis. *World J Cardiol* 2020; 12(7): 303-333
URL: https://www.wjgnet.com/1949-8462/full/v12/i7/303.htm
DOI: https://dx.doi.org/10.4330/wjc.v12.i7.303

INTRODUCTION

The purpose of this review is to identify and contextualise the emerging roles of micro-RNA (miRNA) sequences involved in epigenetic regulation of cholesterol deposition within macrophage "foam" cells, a rapidly developing area of key interest to researchers and clinicians developing new therapeutic strategies to combat coronary heart disease (CHD). CHD, a major cause of global morbidity and mortality, is principally caused by atherosclerosis, a complex, progressive chronic inflammatory disease. Genetic factors contribute to atherosclerosis, in combination with environmental, metabolic and behavioural triggers including elevated serum lipid levels, diabetes, obesity, hypertension and smoking[1]. Atherosclerotic lesions originate at non-random locations of the vasculature[2,3], where alterations in haemodynamic blood flow, such as decreased shear stress and turbulent flow, are sensed by endothelial cells, disrupting homeostatic cellular organisation, increasing permeability of the arteries and enabling the accumulation of circulating cholesterol-rich low-density lipoprotein (LDL) in the intima[2-4]. Local inflammation in endothelial cells is mediated by activation of the pro-inflammatory transcription factor, nuclear factor-κB (NF-κB), in part due to shear stress-mediated inhibition of the anti-inflammatory transcription factor Kruppel-like factor 2[5,6]. This leads to increased expression of adhesion molecules, E-selectin, intercellular adhesion molecule-1 (ICAM-1) and vascular cell adhesion molecule-1, and of pro-inflammatory cytokines and chemoattractants[6]. Further, endothelial expression of lipoxygenase enzymes and production of reactive oxygen species (ROS) oxidatively modify proteoglycan-bound LDL (oxLDL)[7]. This amplifies the local inflammatory response mediated by receptors such as lectin-like oxidised LDL receptor 1 (LOX-1) and toll-like receptor 4 (TLR4) present on endothelial and smooth muscle cells[8-10].

Endothelial expression of adhesion molecules, and chemokine-chemokine receptor interactions, recruit circulating monocytes to the intima, where they differentiate into macrophages in response to macrophage colony-stimulating factor[11]. Intimal macrophages recognise modified components of oxLDL and internalise oxLDL and LDL, becoming "foam" cells due to accumulation of droplets of cholesteryl ester. This occurs *via* interaction with scavenger receptors (SRs), such as SR-A1, SR-B1, cluster of differentiation 36 (CD36, SR-B2), CD68 (SR-D1), LOX-1 (SR-E1), TLR4, and the LDL receptor (LDLR)[7,12-14]. Lipoprotein lipase (LPL) is also implicated in foam cell formation in distinct ways: Inhibition of LPL activity by angiopoietin-like protein 4 decreases lipid uptake in macrophages, whereas genetic deletion of this protein increases lipid uptake, expression of lipid-induced genes and respiration[15]. Additional receptor independent mechanisms such as macro- and micropinocytosis can also lead to the uptake of these lipoproteins[16,17]. The influx of cholesterol-rich lipoproteins through these various mechanisms, as well as the rate limited process of cholesterol efflux (below), leads to the generation of lipid-laden "foam" cells with reduced capacity to migrate from the intima[18-20].

Accumulation of macrophages and lipid-laden foam cells is accompanied by plaque enrichment with additional immune cells[21]. T-helper cells, activated by oxLDL-induced maturation of dendritic cells (DCs), recognise epitopes on apolipoprotein B100 (ApoB100) in native LDL and oxLDL[22,23]. Phenotypically, these T_H cells are primarily of the T_H1 subset, producing pro-inflammatory cytokines such as interferon gamma (IFN-γ) and tumour necrosis factor alpha (TNF-α), but atheroprotective anti-

inflammatory regulatory T cells (T_{regs}) are also present[24,25]. The combination of hyperlipidaemia, endothelial expression of adhesion molecules and chemokines, and deposition of chemokines on endothelial cells by activated platelets, recruits and activates additional immune subsets, including neutrophils[26-30]. Neutrophils express myeloperoxidase that produces hypochlorous acid, that promotes LDL oxidation and foam cell formation and increases retention of LDL in the intima *via* binding to LPL[7,26-31].

As the complexity of the arterial microenvironment increases, atherosclerotic plaques develop a number of key features. Responding to signals such as growth factors, cytokines and oxidised phospholipids (oxPL), vascular smooth muscle cells (VSMCs) undergo phenotypic switching from contractile quiescent VSMCs to synthetic, migratory and proliferative VSMC[32,33]. This leads to dramatic vascular remodelling and arterial thickening *via* production of matrix degrading metalloproteinases and a shift in production from type I and III collagen to type VIII collagen[34-36]. Further, intimal VSMCs accumulate lipids and can take on a foam cell phenotype which, under endoplasmic reticulum (ER) stress or in the presence of increased intracellular free cholesterol, leads to apoptosis and necrosis of both macrophage-derived and VSMC-derived foam cells, forming a hypoxic, necrotic core and extracellular lipid pools[37-41]. Hypoxia inducible factor 1 enhances neovascularisation *via* induction of vascular endothelial growth factor A expression in macrophages and VSMC[42,43], and by increased expression of macrophage SRs and pro-inflammatory mediators and decreased expression of ATP binding cassette (ABC) transporters responsible for cellular cholesterol efflux[44-46].

Macrophage sub-populations within atherosclerotic lesions

Within the arterial intima, macrophages exhibit notable phenotypic plasticity in response to multiple signals from this complex microenvironment and can exhibit pro- or anti-atherosclerotic responses (Figure 1). Pro-inflammatory (M1) macrophages can be generated *in vitro* in response to a variety of stimuli associated with a T_H1 response, such as lipopolysaccharide (LPS) and IFN-γ[47,48], resulting in increased expression of pro-inflammatory mediators such as interleukin (IL)-1β, IL-6, TNF-α, IL-12 and IL-23, and ROS[47,49,50]. Oxidized LDL induces activation of the NF-κB pathway which enhances the pro-inflammatory response in M1-like macrophages and expression of pro-inflammatory mediators in macrophages polarised to the anti-inflammatory (M2) phenotype[51-53]. Further, oxLDL and individual components derived from oxLDL, such as free cholesterol and cholesterol crystals, cholesteryl ester hydroperoxides, and 7-ketocholesteryl-9-carboxynonanoate (Figure 1), have been shown to activate pro-inflammatory pathways including the nod-like receptor protein 3 (NLRP3) inflammasome[54], mitogen activated protein kinase pathway[55,56] and NF-κB signalling[57,58].

Macrophages, however, can adopt a variety of additional immunoregulatory subtypes within the phenotypic spectrum. A subset of anti-inflammatory macrophages (M2a), generated in response to cytokines such as IL-4 and IL-13, are produced as part of the T_H2 response[59,60]. These cells are associated with wound healing *via* production of factors such as fibronectin and transforming growth factor β (TGF-β)[59,60]. Exposure to immune complexes, and to TLR ligands, generates another subset, termed M2b, which have both protective and detrimental roles and express high levels of the anti-inflammatory cytokine IL-10, low levels of pro-inflammatory IL-12, but also other pro-inflammatory mediators including chemoattractant C-C motif chemokine ligand 1 (CCL1)[61-63]. Stimulation of macrophages with glucocorticoids and IL-10 induce macrophage phenotype (M2c), which play a predominant role in clearance of apoptotic cells[64,65]. Finally, a pro-angiogenic population, termed M2d, is induced in murine macrophages in response to adenosine agonists in conjunction with TLR-signalling[66,67].

Interestingly, while some components of oxLDL activate inflammatory pathways, oxysterols and the product of cholesteryl ester oxidation, 9-oxonanoyl cholesterol, induce expression of the anti-inflammatory and pro-fibrotic cytokine TGF-β[68,69]. Consequently, treatment of macrophages with oxLDL can also induce an anti-inflammatory phenotype[70]. This apparent discrepancy between inflammatory versus anti-inflammatory signalling may be due to the degree of oxidation of the LDL particle[71], or the extent of lipid accumulation within cells[72]. Oxidized phospholipids (oxPL) (Figure 1) also induce a distinct macrophage phenotype (Mox) in murine models[73-75]; Mox macrophages exhibit reduced expression of M1, as well as M2-like, macrophage markers and enhanced expression of nuclear factor erythroid 2-related factor 2 (Nrf2) dependent anti-oxidant genes[73]. Further, macrophage subsets found within the plaque microenvironment include M4 macrophages, which are induced by

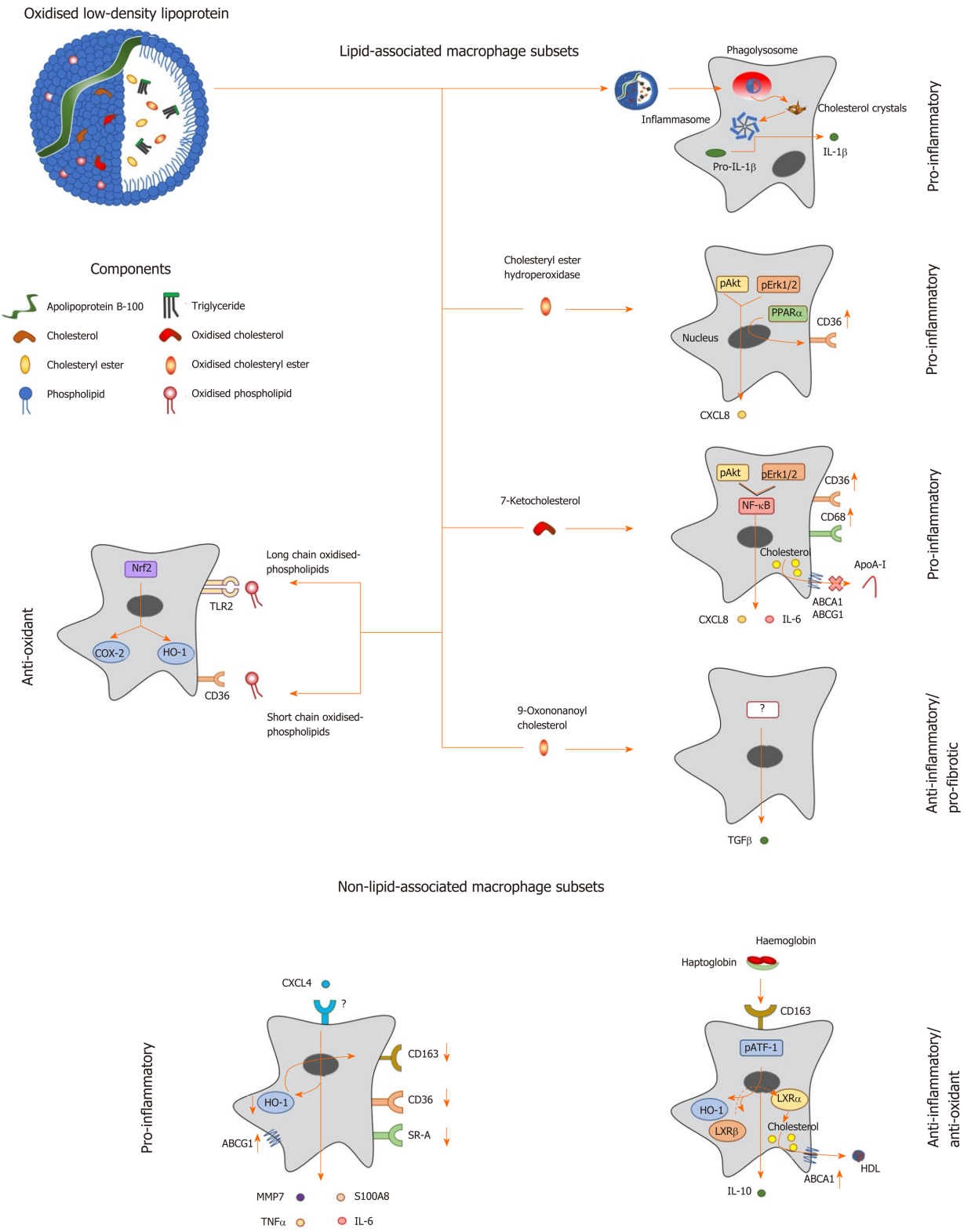

Figure 1 Macrophage phenotype in response to lipids and other factors within atherosclerotic lesions. Oxidized low density lipoprotein particles are composed of a number of components including (modified) apolipoprotein B, (oxidized) free cholesterol, (oxidized) cholesteryl esters and (oxidized) phospholipids, which induce a range of unique transcriptional responses in macrophages (indicated by arrows), resulting in altered expression of secreted cytokines and cell surface receptors, and differing macrophage phenotypes (highlighted in bold). Macrophages can be polarised to a pro-inflammatory phenotype by components of oxidized LDL in a number of differing ways. Cholesterol crystals activate the inflammasome to increase expression of interleukin-1 (IL-1), while cholesteryl ester hydroperoxides activate phospho-extracellular signal-regulated protein kinases 1 and 2 (pERK1/2) and phospho-protein kinase B (pAkt) pathways, resulting in induction of peroxisome proliferator activated receptor alpha and increased expression of C-X-C motif ligand 8 (CXCL8) and the scavenger receptor, cluster of differentiation 36 (CD36). The modified cholesterol metabolite, 7-ketocholesterol, also triggers pAkt and pERK1/2 signalling, resulting in activation of nuclear factor kappa B (NF-κB), and enhanced output of pro-inflammatory cytokines such as IL-6 and CXCL8; this oxysterol also increases expression of CD36 and CD68,

potentiating uptake of modified lipoproteins, and represses expression of ATP binding cassette transporter A1 (ABCA1) and ABCG1, limiting cholesterol removal via apolipoprotein A-I (apoA-I) and high density lipoprotein. By contrast, other components of oxLDL can induce an anti-inflammatory phenotype: For example, 9-oxononanoyl cholesterol induces expression of transforming growth factor β and stimulates fibrosis. Short chain oxidized phospholipids interact with CD36 to activate cyclooxygenase-2 (COX-2) and heme oxygenase-1 (HO-1), while long chain oxidized phospholipids bind toll-like receptor-2, resulting in activation of nuclear factor erythroid-2-related factor 2 which enhances expression of antioxidant genes, including HO-1, to protect cells against further oxidative damage. Other factors found within atherosclerotic lesions can also influence macrophage phenotype: For example, the chemokine CXCL4 induces the expression of pro-inflammatory factors such IL-6, tumor necrosis factor α, matrix metalloproteinase 7 and S100 calcium binding protein A8, while repressing the expression of ABCG1, HO-1, CD36, scavenger receptor-A and CD163. Alternatively an anti-inflammatory and antioxidant phenotype can be induced by the interaction of hemoglobin:haptoglobin complexes with CD163, which activates phospho-activating transcription factor-1, resulting in changes in LXR expression, induction of HO-1 and increased expression of IL-10 and ABCA1. IL: Interleukin; TGF: Transforming growth factor; TNF: Tumor necrosis factor; HO-1: Heme oxygenase-1; MMP: Matrix metalloproteinase; LXR: Liver X receptor; ABCA1: ATP binding cassette transporter A1; HDL: High density lipoprotein; pAkt: Phospho-protein kinase B; NF-κB: Nuclear factor kappa B; pATF-1: Phospho-activating transcription factor-1; PPAR-α: Peroxisome proliferator activated receptor alpha; CXCL: C-X-C motif ligand; ABCG1: ATP binding cassette transporter G1.

chemokine (C-X-C) motif ligand 4 (CXCL4)[76], MHb macrophages, induced by hemoglobin: Haptoglobin complexes[77], and Mhem macrophages, induced by heme[78,79]; both MHb and Mhem macrophages exhibit resistance to cholesterol loading[77-79].

Cholesterol accumulation in macrophage "foam" cells: Responses to excess (oxy)sterol

Macrophages play a vital role in handling excess LDL-cholesterol and/or toxic oxLDL metabolites, *via* esterification to cytosolic lipid droplets by Acyl CoA: Cholesterol Acyltransferase (ACAT-1-/2) or lysosomal sequestration[80]. Autophagy also contributes to lipid droplet formation, with Beclin-1 inhibiting the formation of droplets in response to modified LDL in naïve cells but not in inflammatory activated macrophages[81]. Accumulation of sterol is central to activation of nuclear liver X receptors (LXRs), which lie under the control of oxysterol metabolites of cholesterol; the extent of activation of these transcription factors may also contribute to the heterogeneity of macrophage responses to sterol accumulation[72,82]. LXRs control the expression of ABC transporters (ABCA1, ABCG1/G4) that actively efflux cholesterol from cells to acceptors, such as apolipoprotein (apo) A-I, apoE and high-density lipoprotein (HDL). Binding of apoA-I to ABCA1 triggers an array of cell signalling pathways[83], and mobilisation of stored cholesteryl esters *via* cholesteryl ester hydrolases, releases cholesterol which trafficks to the plasma membrane for efflux as nascent HDL[80,84]. In addition, ABCG1 and ABCG4 aid the formation of more mature forms of HDL, so they work in concert with ABCA1 to initiate the process of reverse cholesterol transport which can return cholesterol to the liver for excretion *via* the classical and alternative bile acid pathways[80,84].

Liver X nuclear receptors form obligate heterodimers with retinoid X receptors which bind directly to the LXR response element, a direct repeat 4 (DR4) motif of the six base pair sequence AGTTCA separated by four base pairs[85-88]. Ligand binding triggers a conformational change in the heterodimer, dissociating nuclear receptor co-repressors [NCOR1/NCOR2 (SMRT)] proteins which undergo ubiquitination and proteasomal degradation, and engaging coactivator proteins (steroid receptor coactivators, PPAR-γ coactivator 1 and nuclear receptor coactivator 6)[87]. Genetic deletion of LXRs in bone marrow derived macrophages, however, reveal a more complex picture: Depending on the target gene, LXR deletion can up- or down-regulate, or effect no change in, gene expression[87].

LXRs contribute to the inactivation of the counter-regulatory system operated by sterol regulatory binding proteins (SREBPs) which belong to the basic helix-loop-helix leucine zipper (bHLH-Zip) family of transcription factors[89]. Three SREBP isoforms exist, encoded by two genes: *SREBF1* (SREBP-1a and SREBP-1c) and *SREBF2* (SREBP-2) which target sterol response elements (SRE). Unlike SREBP-1a which is constitutively expressed and targets all SRE with low specificity, SREBP-1c and SREBP-2 are inducible and regulate the expression of genes encoding proteins involved in fatty acid and cholesterol metabolism, respectively[89,90]; SREBP-2 also transcriptionally regulates the LDL receptor which mediates endocytosis of LDL from the circulation. In sterol-replete cells, SREBP transcription factors remain inactive, sequestered at the ER by binding to a chaperone, SREBP cleavage activating protein (SCAP), which contains a five transmembrane sterol sensing domain and interacts with the ER anchor, insulin-induced gene (INSIG-1/-2). As cholesterol levels fall, the interaction of SCAP with INSIG is lost, allowing SCAP-SREBP to traffick to the Golgi apparatus *via* inclusion in COPII-vesicles[89,90]. Golgi site-1 and site-2 proteases (SP-1,

SP-2) cleave the amino terminal of SREBP-2, releasing a transcriptionally active fragment which is imported into the nucleus to target sterol-responsive genes, including *SREBF2* itself; rapid degradation of nuclear (nSREBP) serves to terminate this signalling pathway[89,90].

LXRs operate in functional opposition to SREBP-2, repressing cholesterol biosynthesis *via* novel negative LXR DNA-response elements in the promoter region of genes encoding squalene synthase and lanosterol 14-demethylase[91-93], and promoting the degradation of LDL receptors by increasing the expression of proprotein convertase subtilisin/kexin type 9 (PCSK9)[94,95]. The E3 ubiquitin ligase, inducible degrader of the LDL receptor (IDOL) is an LXR target gene: IDOL dimers interact with members of the ubiquitin-conjugating enzyme (UBE) 2D family of E2 ubiquitin ligases to transfer ubiquitin to the cytoplasmic tail of members of the LDL receptor family, promoting receptor degradation[94,95]. Oxysterols also bind to Insig-1/2, sequestering SREBPs at the ER, further ensuring repression of cholesterol biosynthesis and uptake[88]. By contrast, LXR agonists induce gene expression of SREBP-1c; fatty acid synthase, and a number of desaturase and elongase enzymes in the fatty acid biosynthetic pathway, are also directly regulated by LXR[87]. Thus, efficient delivery of cholesterol to the ER is needed to inhibit proteolytic processing of SREBP-1c to an active transcription factor[89,90], and to limit increased biosynthesis of fatty acids[87].

LXRs also exert anti-inflammatory effects, some of which are indirect and due to the increased expression of ABCA1[96], and production of anti-inflammatory HDL[97,98]. HDL inhibit TLR signalling in macrophages and cytokine signalling in bone marrow progenitors by removal of cholesterol from lipid rafts[99,100] and induce activating transcription factor 3, suppressing the expression of pro-inflammatory genes[97,98]. Multiple mechanisms exist by which LXRs modulate inflammatory responses, some of which involve transactivation and others transrepression[86-88]. Pathway-specific responses occur: LXR activation inhibits NF-κB dependent induction of pro-inflammatory genes in response to LPS and responses triggered by TLR4 and TNF-α but exerts minimal impact on the pathway mediated by TLR3[86-88]. LXRs also regulate apoptosis and enhance survival of macrophages within lesions, while IFN-γ promotes neointimal hyperplasia and macrophage apoptosis by promoting ubiquitin-dependent LXR degradation[101,102].

However, it should be recognised that the pharmacology of oxysterols is highly complex: A large number of nuclear, and G-protein coupled (GPR), receptors bind these bioactive lipids [*e.g.*, retinoid-related orphan receptors, ER, Epstein-Barr virus induced GPR (EBI2/GPR183) and IL-8 receptor (CXCR2)][93]. This, combined with the complexity of oxysterol metabolism, enzymatic conversion to other species such as esters, bile acids and 3-sulphate derivatives, and tissue- and species-specific effects, makes deciphering the (patho)physiological impact of these molecules particularly challenging[93].

EPIGENETIC MECHANISMS CONTRIBUTING TO "foam cell" FORMATION: THE EMERGING ROLE OF MICRORNA

It is increasingly clear that epigenetic mechanisms such as DNA methylation, histone post-translational modification and changes in expression of non-coding RNA, such as long non-coding RNA (lncRNA) and miRNA, are important contributors to macrophage phenotype and the pathogenesis of "foam cell" formation. Alterations in chromatin structure and gene expression exert both acute and chronic effects on a wide array of biological processes which influence macrophage lipid accumulation and inflammatory responses. For example, DNA methyltransferases catalyse methylation of the 5'-position of cytosine residues, using S-adenosyl-methionine as the methyl donor, resulting in hypermethylation of CpG islands and stable repression of transcription[103,104]. Chromatin histone post-translational modifiers, such as histone acetyltransferases and deacetylases and histone methyltransferases, target lysine and/or arginine residues to induce or repress gene expression, dynamically fine-tuning gene expression by controlling the access of transcription factors to promoter and enhancer regions[105,106].

An additional layer of epigenetic regulation is provided by non-coding RNA sequences, including lncRNA sequences, longer than 200 nucleotides, and miRNA sequences (20-25 nucleotides in size), the focus of this review article, which fine-tune expression of multiple (networks of) genes in response to environmental factors, including oxLDL[107-109]. Sequences encoding miRNA can be found singly or in clusters throughout the genome, located in intron-exon portions of protein-encoding genes or

intergenic regions[110,111]. Transcription is dependent on the activity of RNA polymerase II/III and expression, in relation to intergenic miRNA, can be dependent or independent of host gene expression[111-114]. MicroRNA are frequently found in clusters and can be co-transcribed and separated by splicing, or expressed independently[115]. Transcription and generation of miRNA occurs through both canonical and non-canonical pathways, with less information available on the latter[116]. The canonical pathway involves generation of a hairpin-containing primary miRNA (pri-miRNA) transcript containing a 5′ methylated cap and a 3′ polyadenylated tail required for pri-miRNA processing and transport[112,117]. Processing occurs *via* a microprocessor complex consisting of the double-stranded RNA-binding protein DiGeorge syndrome critical region gene 8 which recognises methyl motifs present in the pri-miRNA[118,119]. This interaction serves as an anchor for a ribonuclease II (RNase III), known as Drosha, which cleaves the hairpin structure from the pri-miRNA transcript generating precursor miRNA (pre-miRNA)[120-122].

Export of pre-miRNA (around 70 nucleotides in length) from the nucleus involves the nucleocytoplasmic transporter factor exportin-5 and Ras-related nuclear protein (Ran)GTP[123]. Recognition and binding to exportin-5 occurs primarily through interaction with the 3′ overhanging sequence of pre-miRNA. Blunt ended pre-miRNA remain capable of interaction while RanGTP is bound to the hairpin structure, following release into the cytoplasm[124,125]; hydrolysis of GTP to GDP results in release of the pre-miRNA[118]. Once localised in the cytoplasm, pre-miRNA is processed by a second RNase III enzyme, Dicer, to a mature miRNA duplex (19-25 nucleotides) through removal of the stem-loop structure[126,127]. The guide strand, which has lower base pairing stability, is loaded onto the RNA-induced silencing complex (RISC) composed of Dicer, transactivation response (TAR) RNA binding protein (TRBP) and Argonaute proteins (1 to 4). After integration into the active RISC complex, miRNAs base pair with their complementary mRNA molecules, guided by their miRNA recognising element[128,129].

Degradation of target mRNA occurs only when the miRNA and the target mRNA match exactly (perfect match) or are nearly exactly complementary to each other; this process is the same as the RNA interference induced by artificial small interfering RNA (siRNA)[130,131]. By contrast, if the complementarity between miRNA and target mRNA is only partial (imperfect match), then more moderate reductions in mRNA levels accompanied by translational repression will occur. Targeting occurs through binding of the seed sequence of RISC-incorporated miRNA to conserved complementary regions found in the 3′UTR of target mRNA[130,131]. Factors such as AU-rich regions near seed region binding sites, and auxiliary binding of the miRNA to transcript can also play a role in determining target specificity, reducing translational efficiency or inducing mRNA destabilisation *via* deadenylation[132-134]. miRNA also exert regulatory functions on gene expression in the nucleus, paradoxically promoting gene expression in certain conditions[135,136]. In eukaryotic cells, miRNA molecules can bind several target sequences, mainly within the 3′-UTR of mRNA with varying degrees of complementarity, so that each single miRNA is able to interact with and regulate a large number of genes. Computational prediction suggests that more than 60% of all mammalian protein-coding genes are conserved targets of miRNA, while each miRNA has target sites in hundreds of different genes[137,138]; miRNAs also display tissue-specific expression[139] and concentration-dependent effects in pathologically affected organs and tissues[140-142].

miRNA not only regulate the transcriptional landscape of the cell, but some sequences exist in the extracellular environment in a variety of different forms; degradation of miRNA is avoided through association with Argonaute RISC catalytic component 2 (Ago2), and to a lesser extent nucleophosmin 1 (NMP1)[143-145]. miRNA are found enriched in extracellular vesicles such as exosomes, microvesicles, and lipoproteins such as HDL[146-148], and represent novel biomarkers of atherosclerosis[149]. Secreted miRNA may elicit pro- and anti-atherosclerotic functions: EC when placed under conditions of atherogenic shear stress release Ago2-bound miR-126-3p which in turn downregulate contractile VSMC markers[150], while delivery of miR-223 by HDL to EC leads to downregulation of ICAM-1[151,152].

miRNA sequences implicated in macrophage "foam" cell formation

Over the last five years, there has been an explosion of interest in the role of miRNA involved in macrophage biology, and in "foam" cell formation in particular. Table 1 [153,155-204] indicates some of the miRNA sequences identified by interrogation of the NCBI PubMed database, as either altered by uptake of modified LDL by macrophages, or implicated in the pathogenesis of foam cell formation. Many of the genes targeted by these sequences play established roles in either lipid metabolism or inflammation,

Table 1 MicroRNA sequences associated with macrophage "foam cell" formation and atheroma

MicroRNA (↑↓)	Macrophage	Stimulus	Target	Outcomes *in vitro*	Outcomes *in vivo*	Ref.
Lethal: (let)-7g-5p (↓)	Human: THP-1 macrophages	Oxidized low density lipoprotein (oxLDL)	Nuclear factor kappa beta (NF-κB) (canonical and non-canonical pathways)	Inhibits phosphorylation of inhibitor kappa B kinase (IKK-κB and inhibitor (I) κB, downregulates sterol regulatory element binding transcription factor (SREBF2) and upregulates ATP binding cassette (ABC) transporter A1 (ABCA1); reduces expression of mitogen-activated protein kinase kinase kinase 1 (MEKK1), IKK-κ and inhibits IKK-κ phosphorylation	Overexpression of let-7 g in apolipoprotein (apo)$E^{-/-}$ mice fed a high fat diet (HFD) reduces macrophage accumulation and aortic plaque area; let-7 g sponge accelerates aortic macrophage accumulation in the same model	Wang *et al*[155], 2017
miR-7-5p	Human: THP-1 macrophages	oxLDL ± puerarin	Serine/threonine kinase 11 (STK11)	Mimic significantly decreases cholesterol efflux and promotes cholesterol deposition	-	Li *et al*[156], 2017
miR-9-5p	Human: THP-1 macrophages	oxLDL	Acyl CoA: Cholesterol acyltransferase (ACAT-1; *SOAT1*)	Mimic decreases levels of ACAT-1 protein, reduces cholesterol esterification and blocks foam cell formation	-	Xu *et al*[157], 2013
miR-10a-5p	Murine: $ApoE^{-/-}$ macrophages	Deletion of dicer	-	Mimic rescues defective oxidation of fatty acids in alternatively activated Dicer-deficient macrophages, limiting foam cell formation and inflammation	Levels of hsa-miR-10a are negatively linked to atheroma progression; blockade of miR-10a exacerbates atheroma in $apoE^{-/-}$ mice (HFD)	Wei *et al*[158], 2018
miR-16-5p (↓)	Murine: RAW 264.7 macrophages	OxLDL	Programmed cell death 4 (PDCD4)	Mimic decreases expression and secretion of pro-inflammatory cytokines (interleukin (IL)-6, Tumour necrosis factor (TNF-α), promotes that of anti-inflammatory IL-10, and suppresses NF-κB expression; inhibitor achieves the reverse	Levels decreased in atheroma in $apoE^{-/-}$ (HFD)	Liang *et al*[159], 2016
miR-17-5p	Human: THP-1 macrophages	oxLDL	Beclin-1	Mimic inhibits the enhancement of autophagy and cholesterol efflux induced by interferon-stimulated gene 15 (ISG15)	-	Huang *et al*[160], 2018
miR-19a-3p	-	-	HMG-Box transcription factor-1 (HBP-1)	-	Serum levels are elevated in atherosclerotic patients, and in aortae susceptible to atherosclerosis. Inhibition decreases atheroma and aortic lipid accumulation in $apoE^{-/-}$ (HFD) mice	Chen *et al*[161], 2017
miR-19b-3p (↑)	Human: THP-1 macrophages; Murine: Peritoneal macrophages	Acetylated LDL (AcLDL)	ABCA1	Mimic inhibits cholesterol efflux to ApoA-I, increasing cholesterol mass	Overexpression of miR-19b decreases reverse cholesterol transport (RCT) *in vivo*; mimic reduces high density lipoprotein (HDL) levels, increases lesion area and lipid content in $apoE^{-}$	Lv *et al*[162], 2014

					$^{/-}$ mice fed a Western diet (WD); inhibitor achieves the reverse	
miR-19b-3p (↓)	Human: THP-1 macrophages; Murine: Peritoneal macrophages	AcLDL + diosgenin	ABCA1	Inhibitor enhances ABCA1 cholesterol efflux	Inhibitor promotes RCT *in vivo*, elevates HDL levels, reduces aortic lipid deposition and plaque area in apoE$^{-/-}$ mice (WD)	Lv *et al*[163], 2015
miR-20a/b (-5p)	Human: THP-1 macrophages; Murine: RAW264.7 macrophages	oxLDL	ABCA1	Mimic decreases cholesterol efflux to apoA-I, and increases macrophage cholesterol content	Mimic reduces hepatic expression of ABCA1 and high-density lipoprotein (HDL) levels, impairs reverse cholesterol transport and promotes atherogenesis in apoE$^{-/-}$ mice	Liang *et al*[164], 2017
miR-21-5p	Murine: RAW 264.7 macrophages	OxLDL ± LPS (lipopoly-saccharide)	Toll like receptor 4 (TLR4); NF-κB	LPS stimulation of miR-21 inhibits foam cell formation and reduces secretion of IL-6, IL-12, TNF-α	-	Feng *et al*[165], 2014
miR-21-5p	Murine: Bone-marrow derived macrophages	AcLDL	Mitogen-activated protein kinase kinase 3 (MKK3)	MiR21$^{-/-}$ macrophages exhibit increased ABCG1 degradation and decreased cholesterol efflux, enhancing foam cell formation.	Most abundant miR in murine macrophages; levels elevated in aortic plaque macrophages isolated from LDL receptor knockout (Ldlr$^{-/-}$) (WD) mice; knockout of miR-21 enhances arterial macrophage accumulation, production of inflammatory cytokines	Canfrán-Duque *et al*[166], 2017
miR-23a-5p (↑) miR-23a-3p	Murine: RAW 264.7 macrophages	oxLDL	ABCA1/G1	Inhibitor enhances cholesterol efflux and decreases foam cell formation via upregulation of ABCA1/G1 expression	Plasma levels correlate with plaque progression and vulnerability in patient with acute ischemic stroke. Long-term systemic delivery of antagomir reduces atheroma and promotes plaque stability (apoE$^{-/-}$ mice)	Yang *et al*[167], 2018
miR-24-3p	Primary: Human monocyte-derived macrophages	Colony stimulating factor (CSF)	Matrix metallo-proteinase (MMP)-14	Inhibitor increases macrophage invasive capacity	Hsa-miR-24 levels inversely correlate with MMP-14 protein, and lesion instability Inhibitor increases lesion size and MMP-14 levels in apoE$^{-/-}$ mice (HFD)	Di Gregoli *et al*[168], 2014
miR-27a/b (-3p)	Human: THP-1 macrophages; Murine: RAW264.7 macrophages	AcLDL	ABCA1	Mimic decreases cholesterol efflux, and increases free cholesterol content in macrophages, but blocks uptake of oxLDL [Lipoprotein lipase (LPL), cluster of differentiation (CD36)] and inhibits cholesterol esterification	-	Zhang *et al*[169], 2014
miR-28a-5p (↑)	Murine: RAW264.7 macrophages	oxLDL	LDL receptor class A domain containing 3 (LRAD3)	-	-	Li *et al*[170], 2018
miR-30c-5p	Human: THP-1 macrophages	oxLDL	Caspase 3	Cluster differentiation (CD) 36-dependent uptake of oxLDL reduces miR-30c-5p, enhancing IL secretion	Low serum levels of hsa-miR-30c-5p predict carotid atherosclerosis. Antagomir impairs endothelial	Ceolotto *et al*[171], 2017

					healing following carotid injury (C57BL/6J mice)	
miR-30c-1-3p (↑)	Murine: RAW264.7 macrophages	oxLDL	Oxidized LDL (lectin-like) receptor 1 (LOX-1)	-	-	Li *et al*[170], 2018
miR-33a/b (-5p) (↑)	Human: THP-1 macrophages	oxLDL ± *C. pneumoniae*	ABCA1	Inhibitor promotes cholesterol efflux compared with *C. pneumoniae* control	-	Zhao *et al*[172], 2014
miR-33a-5p	Human: THP-1 macrophages	Vaspin ± LPS	ABCA1	Vaspin decreases expression of miR-33a *via* inhibition of NF-κB, enhancing cholesterol efflux	-	Gao *et al*[173], 2018
miR-33	Human: THP-1 macrophages; Murine: Peritoneal macrophages	-	Peroxisome proliferator activator receptor coactivator 1 (PGC1A), pyruvate dehydrogenase kinase 4 (PDK4), solute carrier family 25 member 25 (SLC25A25), nuclear respiratory factor 1 (NRF1), transcription factor A, mitochondrial (TFAM)	Inhibitor enhances mitochondrial respiration, and cholesterol efflux to apoA-I	Antagomir reduces atheroma in apoE$^{-/-}$ mice (WD)	Karunakaran *et al*[154], 2015
miR-33	Murine: Peritoneal macrophages	AcLDL	Autophagy protein 5 (Atg5); autophagy-related 12 (Atg12), microtubule-associated protein light chain 3 (Map11c3b), AMP-activated protein kinase κ1 (Prkaa1), lysosomal associated membrane protein 1 (Lamp1), transcription factor EB (TFEB), Forkhead box O-3 (FOXO3)	Mimic inhibits the breakdown of lipid droplets by repressing effectors of macrophage autophagy. Silencing promotes lipid droplet catabolism, aiding ABCA1-dependent cholesterol efflux	Inhibition restores defective autophagy in aorta and macrophages of Ldlr$^{-/-}$ mice	Ouimet *et al*[153], 2017
miR-33a-5p (↑)	Human: THP-1 macrophages	oxLDL	ABCA1	Mimic decreases the expression of ABCA1 and promotes lipid accumulation in macrophages, while the inhibitor achieves the reverse	Levels are elevated in individuals at risk of atherosclerosis	Kim *et al*[174], 2017
miR-34a-5p (↓)	Human: THP-1 macrophages	oxLDL + Hcy	Histone deacetylase 1 (HDAC1)	Overexpression of miR-34a reduces HDAC1 levels in foam cells, while knockdown achieves the reverse; HDAC1 induces homocysteine (Hcy) dependent foam cell formation	Levels of miR-34a decrease, and expression of HDAC1 increases, in the aorta of apoE$^{-/-}$ mice fed a high methionine diet	Zhao *et al*[175], 2017
miR-98-5p (↓)	Murine: Peritoneal macrophages	oxLDL	Oxidized LDL (lectin-like) receptor 1 (LOX-1)	Mimic reduces expression of LOX-1 and inhibits foam cell formation; inhibitor achieves the reverse	Mimic decreases expression of LOX-1 and lipid accumulation in the aortic root in apoE$^{-/-}$ mice (HFD); inhibitor achieves the reverse	Dai *et al*[176], 2018
miR-125b-5p (↑)	Murine: RAW 264.7 macrophages	LPS	NF-κB	Silencing of CD40 downregulates levels of miR-125; LPS stimulates miR-125b expression	miR-125b levels are increased in atherosclerosis; siRNA-*CD40* apoE$^{-/-}$ mice exhibit reductions in lesion area	Hueso *et al*[177], 2016
miR-128- (↓)	Murine: RAW 264.7 macrophages	oxLDL	-	Mimic reverses the pro-atherogenic impact of long non-coding (lnc)RNA NEAT1 on foam cell formation	-	Chen *et al*[178], 2018
miR-133a	Murine: RAW 264.7 macrophages	oxLDL	Testicular orphan nuclear receptor 4 (TR4)	Mimic prevents TR-4 mediated	-	Peng *et al*[179], 2016

				enhancement of lipid uptake via CD36		
miR-134-5p	Human: THP-1 macrophages	oxLDL	Angiopoietin (ANGTPL)/lipoprotein lipase (LPL)	LPL activity and protein, inflammatory cytokines and cholesterol mass enhanced by miR-134 mimic; inverse achieved using an inhibitor	-	Lan *et al*[180], 2016
miR-134-5p	-	-	ANGTPL4/LPL	-	Mimic increases atherosclerotic lesions, release of proinflammatory cytokines and peritoneal macrophage lipid accumulation in apoE$^{-/-}$(HFD) mice; inhibitor achieves the reverse	Ye *et al*[181], 2018
miR-144-3p	Human: THP-1 macrophages;Murine: Peritoneal and J774.1 macrophages	Liver X receptor ligand T0901317	ABCA1	Mimic reduces cholesterol efflux to apoA-I in macrophages	Mimic reduces HDL levels in vivo (C57BL/6); inhibitor achieves the reverse	Ramirez *et al*[182], 2013
miR-144-3p	Human: THP-1 macrophages	oxLDL	ABCA1	Mimic reduces cholesterol efflux and enhances expression of cytokines (IL-1, TNF-α, IL-6)	Agomir inhibits RCT *in vivo*, and accelerates atherosclerosis in apoE$^{-/-}$ mice (HFD). Circulating levels of miR-144-3p correlate with acute myocardial infarction	Hu *et al*[183], 2014
miR-146a-5p	Murine: Peritoneal macrophages (wild type and apoE$^{-/-}$)		NF-κB	Increases in miR-146a inhibit pro-inflammatory responses in macrophages (TNF-α)	miR-146a mimic inhibits inflammation and plaque development in apoE$^{-/-}$ x Ldlr$^{-/-}$ and Ldlr$^{-/-}$ mice (HFD)	Li *et al*[184], 2015
miR-146b-5p (↑)	Human: THP-1 macrophages	oxLDL	TNF receptor (TNFR) associated factor 6 (TRAF6)	Inhibition promotes inflammation and lipid uptake during formation of foam cells	Levels are elevated in foam cells, and clinical specimens from patients with atherosclerosis	Lin *et al*[185], 2017
miR-148a-5p miR-152-3p	-	-	DNA methyl-transferase 1 (DNMT1)	Viral overexpression reduces expression of DNMT1, increases levels of adipocyte differentiation related protein (ADRP) and enhances cholesterol accumulation in foam cells; down-regulation achieves the reverse	Aortic levels increased in hyperhomo-cysteinaemic apoE$^{-/-}$ mice	Yang *et al*[186], 2017
miR-150-5p (↑)	Human: THP-1 macrophages	oxLDL	Adiponectin receptor 2 (ADIPOR2)	Mimic inhibits lipid accumulation, increasing cholesterol efflux to apoA-I and HDL; an inhibitor achieves the reverse. Down-regulation of ADIPOR2 replicates the impact of the miR-150 mimic	-	Li *et al*[187], 2016
miR-155-5p (↑)	Human: Peripheral blood monocytes	oxLDL	-	-	-	Chen *et al*[178], 2009
miR-155-5p (↑)	Murine: RAW 264.7 macrophages	oxLDL	HMG-box transcription factor 1 (HBP1)	Enhances lipid uptake and reactive oxygen species production by macrophages	Antagomir decreases lipid accumulation in macrophages and lesion formation in apoE$^{-/-}$ mice (HFD). Level is up-regulated in CD14^{+} monocytes from coronary	Tian *et al*[188], 2014

					heart disease (CHD) patients	
miR-155-5p (↑)	Human: THP-1 macrophages	oxLDL	Calcium-regulated heat stable protein 1 (CARHPS1)-TNF-α	Mimic blocks lipid uptake and suppresses expression of TNF-α; inhibitor achieves the reverse	Elevated in clinical samples (plaque and plasma) from patients with atherosclerosis	Li *et al*[189], 2016
miR-155-5p	Human: THP-1 macrophages	-	T-cell immunoglobulin and mucin domain-3 (Tim-3)	Mimic enhances expression of cholesteryl ester (CE) hydrolase (CEH). Overexpression inhibits foam cell formation, intracellular CE accumulation and enhances efflux of cholesterol	-	Zhang *et al*[190], 2018
miR-181a-5p (↓)	Human: THP-1 macrophages	oxLDL	Mitogen-activated protein kinase kinase 1 (MEK1)	Activates MEK/ERK/NF-κB, upregulates NLR family leucine-rich repeat protein 3 (NRLP3) inflammasome-related proteins (NRLP, caspase-1, IL-18, IL-1)	-	Song *et al*[191], 2019
miR-181a-5p (↑)	Human: THP-1 macrophages	oxLDL	Toll-like receptor 4 (TLR4)	Decreases expression of CD36 protein, and lipid [Total cholesterol (TC), Triglyceride (TG)] accumulation. Inhibits THP-1 apoptosis, and increases Il-6, IL-1, TNF-α protein expression	-	Du *et al*[192], 2018
miR-188-3p (↑)	-	-	-	-	Overexpression induces intravascular lipid accumulation, suppresses oxidation and macrophage inflammation in apoE$^{-/-}$ mice, and reduces serum levels of Regulated upon activation normal T-cell expressed and secreted (RANTES), LOX1 and inducible Nitric Oxide Synthase (iNOS)	Zhang *et al*[193], 2018
miR-212-3p	Human: THP-1 macrophages	oxLDL	Sirtuin 1 (SIRT1)	Overexpression promotes lipid accumulation during foam cell formation, and reduces ABCA1 expression and cholesterol efflux; depletion achieves the reverse	Levels are decreased in atheroma and macrophages in apoE$^{-/-}$ mice (HFD)	Miao *et al*[194], 2018
miR-216a-5p	Human: THP-1 macrophages	oxLDL	Cystathionine-γ-lyase (CSE)	Mimic inhibits expression of ABCA1, decreases phosphorylation of phosphatidyl-inositol 3-kinase (PI3K) and protein kinase B (AKT), and reduces ABCA1 expression and cholesterol efflux, promoting lipid accumulation; inverse occurs with the inhibitor	-	Gong *et al*[195], 2016
miR-217	-	-	-	-	Serum levels are negatively correlated with plaque development in apoE$^{-/-}$ mice (HFD). Mimic reduces intimal media thickness, reduces levels of pro-atherogenic lipoproteins and inhibits inflammation in the same	Liu *et al*[196], 2018

					model	
miR-221-3p (↓)	Murine: RAW 264.7 macrophages	oxLDL	A disintegrin and metalloprotease-22 (ADAM22)	Mimic reduces foam cell formation and apoptosis; inhibitor achieves the reverse	-	Zhuang *et al*[197], 2019
miR-223 (↓)	Murine: Bone marrow derived macrophages; Murine: RAW264.7 macrophages	LPS, oxLDL	TLR4	Overexpression reduces foam cell formation, and production of pro-inflammatory cytokines via repression of NK-κB signaling; inhibitor achieves the reverse	Elevated levels in aortic lesions in apoE$^{-/-}$ mice (HFD)	Wang *et al*[198], 2015
mir-302a-3p (↓)	Primary: Mouse macrophages	oxLDL, AcLDL	ABCA1	Mimic decreases cholesterol efflux to apoA-I	Inhibitor enhances ABCA1 in hepatic and aortic tissues of Ldlr$^{-/-}$ mice (HFD), increases HDL and reduces plaque size and inflammation	Meiler *et al*[199], 2015
miR-361-5p	Human: THP-1 macrophages	oxLDL	LPL	Mir-361-5p is upregulated by apelin, resulting in suppression of LPL translation, inhibition of lipid accumulation and proinflammatory cytokine secretion	-	Zhang *et al*[200], 2017
miR-378-3p (↑)	Human: THP-1 macrophages; Murine: J774.1 macrophages	oxLDL ± coenzyme Q10	ABCG1	Coenzyme Q10 (Q10) protects cholesterol efflux by reducing expression of miR-378	Q10 promotes RCT and reduces atheroma in apoE$^{-/-}$ mice (HFD)	Wang *et al*[201], 2014
miR-382-5p (↑)	Human: THP-1 macrophages	oxLDL, AcLDL	Nuclear factor 1A (NFIA)	Mimic increases cholesterol content and reduces cholesterol efflux; enhances LPS-stimulated production of pro-inflammatory cytokines (IL-6, TNF-α, IL-1)	-	Hu *et al*[108], 2015
miR-486-5p	Human: THP-1 macrophages	oxLDL	Histone acetyl-transferase 1 (HAT1)	Mimic downregulates the expression of ABCA1, limiting cholesterol efflux and promoting foam cell formation; inhibitor achieves the reverse	-	Liu *et al*[202], 2016
miR-497-5p (↑)	Human: THP-1 macrophages	oxLDL	Apelin	Overexpression of miR-497 promotes cholesterol efflux and decreases cholesterol efflux; inhibitor achieves the reverse	-	Cui *et al*[203], 2017
miR-758-5p	Human: THP-1 macrophages	oxLDL	CD36	Mimic decreases uptake of DiI-labelled OxLDL *via* modulation of CD36; inhibitor achieves the reverse	-	Li *et al*[204], 2017

TargetScan and miRDB were used to confirm mouse miRNA target prediction in humans; where (↑↓) is not indicated, the level of miRNA was not confirmed altered by macrophage lipid accumulation. ABCA1: ATP binding cassette transporter A1; ABCG1: ATP binding cassette transporter G1; oxLDL: Oxidized low density lipoprotein; AcLDL: Acetylated low density lipoprotein; ADAM22: A disintegrin and metalloprotease-22; ADIPOR2: Adiponectin receptor 2); ADRP: Adipocyte differentiation related protein; AKT: Protein kinase B; ANGTPTL4: Angiopoetin-like 4; ApoE: Apolipoprotein E; ATG5: Autophagy protein 5; ATG12: Autophagy-related 12; CARHPS1: Calcium-regulated heat stable protein 1; CD: Cluster of differentiation; CEH: Cholesteryl ester hydrolase 1; CSE: Cystathionine-γ-lyase; CSF: Colony stimulating factors; DNMT1: DNA methyltransferase 1; ERK: extracellular signal-regulated kinase; FOXO3: Forkhead protein O3; HAT1: Histone acetyltransferase 1; HBP-1: HMG-Box transcription factor 1; Hcy: Homocysteine; HDAC1: Histone deacetylase 1; HFD: High fat diet; IL: Interleukin; ISG15: Interferon-stimulated gene 15; IKKα/β: Inhibitor kappa B kinase alpha/beta; iNOS: Inducible nitric oxide synthase; Lamp1: Lysosomal associated membrane protein 1; lncRNA: Long noncoding RNA; LPL: Lipoprotein lipase; LPS: Lipopolysaccharide; LRAD3: Low density lipoprotein

receptor class A domain containing 3; Map11c3b: LC3 microtubule-associated protein light chain 3; MEK1: Mitogen activated protein kinase kinase 1; MEKK1: Mitogen-activated protein kinase kinase kinase 1; MKK3: Mitogen activated protein kinase kinase 3; MMP-14: Matrix metalloproteinase-14; NF-κB: Nuclear factor kappa B; NFAM: Transcription factor A, mitochondrial; NFIA: Nuclear factor 1A; NLRP3: NLR-family, leucine-rich repeat protein 3; NRF1: Nuclear respiratory factor 1; OLR1/LOX1: Oxidized low density lipoprotein (lectin-like) receptor 1; PDCD4: Programmed cell death 4; PDK4: Pyruvate dehydrogenase kinase 4; PGC1-γ: Peroxisome proliferator activated receptor-γ coactivator 1; PI3K: Phosphatidylinositol 3-kinase; Prkaa1: AMP-activated protein kinase-α1; RANTES: Regulated upon activation normal T cell expressed and secreted; SIRT1: Sirtuin 1, NAD-dependent protein deacetylase sirtuin 1; SLC25A25: Solute carrier family 25, member 25; SREBF: Sterol regulatory element-binding transcription factor; STK11: Serine/threonine kinase 11; TC: Total cholesterol; TFEB: Transcription factor EB; TG: Triglyceride; TLR4: Toll-like receptor 4; Tim-3: T-cell immunoglobulin and mucin domain-3; TNF-α: Tumour necrosis factor alpha; TR4: Testicular orphan nuclear receptor 4; TRAF6: TNF receptor (TNFR) associated factor 6; Vaspin: Visceral adipose tissue-derived serine protease inhibitor; WD: Western diet.

but a significant number have no prior links to either process, highlighting the importance of miRNA research in driving the discovery of novel cellular processes contributing to disease.

Multiple miRNA sequences target genes involved in macrophage cholesterol homeostasis

It is well established that miR-33, encoded by an intronic sequence within *SREBF2*, plays a role in modulating cholesterol metabolism, in part by repressing expression of ABCA1[152]. However, this sequence also represses effectors of macrophage autophagy[153] thereby inhibiting the breakdown of lipid droplets, and targets genes central to mitochondrial respiration, which are needed for effective cholesterol efflux to apoA-I[154]. The expressions of ABCA1 and/or ABCG1 within the cholesterol efflux pathway are also targeted by miR-19b[162], miR-20a/b[164], miR-23a-5p[167], miR-27a/b[169], miR-144[182] and miR-378[201] (Table 1), highlighting the complexity of the epigenetic regulation mediated by microRNA sequences. Equally, proteins involved in uptake of modified LDL are also modulated by miRNA sequences: TLR-4 by miR-21[165], miR-181a[192] and miR-223[198], LOX-1 by miR-30[170] and miR-98[176], CD36 by miR-181a[192] and miR-758[204], while LPL is targeted by miR-134[180,181] and miR-361[200] (Figure 2). Storage of cholesterol as droplets of cholesteryl ester is modified by miR-9 targeting of *SOAT1* [157], while cholesterol removal by autophagy is reduced by miR-17-5p dependent repression of Beclin-1[160].

Notably, a mimic of miR-134, which enhances LPL activity and protein expression and increases macrophage cholesterol mass, also promotes the production of inflammatory cytokines[180] and increases atheroma formation in the apoE$^{-/-}$ murine model of atheroma[181]. Sequences repressing ABCA1 (miR-144[182], miR-302[199]) also enhance cytokine expression; a mimic of miR-144[183] accelerates lesion development *in vivo*, and circulating levels of this sequence correlate with acute myocardial infarction[183], while an inhibitor of miR-302 increases aortic and hepatic expression of ABCA1 and reduces plaque size and inflammation in Ldlr$^{-/-}$ mice fed a high fat diet[199].

miRNA sequences linking inflammation with cholesterol accumulation in macrophages

miRNA sequences which target the expression of proteins within cell signalling

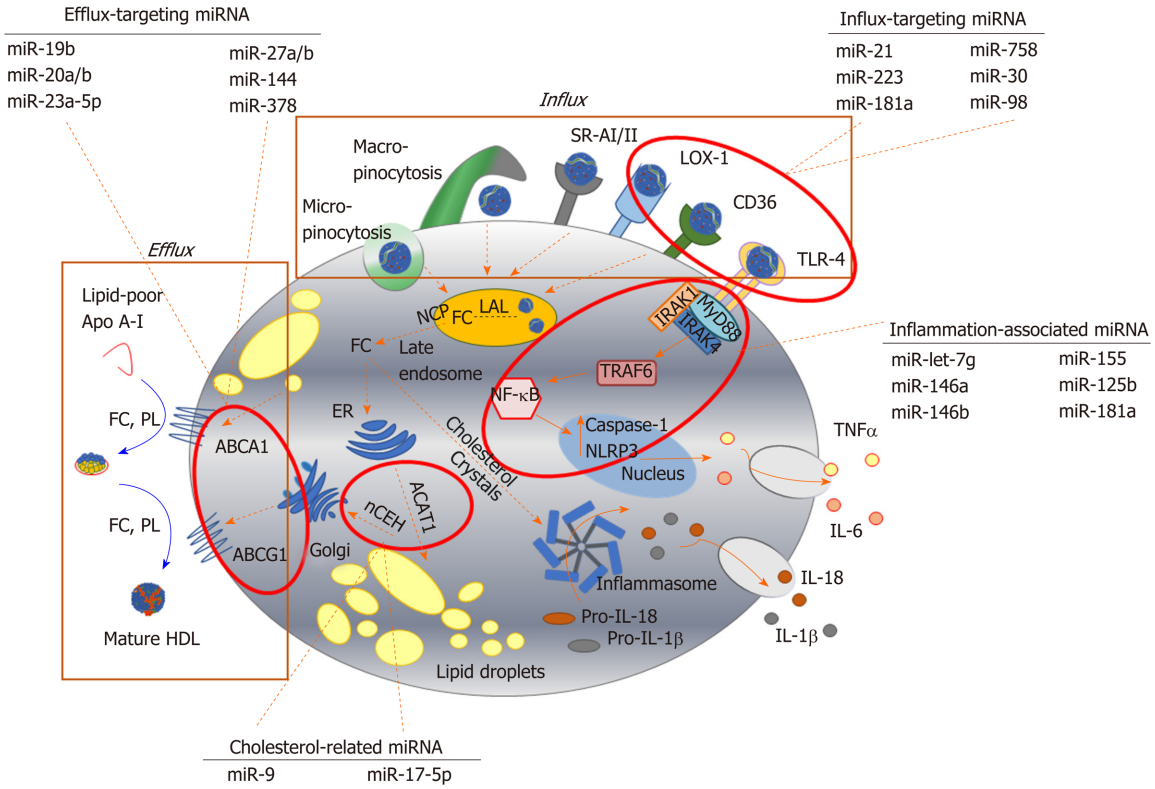

Figure 2 Key pathways involved in foam cell formation regulated by microRNA. Native low-density lipoprotein (LDL) and oxidized LDL is processed in the late endosome/lysosomes by lysosomal acid lipase, generating free cholesterol which is stored in the form of lipid droplets after esterification *via* acyl-CoA cholesteryl acyl transferase or sterol O-acyltransferase 1 at the endoplasmic reticulum. Cholesterol can be removed from the cell by trafficking from the late endosomes, or by hydrolysis of lipid droplets and transport to the plasma membrane to be transferred to lipid-poor apolipoprotein A-I or nascent high-density lipoprotein *via* ABC transporters (ATP binding cassette transporter A1, ATP binding cassette transporter G1). Inflammatory signalling pathways can be activated in foam cells via recognition of oxLDL by toll-like receptor 4 (TLR4), or by intracellular free cholesterol forming cholesterol crystals, leading to the expression and release of inflammatory cytokines. Since their initial discovery, numerous miRNA sequences have been shown to play a role in targeting each of these key steps in the formation of foam cells. For example, influx of modified lipoproteins into macrophages *via* oxidized low-density lipoprotein (lectin-like) receptor 1, cluster of differentiation 36 and TLR4, is reported to be regulated by miR-21, miR-30, miR-98, miR-181a, miR-223 and miR-758. The cholesterol efflux pathway is modulated by distinct sequences, including miR-19b, miR-20a/b, miR-23, miR-27a/b, mir-155 and miR-378, while miR-9 and miR-17 regulate the esterification and hydrolysis of cholesterol droplets. MicroRNA-181a regulates both lipid metabolism and inflammatory response, while let-7g, miR-146a/b, miR125b and miR-155 influence macrophage inflammatory phenotype. Dotted arrows indicate the paths for cholesterol derived from the extracellular environment within the macrophage; solid arrows indicate inflammatory signalling pathways. HDL: High density lipoprotein; ABCA1: ATP binding cassette transporter A1; ABCG1: ATP binding cassette transporter G1; ACAT-1: Acyl-CoA cholesteryl acyl transferase or sterol O-acyltransferase 1; ApoA-I: Apolipoprotein A-I; CD: Cluster of differentiation; ER: Endoplasmic reticulum; FC: Free cholesterol; IL: Interleukin; IRAK: Interleukin 1 receptor associated kinase 4; LAL: Lysosomal acid lipase; LOX-1: Oxidized low-density lipoprotein (lectin-like) receptor 1; MyD88: Myeloid differentiation primary response 88; nCEH: Neutral cholesteryl ester hydrolase; NPC: Niemann-Pick disease type C; NF-κB: Nuclear factor kappa beta; PL: Phospholipid; SR: Scavenger receptor; TLR: Toll-like receptor; TNF-α: Tumour necrosis factor alpha.

pathways mediating inflammatory responses have also been shown to reduce cholesterol accumulation in macrophages (Table 1)[153,155-204]. For instance, let-7g inhibits both canonical (RelA/p50) and non-canonical (RelB/p52) NF-κB signalling pathways, limiting inflammatory (IL-1, IL-6, MCP-1) and apoptotic responses, and decreasing macrophage foam cell formation[155] *in vitro* and *in vivo*. Further, let-7g inhibition of nuclear translocation of RelA/p50 in macrophages treated with OxLDL prevents NF-κB dependent upregulation of *SREBF2* and miR-33a, and results in up-regulation of ABCA1[155]. Indeed, aberrant expression of members of the lethal-7 (let-7) miRNA family have been linked with a number of diseases, including atherosclerosis and cancer[205-207]: Reductions in expression of let-7, which can be mediated by RNA binding protein Lin-28 homolog A (Lin-28), is observed in human carotid plaques from diabetic individuals, and diabetic apoE$^{-/-}$ mice[207].

miR-146a, which also targets the NF-κB pathway, inhibits the production of TNF-α by macrophages *in vitro*, and limits inflammation and plaque development in murine models of atheroma[184]. Plaque development and inflammation are also inhibited by miR-146a which targets the tumour necrosis factor receptor-associated factor (TRAF6)-NF-κB signalling axis[185] thought to underlie many cardiovascular pathologies[208]. Equally, the loss of miR-21, which targets mitogen-activated protein (MAP) kinase kinase 3 (MKK3) within the p38 MAP kinase pathway[166], promotes the degradation of

ABCG1, reducing cholesterol removal and promoting the formation of foam cells *in vitro*. *In vivo*, deletion of miR-21 increases the number of macrophages within arterial lesions, and enhances the production of inflammatory cytokines[166]. Reductions in expression of miR-181a, which targets mitogen-activated protein kinase kinase 1 (MEK1) in the extracellular signal-regulated kinase (ERK)-1/2 pathway, have been linked to upregulation of NRLP3 inflammasome-related proteins[191], while increased expression of this sequence is associated with decreases in macrophage lipid accumulation[192].

Unsurprisingly, given their roles in regulating inflammatory responses, a number of miRNA sequences have been linked with regulating macrophage polarisation to differing phenotypes, recently reviewed by Essandoh *et al*[209]. Notably, miR-9, miR-125b and miR-155 are sequences linked with polarization towards the M1 phenotype[209]; miR-125b and miR-155 are induced by exposure to oxLDL in human macrophages, but mimics of miR-9 and miR-155 are linked with inhibition of foam cell formation by repression of *SOAT1*[157], enhanced expression of cholesteryl ester hydrolase[190], blockade of lipid uptake[189] and increased cholesterol efflux[190], suggesting divergence from the inflammation-lipid accumulation axis. Macrophages are induced to the M2 phenotype by several sequences, including miR-146a and miR-223[209]. miRNA-146a inhibits inflammatory responses in murine macrophages, and also reduces inflammation and plaque formation in murine models of atheroma[184]. Levels of miR-223 are reduced by OxLDL, and LPS, but elevated in murine atherosclerotic lesions, and overexpression of this sequence prevents both foam cell formation and production of inflammatory cytokines[198]. However, much less is known about the impact of miRNA mimics or inhibitors involved in phenotypic modulation after induction of lipid accumulation in macrophages, and whether these molecules can induce phenotypic plasticity or aid lesion regression remains a key question.

Novel and emerging pathways associated with foam cell formation

Importantly, research into microRNA sequences modulated during foam cell formation has highlighted a number of previously unrecognised pathways contributing to this process, which may also prove useful therapeutic targets (Figure 3). For example, the study of miR-155 revealed a previously unsuspected role for calcium-regulated heat stable protein 1 (CARHSP1/CRHSP-24) in foam cell formation[189]. This cytoplasmic protein, a cold shock domain (CSD) protein family member, is found within processing bodies or exosome granules, and was first identified as the physiological substrate for calcineurin (PP2B)[189,210,211]. The conserved CSD domain binds to the AU-rich element (ARE) in the 3-UTR of TNF-α, increasing mRNA stability and enhancing inflammation[210,211]. NF-κB induction of miR-155 by oxLDL in human macrophages is mirrored by increased levels in plasma and atherosclerotic lesions of patients with atherosclerosis[189]. MicroRNA-155 binds directly to the 3′-UTR of CARHSP1 to reduce expression of this protein and TNF-α in macrophage foam cells; knockdown of CARHSP1 inhibits lipid accumulation and TNF-α production, while overexpression of CARHSP1 reverses the protective effects of miR-155[189].

Equally, insight into the hitherto uncharacterised role of programmed cell death 4 (PDC4) in foam cell formation and atherosclerosis was revealed by investigation of the function of miR-16[159]. Expression of PDCD4, which can act as a tumour suppressor, is induced by apoptosis and is known to regulate both inflammatory and apoptotic responses[212-214]. MicroRNA-16 suppresses the activation of inflammatory macrophages by directly targeting the 3′-UTR of PDCD4[159]. Levels of miR-16 decline in macrophages treated with oxLDL and in aortic lesions of apoE$^{-/-}$ mice fed a high fat diet, which also exhibit greater levels of PDCD4 protein. Either knockdown of PDCD4, or transfection with a miR-16 mimic, inhibits the expression and secretion of pro-inflammatory cytokines, and enhances expression and release of the anti-inflammatory factor IL-10, while an inhibitor of miR-16 achieves the reverse; these outcomes are also associated with modulation of ERK, p38 MAP kinase and NF-κB[212].

In other studies, the mechanism of action of molecules such as puerarin, the major bioactive ingredient isolated from *Pueraria lobata* and known as Gegen in traditional Chinese medicine, have been revealed by studies using miRNA[156]. Targeting the 3-UTR region of serine/threonine kinase 11 (STK11) using a miR-7 mimic, revealed that this drug enhances ABCA1-dependent cholesterol efflux *via* a mechanism which involves STK11 activation of AMP kinase and enhanced expression of PPAR-γ-LXR-ABCA1. Finally, it is clear that the contribution of some miRNA targets in foam cells remain to be established. For example, miR-28-5p, which is upregulated in murine macrophages treated with oxLDL, targets LDL receptor class A domain containing 3

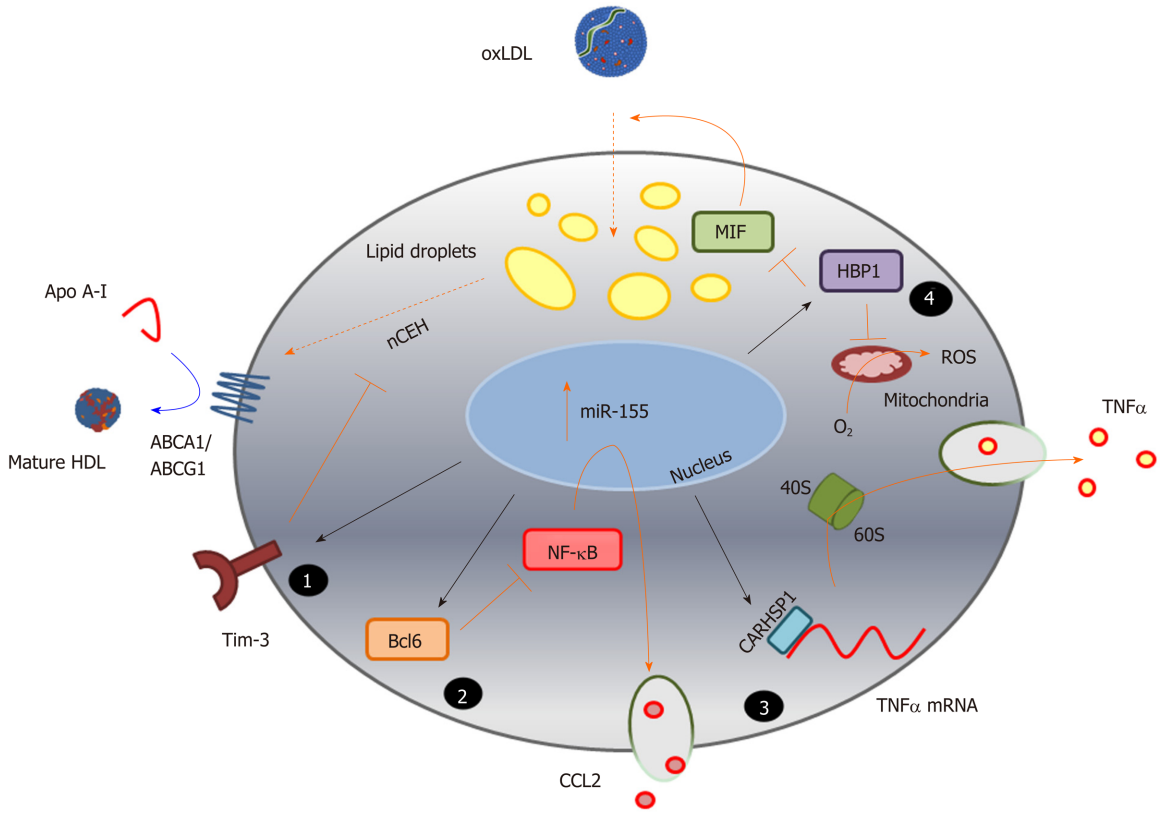

Figure 3 Identification of novel pathways associated with foam cell formation. MicroRNA sequences altered during macrophage foam cell formation reveal novel pathways involved in this process, and highlight the complexity of miRNA function in targeting multiple gene pathways, exemplified here by miR-155 (Table 1). Inhibition of expression of the cell surface immunoregulatory glycoprotein, T-cell immunoglobulin and mucin-domain containing-3 (Tim-3), by miR-155 (1) increases hydrolysis of cholesteryl esters by neutral cholesteryl ester hydrolase, and promotes efflux of this lipid *via* ATP binding cassette transporter A1 and ATP binding cassette transporter G1, to apolipoprotein A-I and high density lipoprotein respectively. MicroRNA-155 also represses expression of the transcriptional repressor B-cell lymphoma 6 protein[236], which increases nuclear factor kappa beta activity and enhances production of the chemokine C-C motif ligand 2 (2); Repression of the cytoplasmic protein, calcium-regulated heat stable protein (CARHSP1) by miR-155, results in reduced binding of this protein to the 3'UTR of the TNFα gene transcript, and to reduced mRNA stability and decreased output of this cytokine (3); MicroRNA-155 also directly targets (represses) HMG-Box transcription factor 1, thereby increasing production of reactive oxygen species and loss of inhibition of macrophage migration inhibitory factor, leading to increased oxidatively modify proteoglycan-bound low density lipoprotein uptake and lipid accumulation (4). The black arrows represent direct targeting by miR-155; orange bars and arrows represent the functions of miR-155 targets in the absence of this miRNA sequence. HDL: High density lipoprotein; ABCA1: ATP binding cassette transporter A1; ABCG1: ATP binding cassette transporter G1; ACAT-1: Acyl-CoA cholesteryl acyl transferase or sterol O-acyltransferase 1; ApoA-I: Apolipoprotein A-I; Bcl6: B-cell lymphoma 6 protein; CARHSP1: Calcium-regulated heat stable protein; CCL2: C-C motif chemokine ligand 2; HBP1: HMG-Box transcription factor 1; MIF: Macrophage migration inhibitory factor; NF-κB: Nuclear factor kappa beta; ROS: Reactive oxygen species; TNF-α: Tumour necrosis factor alpha.

(LRAD3)[170], but the contribution of this novel lipoprotein receptor to foam cell formation has not been investigated: At present, this protein has been linked with amyloid precursor protein trafficking in neurons[215] and with activation of E3 ubiquitin-protein ligase Itchy homolog (Itch) and E3 ubiquitin-protein ligase NEDD4 that promote proteasomal degradation[216].

Pathways targeted by miRNA sequences altered in human macrophage "foam" cells: DIANA/KEGG predictive analysis

It is increasingly recognised that networks of miRNA sequences, and their combined effects on multiple pathways, are important epigenetic determinants of complex phenotypes, just as genome-wide association studies have revealed shared genes and pathways in human disease[217,218]. The (human) sequences described in Table 1 were analysed using DIANA-miRPATH v3.0, and the miRNA versus GO/GOSlim/KEGG entries heat map is shown in Figure 4. This functionality enables identification of miRNA belonging to similar functional categories, and identification of pathways lying under the regulation of similar miRNAs[219].

Several well-established pathways, targeted by multiple and distinct miRNA sequences/clusters, and known to regulate vascular function and atherogenesis, emerge from this predictive analysis. These include adherens junctions, which are a key part of the common signalling network linking age-related disease proteins

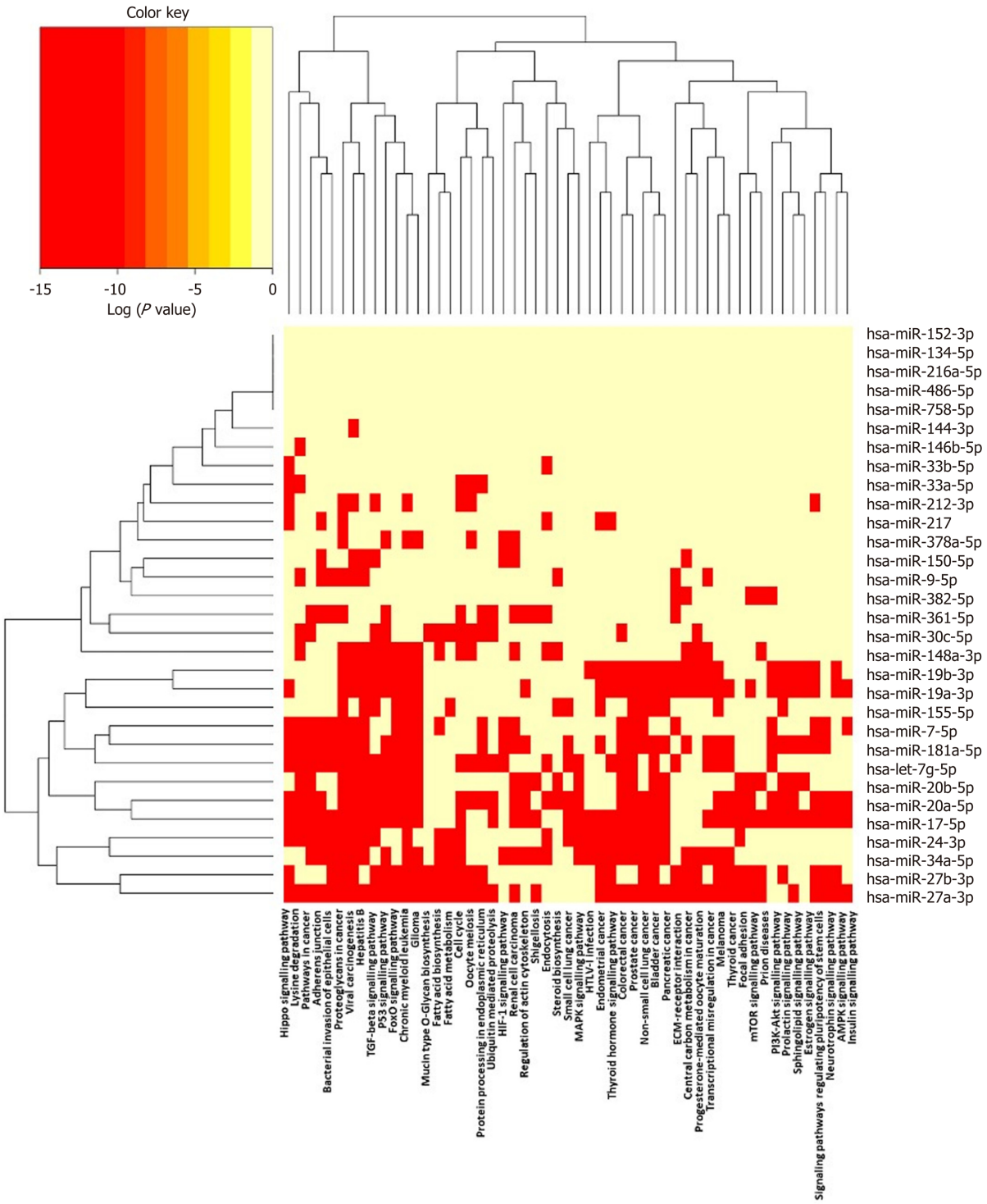

Figure 4 Pathways targeted by miRNA sequences altered in human macrophage "foam" cells: DIANA/KEGG predictive analysis. The human miRNA sequences described in Table 1 were analysed using DIANA-miRPATH v3.0, yielding a heat map of miRNA *vs* Gene Ontology/GOSlim/Kyoto Encyclopedia for Genes and Genomes entries.

(ARDPs) and longevity-associated proteins (LAPs) in the human interactome[220]. The endothelial adherens junction complex, formed of vascular endothelial (VE)-cadherin and associated catenins, is a key determinant of arterial permeability, dysregulation contributing to vascular inflammation and atherosclerosis[221], while attenuating intraplaque vascular leakage reduces macrophage accumulation, necrotic core size and intraplaque haemorrhage[222]. Identification of the TGF-β signalling pathway as a target of miRNA sequences altered in macrophage foam cells is equally unsurprising, given the widely recognised, and extensively reviewed, role of this cytokine in controlling macrophage phenotype[223], atherosclerosis[224] and cardiovascular function[225].

More intriguingly, the Hippo signalling pathway emerges as highly targeted by

multiple miRNA sequences implicated in foam cell formation (Figure 4); originally discovered in *Drosophila* and highly conserved in mammalian cells, this pathway regulates cell survival, proliferation and apoptosis[226]. Li *et al*[170] first showed that target genes of differentially expressed miRNA sequences are enriched in this pathway, in murine RAW264.7 macrophages treated with OxLDL; the Hippo/Yes-associated protein (YAP) signalling pathway is linked with vascular remodelling, pulmonary hypertension, aortic aneurysm, restenosis and angiogenesis, and atherosclerosis[226,227]. Notably, the atheroprotective effect of steady laminar flow in major arteries is linked with inhibition of Hippo/YAP effector function[228] while activation of this pathway is linked with vascular remodelling, and switching of arterial smooth muscle cells to the "synthetic" proliferative phenotype in response to biochemical stretch[229]. The effector function of YAP is linked with accelerated atherosclerosis in apoE$^{-/-}$ mice[230], while the herbal extract *Scutellarin* can protect against atherosclerosis in rats by modulating the Hippo-YAP-Forkhead box (FOXO)3A transduction pathway[231].

Another pathway enriched in targets of multiple miRNA sequences is that involved in bacterial invasion of epithelial cells (Figure 4). Infection and systemic inflammation are linked with atherogenesis in a number of epidemiological studies[232] and vascular cells and macrophages are subject to invasion by bacteria *via* a number of mechanisms, including evasion of autophagy and internalisation *via* lipid rafts. In turn, this has led to the notion of vascular tissue providing a "privileged niche" in which bacteria can persist in dormancy for extended periods of time before becoming activated in phagocytic cells, contributing to the chronic and unresolved inflammation which characterises atherosclerosis[232]. The epigenetic miRNA profile found in macrophage "foam" cells which may modulate susceptibility to bacterial invasion may also suggest key proteins (and pathogens) implicated in this process, and/or highlight possible therapeutic strategies designed to limit the impact of vascular "infectology"[232].

THERAPEUTIC OPTIONS: CLINICAL APPLICATIONS OF MIRNA (TARGETS)

miRNA pathways are excellent candidates for pharmacological manipulation, and have been invoked as biomarkers, diagnostics or therapeutics for a number of disease conditions[140,233,234]. For example, Caruso *et al*[233] monitored dynamic changes in microRNA profiles in lung tissue during the development of pulmonary arterial hypertension (PAH) in hypoxic rodents. The same authors discovered that miR-145 is a useful indicator of hypoxia in mice, and of heritable and idiopathic pulmonary arterial hypertension in patients; down-regulation of miR-145 also had utility in protecting against development of PAH in mice[234]. Further, the "ThyraMIR" testing platform, which examines the expression of a panel of ten miRNA in conjunction with selected disease-associated genes, has been approved for diagnostic use in thyroid cancer when malignancy risk cannot be determined by conventional cytology[235].

Treatments involving miRNAs focus on the concept of specifically influencing levels of miRNAs in certain diseases – including suppression of miRNAs, as well as raising miRNA levels or substituting artificially generated copies[140]. Mimics can be used for gene silencing, by generating artificial, double-stranded miRNA-like RNA fragments, which bind specifically to target mRNA, activating the RISC complex; this results in down-regulation of specific mRNAs and gene suppression (above). Equally, chemically engineered oligonucleotides are capable of silencing single endogenous miRNAs, binding to the target mature miRNA, leading to reduced activation of RISC and up-regulation of specific mRNAs and gene expression. Other approaches involve "target mimicry" using miRNA sponges, masking or erasers[140].

Delivery of disease-specific miRNA mimics or inhibitors remains in the developmental stage with multiple miRNA therapeutics currently in clinical trials. The most advanced trial, currently in Phase II, employs a chemically engineered inhibitor for miR-122 (Miravirsen) which, under normal conditions, binds to the 5′-UTR region of the hepatitis C virus and enhances its transcription[236-243]. By hybridizing to mature miR-122, Miravirsen has been shown to effectively inhibit viral replication with minimal "off target" effects[236-239]. MicroRNA-based clinical trials are also underway for the development of novel treatments for various cancers. Currently in Phase I and Phase II trials, the efficacy of an inhibitor (MRG-106) targeting miR-155 is being investigated for treatment of a variety of lymphomas, reflecting the recognised role of this sequence in driving malignant lymphocyte proliferation[240,241].

Despite the encouraging progression of miRNA therapies, significant challenges

have also been highlighted in some clinical trials. One such promising miRNA therapeutic, the miR-34 mimic "MRX34", was employed in a Phase I trial for patients with advanced liver cancer[242-244]; despite dose-dependent modulation of miR-34 target oncogenes, the study was halted due to serious adverse effects in a small cohort of subjects[242-244]. This study also highlighted a challenging area for the development of miRNA-based therapies: The preclinical studies demonstrated that the liposomal delivery system resulted in elevated miR-34 in multiple tissues in non-human primates[244]. While this may be beneficial for miRNA therapeutics used to treat diseases that can arise in several anatomical locations, in the case of tissue specific diseases, such as atherosclerosis, site-specific homing could dramatically reduce potential off-target effects.

To overcome this issue, liposomes enriched in specific amino acid sequences have been developed which result in increased tissue-specific accumulation. The efficacy of this system, for the delivery of short, siRNA, has been demonstrated *in vivo* in osteoporotic mice[245]. Use of a lipid nanoparticle containing C-C chemokine receptor type 2 (CCR2)-targeting siRNA resulted in high levels of localisation in bone marrow and spleen, significant reductions in monocyte CCR2 expression, decreased myeloid cell infiltration in the plaque and an overall reduction in lesion size in ApoE$^{-/-}$ mice[246]. While this system targets atherosclerotic plaque indirectly, additional delivery mechanisms have been employed in animal studies that may facilitate plaque-directed delivery of miRNA-based therapeutics. Notably, reconstituted HDL (rHDL) can act as a carrier particle for delivery of drugs and microRNA: In ApoE$^{-/-}$ mice, rHDL was used to delivery simvastatin to plaque regions, resulting in reduced local inflammation[247], while miR-223 incorporated into rHDL *in vitro* was able to selectively target cells expressing SR-BI[148].

Thus, many factors need careful consideration in developing miRNA therapeutics for atherosclerosis, including effective vectors and delivery options, and the nature of "off-target" side-effects and/or toxicities which may occur due to disruption of multiple target genes and/or cell signalling networks[248,249]. However, since differing microRNA sequences impact on distinct stages of the atherogenic process[248,249], delivery of a pool of mimics and/or inhibitors may be an attractive therapeutic strategy for treatment of this complex, multicellular disease[248,249]. Defined stages of the disease process could be targeted by distinct miRNA mimics/inhibitors, predicated by serum levels of secreted miRNA sequences. Such approaches, if fully validated, might be used to provide personalised treatment, or be beneficial in targeting asymptomatic patients, or those in whom statin use is contraindicated or ineffective[250-252].

CONCLUSION

Huge advances have been made in understanding the epigenetic factors, and particularly the role of small non-coding miRNA sequences, in regulating macrophage "foam" cell formation and function over the last decade. Networks of genes regulated by multiple miRNA sequences have been revealed, and new pathways discovered which contribute to the atherogenic process, which may ultimately lead to RNA-based therapeutics capable of preventing or regressing the formation of complex atherosclerotic lesions by targeting macrophage function.

REFERENCES

1 **Batty GD**, Kivimäki M, Bell S. Comparison of risk factors for coronary heart disease morbidity versus mortality. *Eur J Prev Cardiol* 2019; 2047487319882512 [PMID: 31619085 DOI: 10.1177/2047487319882512]

2 **Asakura T**, Karino T. Flow patterns and spatial distribution of atherosclerotic lesions in human coronary arteries. *Circ Res* 1990; **66**: 1045-1066 [PMID: 2317887 DOI: 10.1161/01.res.66.4.1045]

3 **Dai G**, Kaazempur-Mofrad MR, Natarajan S, Zhang Y, Vaughn S, Blackman BR, Kamm RD, García-Cardeña G, Gimbrone MA Jr. Distinct endothelial phenotypes evoked by arterial waveforms derived from atherosclerosis-susceptible and -resistant regions of human vasculature. *Proc Natl Acad Sci USA* 2004; **101**: 14871-14876 [PMID: 15466704 DOI: 10.1073/pnas.0406073101]

4 **Skålén K**, Gustafsson M, Rydberg EK, Hultén LM, Wiklund O, Innerarity TL, Borén J. Subendothelial retention of atherogenic lipoproteins in early atherosclerosis. *Nature* 2002; **417**: 750-754 [PMID: 12066187 DOI: 10.1038/nature00804]

5 **Parmar KM**, Larman HB, Dai G, Zhang Y, Wang ET, Moorthy SN, Kratz JR, Lin Z, Jain MK, Gimbrone MA Jr, García-Cardeña G. Integration of flow-dependent endothelial phenotypes by Kruppel-like factor 2. *J Clin Invest* 2006; **116**: 49-58 [PMID: 16341264 DOI: 10.1172/JCI24787]

6 **Wang C**, Baker BM, Chen CS, Schwartz MA. Endothelial cell sensing of flow direction. *Arterioscler*

Thromb Vasc Biol 2013; **33**: 2130-2136 [PMID: 23814115 DOI: 10.1161/ATVBAHA.113.301826]
7 **Yoshida H**, Kisugi R. Mechanisms of LDL oxidation. *Clin Chim Acta* 2010; **411**: 1875-1882 [PMID: 20816951 DOI: 10.1016/j.cca.2010.08.038]
8 **Yang K**, Zhang XJ, Cao LJ, Liu XH, Liu ZH, Wang XQ, Chen QJ, Lu L, Shen WF, Liu Y. Toll-like receptor 4 mediates inflammatory cytokine secretion in smooth muscle cells induced by oxidized low-density lipoprotein. *PLoS One* 2014; **9**: e95935 [PMID: 24755612 DOI: 10.1371/journal.pone.0095935]
9 **Sawamura T**, Kume N, Aoyama T, Moriwaki H, Hoshikawa H, Aiba Y, Tanaka T, Miwa S, Katsura Y, Kita T, Masaki T. An endothelial receptor for oxidized low-density lipoprotein. *Nature* 1997; **386**: 73-77 [PMID: 9052782 DOI: 10.1038/386073a0]
10 **Sambandam T**, Baker JR, Christner JE, Ekborg SL. Specificity of the low density lipoprotein-glycosaminoglycan interaction. *Arterioscler Thromb* 1991; **11**: 561-568 [PMID: 2029496 DOI: 10.1161/01.ATV.11.3.561]
11 **Moore KJ**, Koplev S, Fisher EA, Tabas I, Björkegren JLM, Doran AC, Kovacic JC. Macrophage Trafficking, Inflammatory Resolution, and Genomics in Atherosclerosis: JACC Macrophage in CVD Series (Part 2). *J Am Coll Cardiol* 2018; **72**: 2181-2197 [PMID: 30360827 DOI: 10.1016/j.jacc.2018.08.2147]
12 **PrabhuDas MR**, Baldwin CL, Bollyky PL, Bowdish DME, Drickamer K, Febbraio M, Herz J, Kobzik L, Krieger M, Loike J, McVicker B, Means TK, Moestrup SK, Post SR, Sawamura T, Silverstein S, Speth RC, Telfer JC, Thiele GM, Wang XY, Wright SD, El Khoury J. A Consensus Definitive Classification of Scavenger Receptors and Their Roles in Health and Disease. *J Immunol* 2017; **198**: 3775-3789 [PMID: 28483986 DOI: 10.4049/jimmunol.1700373]
13 **Traber MG**, Kayden HJ. Low density lipoprotein receptor activity in human monocyte-derived macrophages and its relation to atheromatous lesions. *Proc Natl Acad Sci USA* 1980; **77**: 5466-5470 [PMID: 6254083 DOI: 10.1073/pnas.77.9.5466]
14 **Choi SH**, Harkewicz R, Lee JH, Boullier A, Almazan F, Li AC, Witztum JL, Bae YS, Miller YI. Lipoprotein accumulation in macrophages via toll-like receptor-4-dependent fluid phase uptake. *Circ Res* 2009; **104**: 1355-1363 [PMID: 19461045 DOI: 10.1161/CIRCRESAHA.108.192880]
15 **Oteng AB**, Ruppert PMM, Boutens L, Dijk W, van Dierendonck XAMH, Olivecrona G, Stienstra R, Kersten S. Characterization of ANGPTL4 function in macrophages and adipocytes using *Angptl4*-knockout and *Angptl4*-hypomorphic mice. *J Lipid Res* 2019; **60**: 1741-1754 [PMID: 31409739 DOI: 10.1194/jlr.M094128]
16 **Kruth HS**, Jones NL, Huang W, Zhao B, Ishii I, Chang J, Combs CA, Malide D, Zhang WY. Macropinocytosis is the endocytic pathway that mediates macrophage foam cell formation with native low density lipoprotein. *J Biol Chem* 2005; **280**: 2352-2360 [PMID: 15533943 DOI: 10.1074/jbc.M407167200]
17 **Anzinger JJ**, Chang J, Xu Q, Buono C, Li Y, Leyva FJ, Park BC, Greene LE, Kruth HS. Native low-density lipoprotein uptake by macrophage colony-stimulating factor-differentiated human macrophages is mediated by macropinocytosis and micropinocytosis. *Arterioscler Thromb Vasc Biol* 2010; **30**: 2022-2031 [PMID: 20634472 DOI: 10.1161/ATVBAHA.110.210849]
18 **Luo Y**, Duan H, Qian Y, Feng L, Wu Z, Wang F, Feng J, Yang D, Qin Z, Yan X. Macrophagic CD146 promotes foam cell formation and retention during atherosclerosis. *Cell Res* 2017; **27**: 352-372 [PMID: 28084332 DOI: 10.1038/cr.2017.8]
19 **Park YM**, Drazba JA, Vasanji A, Egelhoff T, Febbraio M, Silverstein RL. Oxidized LDL/CD36 interaction induces loss of cell polarity and inhibits macrophage locomotion. *Mol Biol Cell* 2012; **23**: 3057-3068 [PMID: 22718904 DOI: 10.1091/mbc.E11-12-1051]
20 **Llodrá J**, Angeli V, Liu J, Trogan E, Fisher EA, Randolph GJ. Emigration of monocyte-derived cells from atherosclerotic lesions characterizes regressive, but not progressive, plaques. *Proc Natl Acad Sci USA* 2004; **101**: 11779-11784 [PMID: 15280540 DOI: 10.1073/pnas.0403259101]
21 **Galkina E**, Kadl A, Sanders J, Varughese D, Sarembock IJ, Ley K. Lymphocyte recruitment into the aortic wall before and during development of atherosclerosis is partially L-selectin dependent. *J Exp Med* 2006; **203**: 1273-1282 [PMID: 16682495 DOI: 10.1084/jem.20052205]
22 **Nickel T**, Schmauss D, Hanssen H, Sicic Z, Krebs B, Jankl S, Summo C, Fraunberger P, Walli AK, Pfeiler S, Weis M. oxLDL uptake by dendritic cells induces upregulation of scavenger-receptors, maturation and differentiation. *Atherosclerosis* 2009; **205**: 442-450 [PMID: 19203752 DOI: 10.1016/j.atherosclerosis.2009.01.002]
23 **Stemme S**, Faber B, Holm J, Wiklund O, Witztum JL, Hansson GK. T lymphocytes from human atherosclerotic plaques recognize oxidized low density lipoprotein. *Proc Natl Acad Sci USA* 1995; **92**: 3893-3897 [PMID: 7732003 DOI: 10.1073/pnas.92.9.3893]
24 **Frostegård J**, Ulfgren AK, Nyberg P, Hedin U, Swedenborg J, Andersson U, Hansson GK. Cytokine expression in advanced human atherosclerotic plaques: dominance of pro-inflammatory (Th1) and macrophage-stimulating cytokines. *Atherosclerosis* 1999; **145**: 33-43 [PMID: 10428293 DOI: 10.1016/s0021-9150(99)00011-8]
25 **Kimura T**, Kobiyama K, Winkels H, Tse K, Miller J, Vassallo M, Wolf D, Ryden C, Orecchioni M, Dileepan T, Jenkins MK, James EA, Kwok WW, Hanna DB, Kaplan RC, Strickler HD, Durkin HG, Kassaye SG, Karim R, Tien PC, Landay AL, Gange SJ, Sidney J, Sette A, Ley K. Regulatory $CD4^+$ T Cells Recognize Major Histocompatibility Complex Class II Molecule-Restricted Peptide Epitopes of Apolipoprotein B. *Circulation* 2018; **138**: 1130-1143 [PMID: 29588316 DOI: 10.1161/CIRCULATIONAHA.117.031420]
26 **Drechsler M**, Megens RT, van Zandvoort M, Weber C, Soehnlein O. Hyperlipidemia-triggered neutrophilia promotes early atherosclerosis. *Circulation* 2010; **122**: 1837-1845 [PMID: 20956207 DOI: 10.1161/CIRCULATIONAHA.110.961714]
27 **Huo Y**, Schober A, Forlow SB, Smith DF, Hyman MC, Jung S, Littman DR, Weber C, Ley K. Circulating activated platelets exacerbate atherosclerosis in mice deficient in apolipoprotein E. *Nat Med* 2003; **9**: 61-67 [PMID: 12483207 DOI: 10.1038/nm810]
28 **Daugherty A**, Dunn JL, Rateri DL, Heinecke JW. Myeloperoxidase, a catalyst for lipoprotein oxidation, is expressed in human atherosclerotic lesions. *J Clin Invest* 1994; **94**: 437-444 [PMID: 8040285 DOI: 10.1172/JCI117342]

29 **Hazell LJ**, Stocker R. Oxidation of low-density lipoprotein with hypochlorite causes transformation of the lipoprotein into a high-uptake form for macrophages. *Biochem J* 1993; **290**: 165-172 [PMID: 8439285 DOI: 10.1042/bj2900165]

30 **van Leeuwen M**, Gijbels MJ, Duijvestijn A, Smook M, van de Gaar MJ, Heeringa P, de Winther MP, Tervaert JW. Accumulation of myeloperoxidase-positive neutrophils in atherosclerotic lesions in LDLR-/- mice. *Arterioscler Thromb Vasc Biol* 2008; **28**: 84-89 [PMID: 17991873 DOI: 10.1161/ATVBAHA.107.154807]

31 **Auerbach BJ**, Bisgaier CL, Wölle J, Saxena U. Oxidation of low density lipoproteins greatly enhances their association with lipoprotein lipase anchored to endothelial cell matrix. *J Biol Chem* 1996; **271**: 1329-1335 [PMID: 8576120 DOI: 10.1074/jbc.271.3.1329]

32 **Alexander MR**, Murgai M, Moehle CW, Owens GK. Interleukin-1β modulates smooth muscle cell phenotype to a distinct inflammatory state relative to PDGF-DD via NF-κB-dependent mechanisms. *Physiol Genomics* 2012; **44**: 417-429 [PMID: 22318995 DOI: 10.1152/physiolgenomics.00160.2011]

33 **Cherepanova OA**, Pidkovka NA, Sarmento OF, Yoshida T, Gan Q, Adiguzel E, Bendeck MP, Berliner J, Leitinger N, Owens GK. Oxidized phospholipids induce type VIII collagen expression and vascular smooth muscle cell migration. *Circ Res* 2009; **104**: 609-618 [PMID: 19168440 DOI: 10.1161/CIRCRESAHA.108.186064]

34 **Galis ZS**, Muszynski M, Sukhova GK, Simon-Morrissey E, Unemori EN, Lark MW, Amento E, Libby P. Cytokine-stimulated human vascular smooth muscle cells synthesize a complement of enzymes required for extracellular matrix digestion. *Circ Res* 1994; **75**: 181-189 [PMID: 8013077 DOI: 10.1161/01.RES.75.1.181]

35 **Lopes J**, Adiguzel E, Gu S, Liu SL, Hou G, Heximer S, Assoian RK, Bendeck MP. Type VIII collagen mediates vessel wall remodeling after arterial injury and fibrous cap formation in atherosclerosis. *Am J Pathol* 2013; **182**: 2241-2253 [PMID: 23567639 DOI: 10.1016/j.ajpath.2013.02.011]

36 **Jacobsen K**, Lund MB, Shim J, Gunnersen S, Füchtbauer EM, Kjolby M, Carramolino L, Bentzon JF. Diverse cellular architecture of atherosclerotic plaque derives from clonal expansion of a few medial SMCs. *JCI Insight* 2017; **2**: e95890 [PMID: 28978793 DOI: 10.1172/jci.insight.95890]

37 **Allahverdian S**, Chehroudi AC, McManus BM, Abraham T, Francis GA. Contribution of intimal smooth muscle cells to cholesterol accumulation and macrophage-like cells in human atherosclerosis. *Circulation* 2014; **129**: 1551-1559 [PMID: 24481950 DOI: 10.1161/CIRCULATIONAHA.113.005015]

38 **Ball RY**, Stowers EC, Burton JH, Cary NR, Skepper JN, Mitchinson MJ. Evidence that the death of macrophage foam cells contributes to the lipid core of atheroma. *Atherosclerosis* 1995; **114**: 45-54 [PMID: 7605375 DOI: 10.1016/0021-9150(94)05463-s]

39 **Hegyi L**, Skepper JN, Cary NR, Mitchinson MJ. Foam cell apoptosis and the development of the lipid core of human atherosclerosis. *J Pathol* 1996; **180**: 423-429 [PMID: 9014864 DOI: 10.1002/(SICI)1096-9896(199612)180:4<423::AID-PATH677>3.0.CO;2-1]

40 **Tabas I**. Free cholesterol-induced cytotoxicity a possible contributing factor to macrophage foam cell necrosis in advanced atherosclerotic lesions. *Trends Cardiovasc Med* 1997; **7**: 256-263 [PMID: 21235894 DOI: 10.1016/S1050-1738(97)00086-8]

41 **Seimon TA**, Nadolski MJ, Liao X, Magallon J, Nguyen M, Feric NT, Koschinsky ML, Harkewicz R, Witztum JL, Tsimikas S, Golenbock D, Moore KJ, Tabas I. Atherogenic lipids and lipoproteins trigger CD36-TLR2-dependent apoptosis in macrophages undergoing endoplasmic reticulum stress. *Cell Metab* 2010; **12**: 467-482 [PMID: 21035758 DOI: 10.1016/j.cmet.2010.09.010]

42 **Forsythe JA**, Jiang BH, Iyer NV, Agani F, Leung SW, Koos RD, Semenza GL. Activation of vascular endothelial growth factor gene transcription by hypoxia-inducible factor 1. *Mol Cell Biol* 1996; **16**: 4604-4613 [PMID: 8756616 DOI: 10.1128/mcb.16.9.4604]

43 **Sluimer JC**, Gasc JM, van Wanroij JL, Kisters N, Groeneweg M, Sollewijn Gelpke MD, Cleutjens JP, van den Akker LH, Corvol P, Wouters BG, Daemen MJ, Bijnens AP. Hypoxia, hypoxia-inducible transcription factor, and macrophages in human atherosclerotic plaques are correlated with intraplaque angiogenesis. *J Am Coll Cardiol* 2008; **51**: 1258-1265 [PMID: 18371555 DOI: 10.1016/j.jacc.2007.12.025]

44 **Parathath S**, Mick SL, Feig JE, Joaquin V, Grauer L, Habiel DM, Gassmann M, Gardner LB, Fisher EA. Hypoxia is present in murine atherosclerotic plaques and has multiple adverse effects on macrophage lipid metabolism. *Circ Res* 2011; **109**: 1141-1152 [PMID: 21921268 DOI: 10.1161/CIRCRESAHA.111.246363]

45 **Crucet M**, Wüst SJ, Spielmann P, Lüscher TF, Wenger RH, Matter CM. Hypoxia enhances lipid uptake in macrophages: role of the scavenger receptors Lox1, SRA, and CD36. *Atherosclerosis* 2013; **229**: 110-117 [PMID: 23706521 DOI: 10.1016/j.atherosclerosis.2013.04.034]

46 **Folco EJ**, Sukhova GK, Quillard T, Libby P. Moderate hypoxia potentiates interleukin-1β production in activated human macrophages. *Circ Res* 2014; **115**: 875-883 [PMID: 25185259 DOI: 10.1161/CIRCRESAHA.115.304437]

47 **Dalton DK**, Pitts-Meek S, Keshav S, Figari IS, Bradley A, Stewart TA. Multiple defects of immune cell function in mice with disrupted interferon-gamma genes. *Science* 1993; **259**: 1739-1742 [PMID: 8456300 DOI: 10.1126/science.8456300]

48 **Boldrick JC**, Alizadeh AA, Diehn M, Dudoit S, Liu CL, Belcher CE, Botstein D, Staudt LM, Brown PO, Relman DA. Stereotyped and specific gene expression programs in human innate immune responses to bacteria. *Proc Natl Acad Sci USA* 2002; **99**: 972-977 [PMID: 11805339 DOI: 10.1073/pnas.231625398]

49 **Verreck FA**, de Boer T, Langenberg DM, Hoeve MA, Kramer M, Vaisberg E, Kastelein R, Kolk A, de Waal-Malefyt R, Ottenhoff TH. Human IL-23-producing type 1 macrophages promote but IL-10-producing type 2 macrophages subvert immunity to (myco)bacteria. *Proc Natl Acad Sci USA* 2004; **101**: 4560-4565 [PMID: 15070757 DOI: 10.1073/pnas.0400983101]

50 **Deng Z**, Shi F, Zhou Z, Sun F, Sun MH, Sun Q, Chen L, Li D, Jiang CY, Zhao RZ, Cui D, Wang XJ, Jing YF, Xia SJ, Han BM. M1 macrophage mediated increased reactive oxygen species (ROS) influence wound healing via the MAPK signaling in vitro and in vivo. *Toxicol Appl Pharmacol* 2019; **366**: 83-95 [PMID: 30690042 DOI: 10.1016/j.taap.2019.01.022]

51 **Hirose K**, Iwabuchi K, Shimada K, Kiyanagi T, Iwahara C, Nakayama H, Daida H. Different responses to oxidized low-density lipoproteins in human polarized macrophages. *Lipids Health Dis* 2011; **10**: 1 [PMID:

21199582 DOI: 10.1186/1476-511X-10-1]
52 **van Tits LJ**, Stienstra R, van Lent PL, Netea MG, Joosten LA, Stalenhoef AF. Oxidized LDL enhances pro-inflammatory responses of alternatively activated M2 macrophages: a crucial role for Krüppel-like factor 2. *Atherosclerosis* 2011; **214**: 345-349 [PMID: 21167486 DOI: 10.1016/j.atherosclerosis.2010.11.018]
53 **Bae YS**, Lee JH, Choi SH, Kim S, Almazan F, Witztum JL, Miller YI. Macrophages generate reactive oxygen species in response to minimally oxidized low-density lipoprotein: toll-like receptor 4- and spleen tyrosine kinase-dependent activation of NADPH oxidase 2. *Circ Res* 2009; **104**: 210-218, 21p following 218 [PMID: 19096031 DOI: 10.1161/CIRCRESAHA.108.181040]
54 **Duewell P**, Kono H, Rayner KJ, Sirois CM, Vladimer G, Bauernfeind FG, Abela GS, Franchi L, Nuñez G, Schnurr M, Espevik T, Lien E, Fitzgerald KA, Rock KL, Moore KJ, Wright SD, Hornung V, Latz E. NLRP3 inflammasomes are required for atherogenesis and activated by cholesterol crystals. *Nature* 2010; **464**: 1357-1361 [PMID: 20428172 DOI: 10.1038/nature08938]
55 **Kang JH**, Kim JK, Park WH, Park KK, Lee TS, Magae J, Nakajima H, Kim CH, Chang YC. Ascochlorin suppresses oxLDL-induced MMP-9 expression by inhibiting the MEK/ERK signaling pathway in human THP-1 macrophages. *J Cell Biochem* 2007; **102**: 506-514 [PMID: 17407144 DOI: 10.1002/jcb.21312]
56 **Shao Q**, Shen LH, Hu LH, Pu J, Jing Q, He B. Atorvastatin suppresses inflammatory response induced by oxLDL through inhibition of ERK phosphorylation, IκBα degradation, and COX-2 expression in murine macrophages. *J Cell Biochem* 2012; **113**: 611-618 [PMID: 21956776 DOI: 10.1002/jcb.23388]
57 **Harkewicz R**, Hartvigsen K, Almazan F, Dennis EA, Witztum JL, Miller YI. Cholesteryl ester hydroperoxides are biologically active components of minimally oxidized low density lipoprotein. *J Biol Chem* 2008; **283**: 10241-10251 [PMID: 18263582 DOI: 10.1074/jbc.M709006200]
58 **Huang Z**, Li W, Wang R, Zhang F, Chi Y, Wang D, Liu Z, Zhang Y, Matsuura E, Liu Q. 7-ketocholesteryl-9-carboxynonanoate induced nuclear factor-kappa B activation in J774A.1 macrophages. *Life Sci* 2010; **87**: 651-657 [PMID: 20932850 DOI: 10.1016/j.lfs.2010.09.028]
59 **Stein M**, Keshav S, Harris N, Gordon S. Interleukin 4 potently enhances murine macrophage mannose receptor activity: a marker of alternative immunologic macrophage activation. *J Exp Med* 1992; **176**: 287-292 [PMID: 1613462 DOI: 10.1084/jem.176.1.287]
60 **Lee CG**, Homer RJ, Zhu Z, Lanone S, Wang X, Koteliansky V, Shipley JM, Gotwals P, Noble P, Chen Q, Senior RM, Elias JA. Interleukin-13 induces tissue fibrosis by selectively stimulating and activating transforming growth factor beta(1). *J Exp Med* 2001; **194**: 809-821 [PMID: 11560996 DOI: 10.1084/jem.194.6.809]
61 **Sironi M**, Martinez FO, D'Ambrosio D, Gattorno M, Polentarutti N, Locati M, Gregorio A, Iellem A, Cassatella MA, Van Damme J, Sozzani S, Martini A, Sinigaglia F, Vecchi A, Mantovani A. Differential regulation of chemokine production by Fcgamma receptor engagement in human monocytes: association of CCL1 with a distinct form of M2 monocyte activation (M2b, Type 2). *J Leukoc Biol* 2006; **80**: 342-349 [PMID: 16735693 DOI: 10.1189/jlb.1005586]
62 **Gerber JS**, Mosser DM. Reversing lipopolysaccharide toxicity by ligating the macrophage Fc gamma receptors. *J Immunol* 2001; **166**: 6861-6868 [PMID: 11359846 DOI: 10.4049/jimmunol.166.11.6861]
63 **Edwards JP**, Zhang X, Frauwirth KA, Mosser DM. Biochemical and functional characterization of three activated macrophage populations. *J Leukoc Biol* 2006; **80**: 1298-1307 [PMID: 16905575 DOI: 10.1189/jlb.0406249]
64 **Zizzo G**, Hilliard BA, Monestier M, Cohen PL. Efficient clearance of early apoptotic cells by human macrophages requires M2c polarization and MerTK induction. *J Immunol* 2012; **189**: 3508-3520 [PMID: 22942426 DOI: 10.4049/jimmunol.1200662]
65 **Zizzo G**, Cohen PL. IL-17 stimulates differentiation of human anti-inflammatory macrophages and phagocytosis of apoptotic neutrophils in response to IL-10 and glucocorticoids. *J Immunol* 2013; **190**: 5237-5246 [PMID: 23596310 DOI: 10.4049/jimmunol.1203017]
66 **Ferrante CJ**, Pinhal-Enfield G, Elson G, Cronstein BN, Hasko G, Outram S, Leibovich SJ. The adenosine-dependent angiogenic switch of macrophages to an M2-like phenotype is independent of interleukin-4 receptor alpha (IL-4Rα) signaling. *Inflammation* 2013; **36**: 921-931 [PMID: 23504259 DOI: 10.1007/s10753-013-9621-3]
67 **Pinhal-Enfield G**, Ramanathan M, Hasko G, Vogel SN, Salzman AL, Boons GJ, Leibovich SJ. An angiogenic switch in macrophages involving synergy between Toll-like receptors 2, 4, 7, and 9 and adenosine A(2A) receptors. *Am J Pathol* 2003; **163**: 711-721 [PMID: 12875990 DOI: 10.1016/S0002-9440(10)63698-X]
68 **Leonarduzzi G**, Sevanian A, Sottero B, Arkan MC, Biasi F, Chiarpotto E, Basaga H, Poli G. Up-regulation of the fibrogenic cytokine TGF-beta1 by oxysterols: a mechanistic link between cholesterol and atherosclerosis. *FASEB J* 2001; **15**: 1619-1621 [PMID: 11427505 DOI: 10.1096/fj.00-0668fje]
69 **Sottero B**, Gamba P, Longhi M, Robbesyn F, Abuja PM, Schaur RJ, Poli G, Leonarduzzi G. Expression and synthesis of TGFbeta1 is induced in macrophages by 9-oxononanoyl cholesterol, a major cholesteryl ester oxidation product. *Biofactors* 2005; **24**: 209-216 [PMID: 16403982 DOI: 10.1002/biof.5520240125]
70 **Rios FJ**, Koga MM, Pecenin M, Ferracini M, Gidlund M, Jancar S. Oxidized LDL induces alternative macrophage phenotype through activation of CD36 and PAFR. *Mediators Inflamm* 2013; **2013**: 198193 [PMID: 24062612 DOI: 10.1155/2013/198193]
71 **Seo JW**, Yang EJ, Yoo KH, Choi IH. Macrophage Differentiation from Monocytes Is Influenced by the Lipid Oxidation Degree of Low Density Lipoprotein. *Mediators Inflamm* 2015; **2015**: 235797 [PMID: 26294848 DOI: 10.1155/2015/235797]
72 **Kim K**, Shim D, Lee JS, Zaitsev K, Williams JW, Kim KW, Jang MY, Seok Jang H, Yun TJ, Lee SH, Yoon WK, Prat A, Seidah NG, Choi J, Lee SP, Yoon SH, Nam JW, Seong JK, Oh GT, Randolph GJ, Artyomov MN, Cheong C, Choi JH. Transcriptome Analysis Reveals Nonfoamy Rather Than Foamy Plaque Macrophages Are Proinflammatory in Atherosclerotic Murine Models. *Circ Res* 2018; **123**: 1127-1142 [PMID: 30359200 DOI: 10.1161/CIRCRESAHA.118.312804]
73 **Kadl A**, Meher AK, Sharma PR, Lee MY, Doran AC, Johnstone SR, Elliott MR, Gruber F, Han J, Chen W, Kensler T, Ravichandran KS, Isakson BE, Wamhoff BR, Leitinger N. Identification of a novel macrophage

phenotype that develops in response to atherogenic phospholipids via Nrf2. *Circ Res* 2010; **107**: 737-746 [PMID: 20651288 DOI: 10.1161/CIRCRESAHA.109.215715]
74 **Kadl A**, Galkina E, Leitinger N. Induction of CCR2-dependent macrophage accumulation by oxidized phospholipids in the air-pouch model of inflammation. *Arthritis Rheum* 2009; **60**: 1362-1371 [PMID: 19404946 DOI: 10.1002/art.24448]
75 **Kadl A**, Sharma PR, Chen W, Agrawal R, Meher AK, Rudraiah S, Grubbs N, Sharma R, Leitinger N. Oxidized phospholipid-induced inflammation is mediated by Toll-like receptor 2. *Free Radic Biol Med* 2011; **51**: 1903-1909 [PMID: 21925592 DOI: 10.1016/j.freeradbiomed.2011.08.026]
76 **Scheuerer B**, Ernst M, Dürrbaum-Landmann I, Fleischer J, Grage-Griebenow E, Brandt E, Flad HD, Petersen F. The CXC-chemokine platelet factor 4 promotes monocyte survival and induces monocyte differentiation into macrophages. *Blood* 2000; **95**: 1158-1166 [PMID: 10666185 DOI: 10.1182/blood.V95.4.1158.004k31_1158_1166]
77 **Finn AV**, Nakano M, Polavarapu R, Karmali V, Saeed O, Zhao X, Yazdani S, Otsuka F, Davis T, Habib A, Narula J, Kolodgie FD, Virmani R. Hemoglobin directs macrophage differentiation and prevents foam cell formation in human atherosclerotic plaques. *J Am Coll Cardiol* 2012; **59**: 166-177 [PMID: 22154776 DOI: 10.1016/j.jacc.2011.10.852]
78 **Boyle JJ**, Harrington HA, Piper E, Elderfield K, Stark J, Landis RC, Haskard DO. Coronary intraplaque hemorrhage evokes a novel atheroprotective macrophage phenotype. *Am J Pathol* 2009; **174**: 1097-1108 [PMID: 19234137 DOI: 10.2353/ajpath.2009.080431]
79 **Boyle JJ**, Johns M, Kampfer T, Nguyen AT, Game L, Schaer DJ, Mason JC, Haskard DO. Activating transcription factor 1 directs Mhem atheroprotective macrophages through coordinated iron handling and foam cell protection. *Circ Res* 2012; **110**: 20-33 [PMID: 22052915 DOI: 10.1161/CIRCRESAHA.111.247577]
80 **Howles PN**. Cholesterol Absorption and Metabolism. *Methods Mol Biol* 2016; **1438**: 177-197 [PMID: 27150091 DOI: 10.1007/978-1-4939-3661-8_11]
81 **Hadadi-Bechor S**, Haim Y, Pecht T, Gat R, Tarnovscki T, Gericke M, Rudich A. Autophagy differentially regulates macrophage lipid handling depending on the lipid substrate (oleic acid vs. acetylated-LDL) and inflammatory activation state. *Biochim Biophys Acta Mol Cell Biol Lipids* 2019; **1864**: 158527 [PMID: 31520777 DOI: 10.1016/j.bbalip.2019.158527]
82 **Chen W**, Chen G, Head DL, Mangelsdorf DJ, Russell DW. Enzymatic reduction of oxysterols impairs LXR signaling in cultured cells and the livers of mice. *Cell Metab* 2007; **5**: 73-79 [PMID: 17189208 DOI: 10.1016/j.cmet.2006.11.012]
83 **Zhao GJ**, Yin K, Fu YC, Tang CK. The interaction of ApoA-I and ABCA1 triggers signal transduction pathways to mediate efflux of cellular lipids. *Mol Med* 2012; **18**: 149-158 [PMID: 22064972 DOI: 10.2119/molmed.2011.00183]
84 **Yvan-Charvet L**, Wang N, Tall AR. Role of HDL, ABCA1, and ABCG1 transporters in cholesterol efflux and immune responses. *Arterioscler Thromb Vasc Biol* 2010; **30**: 139-143 [PMID: 19797709 DOI: 10.1161/ATVBAHA.108.179283]
85 **Pehkonen P**, Welter-Stahl L, Diwo J, Ryynänen J, Wienecke-Baldacchino A, Heikkinen S, Treuter E, Steffensen KR, Carlberg C. Genome-wide landscape of liver X receptor chromatin binding and gene regulation in human macrophages. *BMC Genomics* 2012; **13**: 50 [PMID: 22292898 DOI: 10.1186/1471-2164-13-50]
86 **Lee SD**, Tontonoz P. Liver X receptors at the intersection of lipid metabolism and atherogenesis. *Atherosclerosis* 2015; **242**: 29-36 [PMID: 26164157 DOI: 10.1016/j.atherosclerosis.2015.06.042]
87 **Schulman IG**. Liver X receptors link lipid metabolism and inflammation. *FEBS Lett* 2017; **591**: 2978-2991 [PMID: 28555747 DOI: 10.1002/1873-3468.12702]
88 **Fessler MB**. The challenges and promise of targeting the Liver X Receptors for treatment of inflammatory disease. *Pharmacol Ther* 2018; **181**: 1-12 [PMID: 28720427 DOI: 10.1016/j.pharmthera.2017.07.010]
89 **Eberlé D**, Hegarty B, Bossard P, Ferré P, Foufelle F. SREBP transcription factors: master regulators of lipid homeostasis. *Biochimie* 2004; **86**: 839-848 [PMID: 15589694 DOI: 10.1016/j.biochi.2004.09.018]
90 **Sato R**. Sterol metabolism and SREBP activation. *Arch Biochem Biophys* 2010; **501**: 177-181 [PMID: 20541520 DOI: 10.1016/j.abb.2010.06.004]
91 **Wang Y**, Rogers PM, Su C, Varga G, Stayrook KR, Burris TP. Regulation of cholesterologenesis by the oxysterol receptor, LXRalpha. *J Biol Chem* 2008; **283**: 26332-26339 [PMID: 18676367 DOI: 10.1074/jbc.M804808200]
92 **Traversari C**, Russo V. Control of the immune system by oxysterols and cancer development. *Curr Opin Pharmacol* 2012; **12**: 729-735 [PMID: 22832233 DOI: 10.1016/j.coph.2012.07.003]
93 **Guillemot-Legris O**, Mutemberezi V, Muccioli GG. Oxysterols in Metabolic Syndrome: From Bystander Molecules to Bioactive Lipids. *Trends Mol Med* 2016; **22**: 594-614 [PMID: 27286741 DOI: 10.1016/j.molmed.2016.05.006]
94 **Zhang L**, Reue K, Fong LG, Young SG, Tontonoz P. Feedback regulation of cholesterol uptake by the LXR-IDOL-LDLR axis. *Arterioscler Thromb Vasc Biol* 2012; **32**: 2541-2546 [PMID: 22936343 DOI: 10.1161/ATVBAHA.112.250571]
95 **Sorrentino V**, Zelcer N. Post-transcriptional regulation of lipoprotein receptors by the E3-ubiquitin ligase inducible degrader of the low-density lipoprotein receptor. *Curr Opin Lipidol* 2012; **23**: 213-219 [PMID: 22510808 DOI: 10.1097/MOL.0b013e3283532947]
96 **Tang C**, Houston BA, Storey C, LeBoeuf RC. Both STAT3 activation and cholesterol efflux contribute to the anti-inflammatory effect of apoA-I/ABCA1 interaction in macrophages. *J Lipid Res* 2016; **57**: 848-857 [PMID: 26989082 DOI: 10.1194/jlr.M065797]
97 **De Nardo D**, Labzin LI, Kono H, Seki R, Schmidt SV, Beyer M, Xu D, Zimmer S, Lahrmann C, Schildberg FA, Vogelhuber J, Kraut M, Ulas T, Kerksiek A, Krebs W, Bode N, Grebe A, Fitzgerald ML, Hernandez NJ, Williams BR, Knolle P, Kneilling M, Röcken M, Lütjohann D, Wright SD, Schultze JL, Latz E. High-density lipoprotein mediates anti-inflammatory reprogramming of macrophages via the transcriptional regulator ATF3. *Nat Immunol* 2014; **15**: 152-160 [PMID: 24317040 DOI: 10.1038/ni.2784]
98 **Fotakis P**, Kothari V, Thomas DG, Westerterp M, Molusky MM, Altin E, Abramowicz S, Wang N, He Y,

Heinecke JW, Bornfeldt KE, Tall AR. Anti-Inflammatory Effects of HDL (High-Density Lipoprotein) in Macrophages Predominate Over Proinflammatory Effects in Atherosclerotic Plaques. *Arterioscler Thromb Vasc Biol* 2019; **39**: e253-e272 [PMID: 31578081 DOI: 10.1161/ATVBAHA.119.313253]

99 **Azzam KM**, Fessler MB. Crosstalk between reverse cholesterol transport and innate immunity. *Trends Endocrinol Metab* 2012; **23**: 169-178 [PMID: 22406271 DOI: 10.1016/j.tem.2012.02.001]

100 **Fessler MB**, Parks JS. Intracellular lipid flux and membrane microdomains as organizing principles in inflammatory cell signaling. *J Immunol* 2011; **187**: 1529-1535 [PMID: 21810617 DOI: 10.4049/jimmunol.1100253]

101 **Röszer T**. Transcriptional control of apoptotic cell clearance by macrophage nuclear receptors. *Apoptosis* 2017; **22**: 284-294 [PMID: 27787652 DOI: 10.1007/s10495-016-1310-x]

102 **Zhao Q**, Zhou D, You H, Lou B, Zhang Y, Tian Y, Guo N, Chen X, Liu Y, Wu Y, Yuan Z, Zhou J. IFN-γ aggravates neointimal hyperplasia by inducing endoplasmic reticulum stress and apoptosis in macrophages by promoting ubiquitin-dependent liver X receptor-α degradation. *FASEB J* 2017; **31**: 5321-5331 [PMID: 28798155 DOI: 10.1096/fj.201700327R]

103 **Du HP**, Li J, You SJ, Wang YL, Wang F, Cao YJ, Hu LF, Liu CF. DNA methylation in cystathionine-γ-lyase (CSE) gene promoter induced by ox-LDL in macrophages and in apoE knockout mice. *Biochem Biophys Res Commun* 2016; **469**: 776-782 [PMID: 26692478 DOI: 10.1016/j.bbrc.2015.11.132]

104 **Chistiakov DA**, Orekhov AN, Bobryshev YV. Treatment of cardiovascular pathology with epigenetically active agents: Focus on natural and synthetic inhibitors of DNA methylation and histone deacetylation. *Int J Cardiol* 2017; **227**: 66-82 [PMID: 27852009 DOI: 10.1016/j.ijcard.2016.11.204]

105 **Wang X**, Wang S, Yao G, Yu D, Chen K, Tong Q, Ye L, Wu C, Sun Y, Li H, Hermann DM, Doeppner TR, Jin F, Dai Y, Wu J. Identification of the histone lysine demethylase KDM4A/JMJD2A as a novel epigenetic target in M1 macrophage polarization induced by oxidized LDL. *Oncotarget* 2017; **8**: 114442-114456 [PMID: 29383092 DOI: 10.18632/oncotarget.17748]

106 **Bekkering S**, Joosten LA, van der Meer JW, Netea MG, Riksen NP. The epigenetic memory of monocytes and macrophages as a novel drug target in atherosclerosis. *Clin Ther* 2015; **37**: 914-923 [PMID: 25704108 DOI: 10.1016/j.clinthera.2015.01.008]

107 **Shan K**, Jiang Q, Wang XQ, Wang YN, Yang H, Yao MD, Liu C, Li XM, Yao J, Liu B, Zhang YY, J Y, Yan B. Role of long non-coding RNA-RNCR3 in atherosclerosis-related vascular dysfunction. *Cell Death Dis* 2016; **7**: e2248 [PMID: 27253412 DOI: 10.1038/cddis.2016.145]

108 **Hu YW**, Zhao JY, Li SF, Huang JL, Qiu YR, Ma X, Wu SG, Chen ZP, Hu YR, Yang JY, Wang YC, Gao JJ, Sha YH, Zheng L, Wang Q. RP5-833A20.1/miR-382-5p/NFIA-dependent signal transduction pathway contributes to the regulation of cholesterol homeostasis and inflammatory reaction. *Arterioscler Thromb Vasc Biol* 2015; **35**: 87-101 [PMID: 25265644 DOI: 10.1161/ATVBAHA.114.304296]

109 **Giral H**, Kratzer A, Landmesser U. MicroRNAs in lipid metabolism and atherosclerosis. *Best Pract Res Clin Endocrinol Metab* 2016; **30**: 665-676 [PMID: 27923459 DOI: 10.1016/j.beem.2016.11.010]

110 **Rodriguez A**, Griffiths-Jones S, Ashurst JL, Bradley A. Identification of mammalian microRNA host genes and transcription units. *Genome Res* 2004; **14**: 1902-1910 [PMID: 15364901 DOI: 10.1101/gr.2722704]

111 **Baskerville S**, Bartel DP. Microarray profiling of microRNAs reveals frequent coexpression with neighboring miRNAs and host genes. *RNA* 2005; **11**: 241-247 [PMID: 15701730 DOI: 10.1261/rna.7240905]

112 **Lee Y**, Kim M, Han J, Yeom KH, Lee S, Baek SH, Kim VN. MicroRNA genes are transcribed by RNA polymerase II. *EMBO J* 2004; **23**: 4051-4060 [PMID: 15372072 DOI: 10.1038/sj.emboj.7600385]

113 **Borchert GM**, Lanier W, Davidson BL. RNA polymerase III transcribes human microRNAs. *Nat Struct Mol Biol* 2006; **13**: 1097-1101 [PMID: 17099701 DOI: 10.1038/nsmb1167]

114 **Monteys AM**, Spengler RM, Wan J, Tecedor L, Lennox KA, Xing Y, Davidson BL. Structure and activity of putative intronic miRNA promoters. *RNA* 2010; **16**: 495-505 [PMID: 20075166 DOI: 10.1261/rna.1731910]

115 **Ramalingam P**, Palanichamy JK, Singh A, Das P, Bhagat M, Kassab MA, Sinha S, Chattopadhyay P. Biogenesis of intronic miRNAs located in clusters by independent transcription and alternative splicing. *RNA* 2014; **20**: 76-87 [PMID: 24226766 DOI: 10.1261/rna.041814.113]

116 **Abdelfattah AM**, Park C, Choi MY. Update on non-canonical microRNAs. *Biomol Concepts* 2014; **5**: 275-287 [PMID: 25372759 DOI: 10.1515/bmc-2014-0012]

117 **Cai X**, Hagedorn CH, Cullen BR. Human microRNAs are processed from capped, polyadenylated transcripts that can also function as mRNAs. *RNA* 2004; **10**: 1957-1966 [PMID: 15525708 DOI: 10.1261/rna.7135204]

118 **Han J**, Lee Y, Yeom KH, Kim YK, Jin H, Kim VN. The Drosha-DGCR8 complex in primary microRNA processing. *Genes Dev* 2004; **18**: 3016-3027 [PMID: 15574589 DOI: 10.1101/gad.1262504]

119 **Alarcón CR**, Lee H, Goodarzi H, Halberg N, Tavazoie SF. N6-methyladenosine marks primary microRNAs for processing. *Nature* 2015; **519**: 482-485 [PMID: 25799998 DOI: 10.1038/nature14281]

120 **Yeom KH**, Lee Y, Han J, Suh MR, Kim VN. Characterization of DGCR8/Pasha, the essential cofactor for Drosha in primary miRNA processing. *Nucleic Acids Res* 2006; **34**: 4622-4629 [PMID: 16963499 DOI: 10.1093/nar/gkl458]

121 **Han J**, Lee Y, Yeom KH, Nam JW, Heo I, Rhee JK, Sohn SY, Cho Y, Zhang BT, Kim VN. Molecular basis for the recognition of primary microRNAs by the Drosha-DGCR8 complex. *Cell* 2006; **125**: 887-901 [PMID: 16751099 DOI: 10.1016/j.cell.2006.03.043]

122 **Lee Y**, Ahn C, Han J, Choi H, Kim J, Yim J, Lee J, Provost P, Rådmark O, Kim S, Kim VN. The nuclear RNase III Drosha initiates microRNA processing. *Nature* 2003; **425**: 415-419 [PMID: 14508493 DOI: 10.1038/nature01957]

123 **Bohnsack MT**, Czaplinski K, Gorlich D. Exportin 5 is a RanGTP-dependent dsRNA-binding protein that mediates nuclear export of pre-miRNAs. *RNA* 2004; **10**: 185-191 [PMID: 14730017 DOI: 10.1261/rna.5167604]

124 **Zeng Y**, Cullen BR. Structural requirements for pre-microRNA binding and nuclear export by Exportin 5. *Nucleic Acids Res* 2004; **32**: 4776-4785 [PMID: 15356295 DOI: 10.1093/nar/gkh824]

125 **Wang X**, Xu X, Ma Z, Huo Y, Xiao Z, Li Y, Wang Y. Dynamic mechanisms for pre-miRNA binding and

export by Exportin-5. *RNA* 2011; **17**: 1511-1528 [PMID: 21712399 DOI: 10.1261/rna.2732611]
126 **Hutvágner G**, McLachlan J, Pasquinelli AE, Bálint E, Tuschl T, Zamore PD. A cellular function for the RNA-interference enzyme Dicer in the maturation of the let-7 small temporal RNA. *Science* 2001; **293**: 834-838 [PMID: 11452083 DOI: 10.1126/science.1062961]
127 **Zhang H**, Kolb FA, Jaskiewicz L, Westhof E, Filipowicz W. Single processing center models for human Dicer and bacterial RNase III. *Cell* 2004; **118**: 57-68 [PMID: 15242644 DOI: 10.1016/j.cell.2004.06.017]
128 **Yoda M**, Kawamata T, Paroo Z, Ye X, Iwasaki S, Liu Q, Tomari Y. ATP-dependent human RISC assembly pathways. *Nat Struct Mol Biol* 2010; **17**: 17-23 [PMID: 19966796 DOI: 10.1038/nsmb.1733]
129 **Gregory RI**, Chendrimada TP, Cooch N, Shiekhattar R. Human RISC couples microRNA biogenesis and posttranscriptional gene silencing. *Cell* 2005; **123**: 631-640 [PMID: 16271387 DOI: 10.1016/j.cell.2005.10.022]
130 **Lewis BP**, Shih IH, Jones-Rhoades MW, Bartel DP, Burge CB. Prediction of mammalian microRNA targets. *Cell* 2003; **115**: 787-798 [PMID: 14697198 DOI: 10.1016/s0092-8674(03)01018-3]
131 **Lewis BP**, Burge CB, Bartel DP. Conserved seed pairing, often flanked by adenosines, indicates that thousands of human genes are microRNA targets. *Cell* 2005; **120**: 15-20 [PMID: 15652477 DOI: 10.1016/j.cell.2004.12.035]
132 **Grimson A**, Farh KK, Johnston WK, Garrett-Engele P, Lim LP, Bartel DP. MicroRNA targeting specificity in mammals: determinants beyond seed pairing. *Mol Cell* 2007; **27**: 91-105 [PMID: 17612493 DOI: 10.1016/j.molcel.2007.06.017]
133 **Moore MJ**, Scheel TK, Luna JM, Park CY, Fak JJ, Nishiuchi E, Rice CM, Darnell RB. miRNA-target chimeras reveal miRNA 3'-end pairing as a major determinant of Argonaute target specificity. *Nat Commun* 2015; **6**: 8864 [PMID: 26602609 DOI: 10.1038/ncomms9864]
134 **Guo H**, Ingolia NT, Weissman JS, Bartel DP. Mammalian microRNAs predominantly act to decrease target mRNA levels. *Nature* 2010; **466**: 835-840 [PMID: 20703300 DOI: 10.1038/nature09267]
135 **Wu L**, Fan J, Belasco JG. MicroRNAs direct rapid deadenylation of mRNA. *Proc Natl Acad Sci USA* 2006; **103**: 4034-4039 [PMID: 16495412 DOI: 10.1073/pnas.0510928103]
136 **Benhamed M**, Herbig U, Ye T, Dejean A, Bischof O. Senescence is an endogenous trigger for microRNA-directed transcriptional gene silencing in human cells. *Nat Cell Biol* 2012; **14**: 266-275 [PMID: 22366686 DOI: 10.1038/ncb2443]
137 **Friedman RC**, Farh KK, Burge CB, Bartel DP. Most mammalian mRNAs are conserved targets of microRNAs. *Genome Res* 2009; **19**: 92-105 [PMID: 18955434 DOI: 10.1101/gr.082701.108]
138 **Bushati N**, Cohen SM. microRNA functions. *Annu Rev Cell Dev Biol* 2007; **23**: 175-205 [PMID: 17506695 DOI: 10.1146/annurev.cellbio.23.090506.123406]
139 **Deng Q**, Hu H, Yu X, Liu S, Wang L, Chen W, Zhang C, Zeng Z, Cao Y, Xu-Monette ZY, Li L, Zhang M, Rosenfeld S, Bao S, Hsi E, Young KH, Lu Z, Li Y. Tissue-specific microRNA expression alters cancer susceptibility conferred by a TP53 noncoding variant. *Nat Commun* 2019; **10**: 5061 [PMID: 31699989 DOI: 10.1038/s41467-019-13002-x]
140 **Schulte C**, Zeller T. microRNA-based diagnostics and therapy in cardiovascular disease-Summing up the facts. *Cardiovasc Diagn Ther* 2015; **5**: 17-36 [PMID: 25774345 DOI: 10.3978/j.issn.2223-3652.2014.12.03]
141 **Genemaras AA**, Ennis H, Kaplan L, Huang CY. Inflammatory cytokines induce specific time- and concentration-dependent MicroRNA release by chondrocytes, synoviocytes, and meniscus cells. *J Orthop Res* 2016; **34**: 779-790 [PMID: 26505891 DOI: 10.1002/jor.23086]
142 **De Rosa R**, De Rosa S, Leistner D, Boeckel JN, Keller T, Fichtlscherer S, Dimmeler S, Zeiher AM. Transcoronary Concentration Gradient of microRNA-133a and Outcome in Patients With Coronary Artery Disease. *Am J Cardiol* 2017; **120**: 15-24 [PMID: 28511772 DOI: 10.1016/j.amjcard.2017.03.264]
143 **Arroyo JD**, Chevillet JR, Kroh EM, Ruf IK, Pritchard CC, Gibson DF, Mitchell PS, Bennett CF, Pogosova-Agadjanyan EL, Stirewalt DL, Tait JF, Tewari M. Argonaute2 complexes carry a population of circulating microRNAs independent of vesicles in human plasma. *Proc Natl Acad Sci USA* 2011; **108**: 5003-5008 [PMID: 21383194 DOI: 10.1073/pnas.1019055108]
144 **Turchinovich A**, Weiz L, Langheinz A, Burwinkel B. Characterization of extracellular circulating microRNA. *Nucleic Acids Res* 2011; **39**: 7223-7233 [PMID: 21609964 DOI: 10.1093/nar/gkr254]
145 **Wang K**, Zhang S, Weber J, Baxter D, Galas DJ. Export of microRNAs and microRNA-protective protein by mammalian cells. *Nucleic Acids Res* 2010; **38**: 7248-7259 [PMID: 20615901 DOI: 10.1093/nar/gkq601]
146 **Kapustin AN**, Chatrou ML, Drozdov I, Zheng Y, Davidson SM, Soong D, Furmanik M, Sanchis P, De Rosales RT, Alvarez-Hernandez D, Shroff R, Yin X, Muller K, Skepper JN, Mayr M, Reutelingsperger CP, Chester A, Bertazzo S, Schurgers LJ, Shanahan CM. Vascular smooth muscle cell calcification is mediated by regulated exosome secretion. *Circ Res* 2015; **116**: 1312-1323 [PMID: 25711438 DOI: 10.1161/CIRCRESAHA.116.305012]
147 **Li L**, Zhu D, Huang L, Zhang J, Bian Z, Chen X, Liu Y, Zhang CY, Zen K. Argonaute 2 complexes selectively protect the circulating microRNAs in cell-secreted microvesicles. *PLoS One* 2012; **7**: e46957 [PMID: 23077538 DOI: 10.1371/journal.pone.0046957]
148 **Vickers KC**, Palmisano BT, Shoucri BM, Shamburek RD, Remaley AT. MicroRNAs are transported in plasma and delivered to recipient cells by high-density lipoproteins. *Nat Cell Biol* 2011; **13**: 423-433 [PMID: 21423178 DOI: 10.1038/ncb2210]
149 **Parahuleva MS**, Lipps C, Parviz B, Hölschermann H, Schieffer B, Schulz R, Euler G. MicroRNA expression profile of human advanced coronary atherosclerotic plaques. *Sci Rep* 2018; **8**: 7823 [PMID: 29777114 DOI: 10.1038/s41598-018-25690-4]
150 **Zhu JJ**, Liu YF, Zhang YP, Zhao CR, Yao WJ, Li YS, Wang KC, Huang TS, Pang W, Wang XF, Wang X, Chien S, Zhou J. VAMP3 and SNAP23 mediate the disturbed flow-induced endothelial microRNA secretion and smooth muscle hyperplasia. *Proc Natl Acad Sci USA* 2017; **114**: 8271-8276 [PMID: 28716920 DOI: 10.1073/pnas.1700561114]
151 **Tabet F**, Vickers KC, Cuesta Torres LF, Wiese CB, Shoucri BM, Lambert G, Catherinet C, Prado-Lourenco L, Levin MG, Thacker S, Sethupathy P, Barter PJ, Remaley AT, Rye KA. HDL-transferred microRNA-223 regulates ICAM-1 expression in endothelial cells. *Nat Commun* 2014; **5**: 3292 [PMID:

24576947 DOI: 10.1038/ncomms4292]
152 **Najafi-Shoushtari SH**, Kristo F, Li Y, Shioda T, Cohen DE, Gerszten RE, Näär AM. MicroRNA-33 and the SREBP host genes cooperate to control cholesterol homeostasis. *Science* 2010; **328**: 1566-1569 [PMID: 20466882 DOI: 10.1126/science.1189123]
153 **Ouimet M**, Ediriweera H, Afonso MS, Ramkhelawon B, Singaravelu R, Liao X, Bandler RC, Rahman K, Fisher EA, Rayner KJ, Pezacki JP, Tabas I, Moore KJ. microRNA-33 Regulates Macrophage Autophagy in Atherosclerosis. *Arterioscler Thromb Vasc Biol* 2017; **37**: 1058-1067 [PMID: 28428217 DOI: 10.1161/ATVBAHA.116.308916]
154 **Karunakaran D**, Thrush AB, Nguyen MA, Richards L, Geoffrion M, Singaravelu R, Ramphos E, Shangari P, Ouimet M, Pezacki JP, Moore KJ, Perisic L, Maegdefessel L, Hedin U, Harper ME, Rayner KJ. Macrophage Mitochondrial Energy Status Regulates Cholesterol Efflux and Is Enhanced by Anti-miR33 in Atherosclerosis. *Circ Res* 2015; **117**: 266-278 [PMID: 26002865 DOI: 10.1161/CIRCRESAHA.117.305624]
155 **Wang YS**, Hsi E, Cheng HY, Hsu SH, Liao YC, Juo SH. Let-7g suppresses both canonical and non-canonical NF-κB pathways in macrophages leading to anti-atherosclerosis. *Oncotarget* 2017; **8**: 101026-101041 [PMID: 29254143 DOI: 10.18632/oncotarget.18197]
156 **Li CH**, Gong D, Chen LY, Zhang M, Xia XD, Cheng HP, Huang C, Zhao ZW, Zheng XL, Tang XE, Tang CK. Puerarin promotes ABCA1-mediated cholesterol efflux and decreases cellular lipid accumulation in THP-1 macrophages. *Eur J Pharmacol* 2017; **811**: 74-86 [PMID: 28576406 DOI: 10.1016/j.ejphar.2017.05.055]
157 **Xu J**, Hu G, Lu M, Xiong Y, Li Q, Chang CC, Song B, Chang T, Li B. MiR-9 reduces human acyl-coenzyme A:cholesterol acyltransferase-1 to decrease THP-1 macrophage-derived foam cell formation. *Acta Biochim Biophys Sin (Shanghai)* 2013; **45**: 953-962 [PMID: 24028971 DOI: 10.1093/abbs/gmt096]
158 **Wei Y**, Corbalán-Campos J, Gurung R, Natarelli L, Zhu M, Exner N, Erhard F, Greulich F, Geißler C, Uhlenhaut NH, Zimmer R, Schober A. Dicer in Macrophages Prevents Atherosclerosis by Promoting Mitochondrial Oxidative Metabolism. *Circulation* 2018; **138**: 2007-2020 [PMID: 29748186 DOI: 10.1161/CIRCULATIONAHA.117.031589]
159 **Liang X**, Xu Z, Yuan M, Zhang Y, Zhao B, Wang J, Zhang A, Li G. MicroRNA-16 suppresses the activation of inflammatory macrophages in atherosclerosis by targeting PDCD4. *Int J Mol Med* 2016; **37**: 967-975 [PMID: 26936421 DOI: 10.3892/ijmm.2016.2497]
160 **Huang C**, Yu XH, Zheng XL, Ou X, Tang CK. Interferon-stimulated gene 15 promotes cholesterol efflux by activating autophagy via the miR-17-5p/Beclin-1 pathway in THP-1 macrophage-derived foam cells. *Eur J Pharmacol* 2018; **827**: 13-21 [PMID: 29518394 DOI: 10.1016/j.ejphar.2018.02.042]
161 **Chen H**, Li X, Liu S, Gu L, Zhou X. MircroRNA-19a promotes vascular inflammation and foam cell formation by targeting HBP-1 in atherogenesis. *Sci Rep* 2017; **7**: 12089 [PMID: 28935967 DOI: 10.1038/s41598-017-12167-z]
162 **Lv YC**, Tang YY, Peng J, Zhao GJ, Yang J, Yao F, Ouyang XP, He PP, Xie W, Tan YL, Zhang M, Liu D, Tang DP, Cayabyab FS, Zheng XL, Zhang DW, Tian GP, Tang CK. MicroRNA-19b promotes macrophage cholesterol accumulation and aortic atherosclerosis by targeting ATP-binding cassette transporter A1. *Atherosclerosis* 2014; **236**: 215-226 [PMID: 25084135 DOI: 10.1016/j.atherosclerosis.2014.07.005]
163 **Lv YC**, Yang J, Yao F, Xie W, Tang YY, Ouyang XP, He PP, Tan YL, Li L, Zhang M, Liu D, Cayabyab FS, Zheng XL, Tang CK. Diosgenin inhibits atherosclerosis via suppressing the MiR-19b-induced downregulation of ATP-binding cassette transporter A1. *Atherosclerosis* 2015; **240**: 80-89 [PMID: 25765596 DOI: 10.1016/j.atherosclerosis.2015.02.044]
164 **Liang B**, Wang X, Song X, Bai R, Yang H, Yang Z, Xiao C, Bian Y. MicroRNA-20a/b regulates cholesterol efflux through post-transcriptional repression of ATP-binding cassette transporter A1. *Biochim Biophys Acta Mol Cell Biol Lipids* 2017; **1862**: 929-938 [PMID: 28602962 DOI: 10.1016/j.bbalip.2017.06.002]
165 **Feng J**, Li A, Deng J, Yang Y, Dang L, Ye Y, Li Y, Zhang W. miR-21 attenuates lipopolysaccharide-induced lipid accumulation and inflammatory response: potential role in cerebrovascular disease. *Lipids Health Dis* 2014; **13**: 27 [PMID: 24502419 DOI: 10.1186/1476-511X-13-27]
166 **Canfrán-Duque A**, Rotllan N, Zhang X, Fernández-Fuertes M, Ramírez-Hidalgo C, Araldi E, Daimiel L, Busto R, Fernández-Hernando C, Suárez Y. Macrophage deficiency of miR-21 promotes apoptosis, plaque necrosis, and vascular inflammation during atherogenesis. *EMBO Mol Med* 2017; **9**: 1244-1262 [PMID: 28674080 DOI: 10.15252/emmm.201607492]
167 **Yang S**, Ye ZM, Chen S, Luo XY, Chen SL, Mao L, Li Y, Jin H, Yu C, Xiang FX, Xie MX, Chang J, Xia YP, Hu B. MicroRNA-23a-5p promotes atherosclerotic plaque progression and vulnerability by repressing ATP-binding cassette transporter A1/G1 in macrophages. *J Mol Cell Cardiol* 2018; **123**: 139-149 [PMID: 30227118 DOI: 10.1016/j.yjmcc.2018.09.004]
168 **Di Gregoli K**, Jenkins N, Salter R, White S, Newby AC, Johnson JL. MicroRNA-24 regulates macrophage behavior and retards atherosclerosis. *Arterioscler Thromb Vasc Biol* 2014; **34**: 1990-2000 [PMID: 24990232 DOI: 10.1161/ATVBAHA.114.304088]
169 **Zhang M**, Wu JF, Chen WJ, Tang SL, Mo ZC, Tang YY, Li Y, Wang JL, Liu XY, Peng J, Chen K, He PP, Lv YC, Ouyang XP, Yao F, Tang DP, Cayabyab FS, Zhang DW, Zheng XL, Tian GP, Tang CK. MicroRNA-27a/b regulates cellular cholesterol efflux, influx and esterification/hydrolysis in THP-1 macrophages. *Atherosclerosis* 2014; **234**: 54-64 [PMID: 24608080 DOI: 10.1016/j.atherosclerosis.2014.02.008]
170 **Li X**, Feng S, Luo Y, Long K, Lin Z, Ma J, Jiang A, Jin L, Tang Q, Li M, Wang X. Expression profiles of microRNAs in oxidized low-density lipoprotein-stimulated RAW 264.7 cells. *In Vitro Cell Dev Biol Anim* 2018; **54**: 99-110 [PMID: 29322359 DOI: 10.1007/s11626-017-0225-3]
171 **Ceolotto G**, Giannella A, Albiero M, Kuppusamy M, Radu C, Simioni P, Garlaschelli K, Baragetti A, Catapano AL, Iori E, Fadini GP, Avogaro A, Vigili de Kreutzenberg S. miR-30c-5p regulates macrophage-mediated inflammation and pro-atherosclerosis pathways. *Cardiovasc Res* 2017; **113**: 1627-1638 [PMID: 29016810 DOI: 10.1093/cvr/cvx157]
172 **Zhao GJ**, Mo ZC, Tang SL, Ouyang XP, He PP, Lv YC, Yao F, Tan YL, Xie W, Shi JF, Wang Y, Zhang

M, Liu D, Tang DP, Zheng XL, Tian GP, Tang CK. Chlamydia pneumoniae negatively regulates ABCA1 expression via TLR2-Nuclear factor-kappa B and miR-33 pathways in THP-1 macrophage-derived foam cells. *Atherosclerosis* 2014; **235**: 519-525 [PMID: 24953492 DOI: 10.1016/j.atherosclerosis.2014.05.943]

173 **Gao JH**, Zeng MY, Yu XH, Zeng GF, He LH, Zheng XL, Zhang DW, Ouyang XP, Tang CK. Visceral adipose tissue-derived serine protease inhibitor accelerates cholesterol efflux by up-regulating ABCA1 expression via the NF-κB/miR-33a pathway in THP-1 macropahge-derived foam cells. *Biochem Biophys Res Commun* 2018; **500**: 318-324 [PMID: 29653102 DOI: 10.1016/j.bbrc.2018.04.066]

174 **Kim SH**, Kim GJ, Umemura T, Lee SG, Cho KJ. Aberrant expression of plasma microRNA-33a in an atherosclerosis-risk group. *Mol Biol Rep* 2017; **44**: 79-88 [PMID: 27664032 DOI: 10.1007/s11033-016-4082-z]

175 **Zhao Q**, Li S, Li N, Yang X, Ma S, Yang A, Zhang H, Yang S, Mao C, Xu L, Gao T, Yang X, Zhang H, Jiang Y. miR-34a Targets HDAC1-Regulated H3K9 Acetylation on Lipid Accumulation Induced by Homocysteine in Foam Cells. *J Cell Biochem* 2017; **118**: 4617-4627 [PMID: 28485501 DOI: 10.1002/jcb.26126]

176 **Dai Y**, Wu X, Dai D, Li J, Mehta JL. MicroRNA-98 regulates foam cell formation and lipid accumulation through repression of LOX-1. *Redox Biol* 2018; **16**: 255-262 [PMID: 29549823 DOI: 10.1016/j.redox.2018.03.003]

177 **Hueso M**, De Ramon L, Navarro E, Ripoll E, Cruzado JM, Grinyo JM, Torras J. Silencing of CD40 in vivo reduces progression of experimental atherogenesis through an NF-κB/miR-125b axis and reveals new potential mediators in the pathogenesis of atherosclerosis. *Atherosclerosis* 2016; **255**: 80-89 [PMID: 27835742 DOI: 10.1016/j.atherosclerosis.2016.11.002]

178 **Chen T**, Huang Z, Wang L, Wang Y, Wu F, Meng S, Wang C. MicroRNA-125a-5p partly regulates the inflammatory response, lipid uptake, and ORP9 expression in oxLDL-stimulated monocyte/macrophages. *Cardiovasc Res* 2009; **83**: 131-139 [PMID: 19377067 DOI: 10.1093/cvr/cvp121]

179 **Peng XP**, Huang L, Liu ZH. miRNA-133a attenuates lipid accumulation via TR4-CD36 pathway in macrophages. *Biochimie* 2016; **127**: 79-85 [PMID: 27109382 DOI: 10.1016/j.biochi.2016.04.012]

180 **Lan G**, Xie W, Li L, Zhang M, Liu D, Tan YL, Cheng HP, Gong D, Huang C, Zheng XL, Yin WD, Tang CK. MicroRNA-134 actives lipoprotein lipase-mediated lipid accumulation and inflammatory response by targeting angiopoietin-like 4 in THP-1 macrophages. *Biochem Biophys Res Commun* 2016; **472**: 410-417 [PMID: 26546816 DOI: 10.1016/j.bbrc.2015.10.158]

181 **Ye Q**, Tian GP, Cheng HP, Zhang X, Ou X, Yu XH, Tan RQ, Yang FY, Gong D, Huang C, Pan YJ, Zhang J, Chen LY, Zhao ZW, Xie W, Li L, Zhang M, Xia XD, Zheng XL, Tang CK. MicroRNA-134 Promotes the Development of Atherosclerosis Via the ANGPTL4/LPL Pathway in Apolipoprotein E Knockout Mice. *J Atheroscler Thromb* 2018; **25**: 244-253 [PMID: 28867683 DOI: 10.5551/jat.40212]

182 **Ramírez CM**, Rotllan N, Vlassov AV, Dávalos A, Li M, Goedeke L, Aranda JF, Cirera-Salinas D, Araldi E, Salerno A, Wanschel A, Zavadil J, Castrillo A, Kim J, Suárez Y, Fernández-Hernando C. Control of cholesterol metabolism and plasma high-density lipoprotein levels by microRNA-144. *Circ Res* 2013; **112**: 1592-1601 [PMID: 23519695 DOI: 10.1161/CIRCRESAHA.112.300626]

183 **Hu YW**, Hu YR, Zhao JY, Li SF, Ma X, Wu SG, Lu JB, Qiu YR, Sha YH, Wang YC, Gao JJ, Zheng L, Wang Q. An agomir of miR-144-3p accelerates plaque formation through impairing reverse cholesterol transport and promoting pro-inflammatory cytokine production. *PLoS One* 2014; **9**: e94997 [PMID: 24733347 DOI: 10.1371/journal.pone.0094997]

184 **Li K**, Ching D, Luk FS, Raffai RL. Apolipoprotein E enhances microRNA-146a in monocytes and macrophages to suppress nuclear factor-κB-driven inflammation and atherosclerosis. *Circ Res* 2015; **117**: e1-e11 [PMID: 25904598 DOI: 10.1161/CIRCRESAHA.117.305844]

185 **Lin N**, An Y. Blockade of 146b-5p promotes inflammation in atherosclerosis-associated foam cell formation by targeting TRAF6. *Exp Ther Med* 2017; **14**: 5087-5092 [PMID: 29201219 DOI: 10.3892/etm.2017.5121]

186 **Yang A**, Sun Y, Gao Y, Yang S, Mao C, Ding N, Deng M, Wang Y, Yang X, Jia Y, Zhang H, Jiang Y. Reciprocal Regulation Between miR-148a/152 and DNA Methyltransferase 1 Is Associated with Hyperhomocysteinemia-Accelerated Atherosclerosis. *DNA Cell Biol* 2017; **36**: 462-474 [PMID: 28472596 DOI: 10.1089/dna.2017.3651]

187 **Li J**, Zhang S. microRNA-150 inhibits the formation of macrophage foam cells through targeting adiponectin receptor 2. *Biochem Biophys Res Commun* 2016; **476**: 218-224 [PMID: 27216461 DOI: 10.1016/j.bbrc.2016.05.096]

188 **Tian FJ**, An LN, Wang GK, Zhu JQ, Li Q, Zhang YY, Zeng A, Zou J, Zhu RF, Han XS, Shen N, Yang HT, Zhao XX, Huang S, Qin YW, Jing Q. Elevated microRNA-155 promotes foam cell formation by targeting HBP1 in atherogenesis. *Cardiovasc Res* 2014; **103**: 100-110 [PMID: 24675724 DOI: 10.1093/cvr/cvu070]

189 **Li X**, Kong D, Chen H, Liu S, Hu H, Wu T, Wang J, Chen W, Ning Y, Li Y, Lu Z. miR-155 acts as an anti-inflammatory factor in atherosclerosis-associated foam cell formation by repressing calcium-regulated heat stable protein 1. *Sci Rep* 2016; **6**: 21789 [PMID: 26899994 DOI: 10.1038/srep21789]

190 **Zhang F**, Zhao J, Sun D, Wei N. MiR-155 inhibits transformation of macrophages into foam cells via regulating CEH expression. *Biomed Pharmacother* 2018; **104**: 645-651 [PMID: 29803178 DOI: 10.1016/j.biopha.2018.05.068]

191 **Song J**, Yang S, Yin R, Xiao Q, Ma A, Pan X. MicroRNA-181a regulates the activation of the NLRP3 inflammatory pathway by targeting MEK1 in THP-1 macrophages stimulated by ox-LDL. *J Cell Biochem* 2019; **120**: 13640-13650 [PMID: 30938884 DOI: 10.1002/jcb.28637]

192 **Du XJ**, Lu JM, Sha Y. MiR-181a inhibits vascular inflammation induced by ox-LDL via targeting TLR4 in human macrophages. *J Cell Physiol* 2018; **233**: 6996-7003 [PMID: 29737518 DOI: 10.1002/jcp.26622]

193 **Zhang XF**, Yang Y, Yang XY, Tong Q. MiR-188-3p upregulation results in the inhibition of macrophage proinflammatory activities and atherosclerosis in ApoE-deficient mice. *Thromb Res* 2018; **171**: 55-61 [PMID: 30253270 DOI: 10.1016/j.thromres.2018.09.043]

194 **Miao H**, Zeng H, Gong H. microRNA-212 promotes lipid accumulation and attenuates cholesterol efflux in THP-1 human macrophages by targeting SIRT1. *Gene* 2018; **643**: 55-60 [PMID: 29174964 DOI: 10.1016/j.gene.2017.11.058]

195 **Gong D**, Cheng HP, Xie W, Zhang M, Liu D, Lan G, Huang C, Zhao ZW, Chen LY, Yao F, Tan YL, Li L, Xia XD, Zheng XL, Wang ZB, Tang CK. Cystathionine γ-lyase(CSE)/hydrogen sulfide system is regulated by miR-216a and influences cholesterol efflux in macrophages via the PI3K/AKT/ABCA1 pathway. *Biochem Biophys Res Commun* 2016; **470**: 107-116 [PMID: 26772887 DOI: 10.1016/j.bbrc.2016.01.003]

196 **Liu H**, Li X, Song Y, Wang Z. MicroRNA-217 attenuates intima-media complex thickness of ascending aorta measured by ultrasound bio-microscopy and inhibits inflammation and lipid metabolism in atherosclerotic models of ApoE$^{-/-}$ mice. *Lipids Health Dis* 2018; **17**: 170 [PMID: 30041636 DOI: 10.1186/s12944-018-0825-2]

197 **Zhuang X**, Li R, Maimaitijiang A, Liu R, Yan F, Hu H, Gao X, Shi H. miR-221-3p inhibits oxidized low-density lipoprotein induced oxidative stress and apoptosis via targeting a disintegrin and metalloprotease-22. *J Cell Biochem* 2019; **120**: 6304-6314 [PMID: 30362166 DOI: 10.1002/jcb.27917]

198 **Wang J**, Bai X, Song Q, Fan F, Hu Z, Cheng G, Zhang Y. miR-223 Inhibits Lipid Deposition and Inflammation by Suppressing Toll-Like Receptor 4 Signaling in Macrophages. *Int J Mol Sci* 2015; **16**: 24965-24982 [PMID: 26492242 DOI: 10.3390/ijms161024965]

199 **Meiler S**, Baumer Y, Toulmin E, Seng K, Boisvert WA. MicroRNA 302a is a novel modulator of cholesterol homeostasis and atherosclerosis. *Arterioscler Thromb Vasc Biol* 2015; **35**: 323-331 [PMID: 25524771 DOI: 10.1161/ATVBAHA.114.304878]

200 **Zhang X**, Ye Q, Gong D, Lv Y, Cheng H, Huang C, Chen L, Zhao Z, Li L, Wei X, Zhang M, Xia X, Yu X, Zheng X, Wang S, Wang Z, Tang C. Apelin-13 inhibits lipoprotein lipase expression via the APJ/PKCα/miR-361-5p signaling pathway in THP-1 macrophage-derived foam cells. *Acta Biochim Biophys Sin (Shanghai)* 2017; **49**: 530-540 [PMID: 28444107 DOI: 10.1093/abbs/gmx038]

201 **Wang D**, Yan X, Xia M, Yang Y, Li D, Li X, Song F, Ling W. Coenzyme Q10 promotes macrophage cholesterol efflux by regulation of the activator protein-1/miR-378/ATP-binding cassette transporter G1-signaling pathway. *Arterioscler Thromb Vasc Biol* 2014; **34**: 1860-1870 [PMID: 24675662 DOI: 10.1161/ATVBAHA.113.302879]

202 **Liu D**, Zhang M, Xie W, Lan G, Cheng HP, Gong D, Huang C, Lv YC, Yao F, Tan YL, Li L, Zheng XL, Tang CK. MiR-486 regulates cholesterol efflux by targeting HAT1. *Biochem Biophys Res Commun* 2016; **472**: 418-424 [PMID: 26654953 DOI: 10.1016/j.bbrc.2015.11.128]

203 **Cui J**, Ren Z, Zou W, Jiang Y. miR-497 accelerates oxidized low-density lipoprotein-induced lipid accumulation in macrophages by repressing the expression of apelin. *Cell Biol Int* 2017; **41**: 1012-1019 [PMID: 28653788 DOI: 10.1002/cbin.10808]

204 **Li BR**, Xia LQ, Liu J, Liao LL, Zhang Y, Deng M, Zhong HJ, Feng TT, He PP, Ouyang XP. miR-758-5p regulates cholesterol uptake via targeting the CD36 3'UTR. *Biochem Biophys Res Commun* 2017; **494**: 384-389 [PMID: 28965954 DOI: 10.1016/j.bbrc.2017.09.150]

205 **Stahlhut C**, Slack FJ. Combinatorial Action of MicroRNAs let-7 and miR-34 Effectively Synergizes with Erlotinib to Suppress Non-small Cell Lung Cancer Cell Proliferation. *Cell Cycle* 2015; **14**: 2171-2180 [PMID: 25714397 DOI: 10.1080/15384101.2014.1003008]

206 **Wu G**, Huang P, Ju X, Li Z, Wang Y. Lin28B over-expression mediates the repression of let-7 by hepatitis B virus X protein in hepatoma cells. *Int J Clin Exp Med* 2015; **8**: 15108-15116 [PMID: 26628994]

207 **Brennan E**, Wang B, McClelland A, Mohan M, Marai M, Beuscart O, Derouiche S, Gray S, Pickering R, Tikellis C, de Gaetano M, Barry M, Belton O, Ali-Shah ST, Guiry P, Jandeleit-Dahm KAM, Cooper ME, Godson C, Kantharidis P. Protective Effect of let-7 miRNA Family in Regulating Inflammation in Diabetes-Associated Atherosclerosis. *Diabetes* 2017; **66**: 2266-2277 [PMID: 28487436 DOI: 10.2337/db16-1405]

208 **Abdullah M**, Berthiaume JM, Willis MS. Tumor necrosis factor receptor-associated factor 6 as a nuclear factor kappa B-modulating therapeutic target in cardiovascular diseases: at the heart of it all. *Transl Res* 2018; **195**: 48-61 [PMID: 29175266 DOI: 10.1016/j.trsl.2017.10.012]

209 **Essandoh K**, Li Y, Huo J, Fan GC. MiRNA-Mediated Macrophage Polarization and its Potential Role in the Regulation of Inflammatory Response. *Shock* 2016; **46**: 122-131 [PMID: 26954942 DOI: 10.1097/SHK.0000000000000604]

210 **Pfeiffer JR**, McAvoy BL, Fecteau RE, Deleault KM, Brooks SA. CARHSP1 is required for effective tumor necrosis factor alpha mRNA stabilization and localizes to processing bodies and exosomes. *Mol Cell Biol* 2011; **31**: 277-286 [PMID: 21078874 DOI: 10.1128/MCB.00775-10]

211 **Lindquist JA**, Brandt S, Bernhardt A, Zhu C, Mertens PR. The role of cold shock domain proteins in inflammatory diseases. *J Mol Med (Berl)* 2014; **92**: 207-216 [PMID: 24562821 DOI: 10.1007/s00109-014-1136-3]

212 **Lankat-Buttgereit B**, Göke R. The tumour suppressor Pdcd4: recent advances in the elucidation of function and regulation. *Biol Cell* 2009; **101**: 309-317 [PMID: 19356152 DOI: 10.1042/BC20080191]

213 **Liu X**, Cheng Y, Yang J, Krall TJ, Huo Y, Zhang C. An essential role of PDCD4 in vascular smooth muscle cell apoptosis and proliferation: implications for vascular disease. *Am J Physiol Cell Physiol* 2010; **298**: C1481-C1488 [PMID: 20357187 DOI: 10.1152/ajpcell.00413.2009]

214 **Vikhreva PN**, Kalinichenko SV, Korobko IV. Programmed cell death 4 mechanism of action: The model to be updated? *Cell Cycle* 2017; **16**: 1761-1764 [PMID: 28853972 DOI: 10.1080/15384101.2017.1371881]

215 **Ranganathan S**, Noyes NC, Migliorini M, Winkles JA, Battey FD, Hyman BT, Smith E, Yepes M, Mikhailenko I, Strickland DK. LRAD3, a novel low-density lipoprotein receptor family member that modulates amyloid precursor protein trafficking. *J Neurosci* 2011; **31**: 10836-10846 [PMID: 21795536 DOI: 10.1523/JNEUROSCI.5065-10.2011]

216 **Noyes NC**, Hampton B, Migliorini M, Strickland DK. Regulation of Itch and Nedd4 E3 Ligase Activity and Degradation by LRAD3. *Biochemistry* 2016; **55**: 1204-1213 [PMID: 26854353 DOI: 10.1021/acs.biochem.5b01218]

217 **Cora' D**, Re A, Caselle M, Bussolino F. MicroRNA-mediated regulatory circuits: outlook and perspectives. *Phys Biol* 2017; **14**: 045001 [PMID: 28586314 DOI: 10.1088/1478-3975/aa6f21]

218 **Gui H**, Kwan JS, Sham PC, Cherny SS, Li M. Sharing of Genes and Pathways Across Complex Phenotypes: A Multilevel Genome-Wide Analysis. *Genetics* 2017; **206**: 1601-1609 [PMID: 28495956 DOI: 10.1534/genetics.116.198150]

219 **Vlachos IS**, Zagganas K, Paraskevopoulou MD, Georgakilas G, Karagkouni D, Vergoulis T, Dalamagas T,

Hatzigeorgiou AG. DIANA-miRPath v3.0: deciphering microRNA function with experimental support. *Nucleic Acids Res* 2015; **43**: W460-W466 [PMID: 25977294 DOI: 10.1093/nar/gkv403]
220 **Wolfson M**, Budovsky A, Tacutu R, Fraifeld V. The signaling hubs at the crossroad of longevity and age-related disease networks. *Int J Biochem Cell Biol* 2009; **41**: 516-520 [PMID: 18793745 DOI: 10.1016/j.biocel.2008.08.026]
221 **Vestweber D**. VE-cadherin: the major endothelial adhesion molecule controlling cellular junctions and blood vessel formation. *Arterioscler Thromb Vasc Biol* 2008; **28**: 223-232 [PMID: 18162609 DOI: 10.1161/ATVBAHA.107.158014]
222 **Haasdijk RA**, Den Dekker WK, Cheng C, Tempel D, Szulcek R, Bos FL, Hermkens DM, Chrifi I, Brandt MM, Van Dijk C, Xu YJ, Van De Kamp EH, Blonden LA, Van Bezu J, Sluimer JC, Biessen EA, Van Nieuw Amerongen GP, Duckers HJ. THSD1 preserves vascular integrity and protects against intraplaque haemorrhaging in ApoE-/- mice. *Cardiovasc Res* 2016; **110**: 129-139 [PMID: 26822228 DOI: 10.1093/cvr/cvw015]
223 **Shapouri-Moghaddam A**, Mohammadian S, Vazini H, Taghadosi M, Esmaeili SA, Mardani F, Seifi B, Mohammadi A, Afshari JT, Sahebkar A. Macrophage plasticity, polarization, and function in health and disease. *J Cell Physiol* 2018; **233**: 6425-6440 [PMID: 29319160 DOI: 10.1002/jcp.26429]
224 **Toma I**, McCaffrey TA. Transforming growth factor-β and atherosclerosis: interwoven atherogenic and atheroprotective aspects. *Cell Tissue Res* 2012; **347**: 155-175 [PMID: 21626289 DOI: 10.1007/s00441-011-1189-3]
225 **Goumans MJ**, Ten Dijke P. TGF-β Signaling in Control of Cardiovascular Function. *Cold Spring Harb Perspect Biol* 2018; **10**: a022210 [PMID: 28348036 DOI: 10.1101/cshperspect.a022210]
226 **Zhao B**, Tumaneng K, Guan KL. The Hippo pathway in organ size control, tissue regeneration and stem cell self-renewal. *Nat Cell Biol* 2011; **13**: 877-883 [PMID: 21808241 DOI: 10.1038/ncb2303]
227 **Virbasius JV**, Czech MP. Map4k4 Signaling Nodes in Metabolic and Cardiovascular Diseases. *Trends Endocrinol Metab* 2016; **27**: 484-492 [PMID: 27160798 DOI: 10.1016/j.tem.2016.04.006]
228 **Xu S**, Koroleva M, Yin M, Jin ZG. Atheroprotective laminar flow inhibits Hippo pathway effector YAP in endothelial cells. *Transl Res* 2016; **176**: 18-28.e2 [PMID: 27295628 DOI: 10.1016/j.trsl.2016.05.003]
229 **Wang Y**, Cao W, Cui J, Yu Y, Zhao Y, Shi J, Wu J, Xia Z, Yu B, Liu J. Arterial Wall Stress Induces Phenotypic Switching of Arterial Smooth Muscle Cells in Vascular Remodeling by Activating the YAP/TAZ Signaling Pathway. *Cell Physiol Biochem* 2018; **51**: 842-853 [PMID: 30466081 DOI: 10.1159/000495376]
230 **Xiao J**, Jin K, Wang J, Ma J, Zhang J, Jiang N, Wang H, Luo X, Fei J, Wang Z, Yang X, Ma D. Conditional knockout of TFPI-1 in VSMCs of mice accelerates atherosclerosis by enhancing AMOT/YAP pathway. *Int J Cardiol* 2017; **228**: 605-614 [PMID: 27875740 DOI: 10.1016/j.ijcard.2016.11.195]
231 **Fu Y**, Sun S, Sun H, Peng J, Ma X, Bao L, Ji R, Luo C, Gao C, Zhang X, Jin Y. Scutellarin exerts protective effects against atherosclerosis in rats by regulating the Hippo-FOXO3A and PI3K/AKT signaling pathways. *J Cell Physiol* 2019; **234**: 18131-18145 [PMID: 30891776 DOI: 10.1002/jcp.28446]
232 **Kozarov E**. Bacterial invasion of vascular cell types: vascular infectology and atherogenesis. *Future Cardiol* 2012; **8**: 123-138 [PMID: 22185451 DOI: 10.2217/fca.11.75]
233 **Caruso P**, MacLean MR, Khanin R, McClure J, Soon E, Southgate M, MacDonald RA, Greig JA, Robertson KE, Masson R, Denby L, Dempsie Y, Long L, Morrell NW, Baker AH. Dynamic changes in lung microRNA profiles during the development of pulmonary hypertension due to chronic hypoxia and monocrotaline. *Arterioscler Thromb Vasc Biol* 2010; **30**: 716-723 [PMID: 20110569 DOI: 10.1161/ATVBAHA.109.202028]
234 **Caruso P**, Dempsie Y, Stevens HC, McDonald RA, Long L, Lu R, White K, Mair KM, McClure JD, Southwood M, Upton P, Xin M, van Rooij E, Olson EN, Morrell NW, MacLean MR, Baker AH. A role for miR-145 in pulmonary arterial hypertension: evidence from mouse models and patient samples. *Circ Res* 2012; **111**: 290-300 [PMID: 22715469 DOI: 10.1161/CIRCRESAHA.112.267591]
235 **Sistrunk JW**, Shifrin A, Frager M, Bardales RH, Thomas J, Fishman N, Goldberg P, Guttler R, Grant E. Clinical performance of multiplatform mutation panel and microRNA risk classifier in indeterminate thyroid nodules. *J Am Soc Cytopathol* 2020 [PMID: 32247769 DOI: 10.1016/j.jasc.2020.02.002]
236 **Jopling CL**, Yi M, Lancaster AM, Lemon SM, Sarnow P. Modulation of hepatitis C virus RNA abundance by a liver-specific MicroRNA. *Science* 2005; **309**: 1577-1581 [PMID: 16141076 DOI: 10.1126/science.1113329]
237 **Chang J**, Guo JT, Jiang D, Guo H, Taylor JM, Block TM. Liver-specific microRNA miR-122 enhances the replication of hepatitis C virus in nonhepatic cells. *J Virol* 2008; **82**: 8215-8223 [PMID: 18550664 DOI: 10.1128/JVI.02575-07]
238 **Gebert LF**, Rebhan MA, Crivelli SE, Denzler R, Stoffel M, Hall J. Miravirsen (SPC3649) can inhibit the biogenesis of miR-122. *Nucleic Acids Res* 2014; **42**: 609-621 [PMID: 24068553 DOI: 10.1093/nar/gkt852]
239 **Janssen HL**, Reesink HW, Lawitz EJ, Zeuzem S, Rodriguez-Torres M, Patel K, van der Meer AJ, Patick AK, Chen A, Zhou Y, Persson R, King BD, Kauppinen S, Levin AA, Hodges MR. Treatment of HCV infection by targeting microRNA. *N Engl J Med* 2013; **368**: 1685-1694 [PMID: 23534542 DOI: 10.1056/NEJMoa1209026]
240 **Seto AG**, Beatty X, Lynch JM, Hermreck M, Tetzlaff M, Duvic M, Jackson AL. Cobomarsen, an oligonucleotide inhibitor of miR-155, co-ordinately regulates multiple survival pathways to reduce cellular proliferation and survival in cutaneous T-cell lymphoma. *Br J Haematol* 2018; **183**: 428-444 [PMID: 30125933 DOI: 10.1111/bjh.15547]
241 **Kopp KL**, Ralfkiaer U, Gjerdrum LM, Helvad R, Pedersen IH, Litman T, Jønson L, Hagedorn PH, Krejsgaard T, Gniadecki R, Bonefeld CM, Skov L, Geisler C, Wasik MA, Ralfkiaer E, Ødum N, Woetmann A. STAT5-mediated expression of oncogenic miR-155 in cutaneous T-cell lymphoma. *Cell Cycle* 2013; **12**: 1939-1947 [PMID: 23676217 DOI: 10.4161/cc.24987]
242 **Beg MS**, Brenner AJ, Sachdev J, Borad M, Kang YK, Stoudemire J, Smith S, Bader AG, Kim S, Hong DS. Phase I study of MRX34, a liposomal miR-34a mimic, administered twice weekly in patients with advanced solid tumors. *Invest New Drugs* 2017; **35**: 180-188 [PMID: 27917453 DOI: 10.1007/s10637-016-0407-y]
243 **Hong DS**, Kang YK, Borad M, Sachdev J, Ejadi S, Lim HY, Brenner AJ, Park K, Lee JL, Kim TY, Shin S,

Becerra CR, Falchook G, Stoudemire J, Martin D, Kelnar K, Peltier H, Bonato V, Bader AG, Smith S, Kim S, O'Neill V, Beg MS. Phase 1 study of MRX34, a liposomal miR-34a mimic, in patients with advanced solid tumours. *Br J Cancer* 2020; **122**: 1630-1637 [PMID: 32238921 DOI: 10.1038/s41416-020-0802-1]

244 **Kelnar K**, Bader AG. A qRT-PCR Method for Determining the Biodistribution Profile of a miR-34a Mimic. *Methods Mol Biol* 2015; **1317**: 125-133 [PMID: 26072405 DOI: 10.1007/978-1-4939-2727-2_8]

245 **Zhang G**, Guo B, Wu H, Tang T, Zhang BT, Zheng L, He Y, Yang Z, Pan X, Chow H, To K, Li Y, Li D, Wang X, Wang Y, Lee K, Hou Z, Dong N, Li G, Leung K, Hung L, He F, Zhang L, Qin L. A delivery system targeting bone formation surfaces to facilitate RNAi-based anabolic therapy. *Nat Med* 2012; **18**: 307-314 [PMID: 22286306 DOI: 10.1038/nm.2617]

246 **Leuschner F**, Dutta P, Gorbatov R, Novobrantseva TI, Donahoe JS, Courties G, Lee KM, Kim JI, Markmann JF, Marinelli B, Panizzi P, Lee WW, Iwamoto Y, Milstein S, Epstein-Barash H, Cantley W, Wong J, Cortez-Retamozo V, Newton A, Love K, Libby P, Pittet MJ, Swirski FK, Koteliansky V, Langer R, Weissleder R, Anderson DG, Nahrendorf M. Therapeutic siRNA silencing in inflammatory monocytes in mice. *Nat Biotechnol* 2011; **29**: 1005-1010 [PMID: 21983520 DOI: 10.1038/nbt.1989]

247 **Duivenvoorden R**, Tang J, Cormode DP, Mieszawska AJ, Izquierdo-Garcia D, Ozcan C, Otten MJ, Zaidi N, Lobatto ME, van Rijs SM, Priem B, Kuan EL, Martel C, Hewing B, Sager H, Nahrendorf M, Randolph GJ, Stroes ES, Fuster V, Fisher EA, Fayad ZA, Mulder WJ. A statin-loaded reconstituted high-density lipoprotein nanoparticle inhibits atherosclerotic plaque inflammation. *Nat Commun* 2014; **5**: 3065 [PMID: 24445279 DOI: 10.1038/ncomms4065]

248 **Laffont B**, Rayner KJ. MicroRNAs in the Pathobiology and Therapy of Atherosclerosis. *Can J Cardiol* 2017; **33**: 313-324 [PMID: 28232017 DOI: 10.1016/j.cjca.2017.01.001]

249 **Nazari-Jahantigh M**, Wei Y, Noels H, Akhtar S, Zhou Z, Koenen RR, Heyll K, Gremse F, Kiessling F, Grommes J, Weber C, Schober A. MicroRNA-155 promotes atherosclerosis by repressing Bcl6 in macrophages. *J Clin Invest* 2012; **122**: 4190-4202 [PMID: 23041630 DOI: 10.1172/JCI61716]

250 **Esper RJ**, Nordaby RA. Cardiovascular events, diabetes and guidelines: the virtue of simplicity. *Cardiovasc Diabetol* 2019; **18**: 42 [PMID: 30922303 DOI: 10.1186/s12933-019-0844-y]

251 **Kataoka Y**, St John J, Wolski K, Uno K, Puri R, Tuzcu EM, Nissen SE, Nicholls SJ. Atheroma progression in hyporesponders to statin therapy. *Arterioscler Thromb Vasc Biol* 2015; **35**: 990-995 [PMID: 25722430 DOI: 10.1161/ATVBAHA.114.304477]

252 **Nozue T**, Yamamoto S, Tohyama S, Fukui K, Umezawa S, Onishi Y, Kunishima T, Sato A, Nozato T, Miyake S, Takeyama Y, Morino Y, Yamauchi T, Muramatsu T, Hibi K, Terashima M, Michishita I; TRUTH Investigators. Comparison of arterial remodeling and changes in plaque composition between patients with progression versus regression of coronary atherosclerosis during statin therapy (from the TRUTH study). *Am J Cardiol* 2012; **109**: 1247-1253 [PMID: 22325089 DOI: 10.1016/j.amjcard.2011.12.016]

World Journal of Cardiology

Submit a Manuscript: https://www.f6publishing.com

World J Cardiol 2020 July 26; 12(7): 334-341

DOI: 10.4330/wjc.v12.i7.334

ISSN 1949-8462 (online)

MINIREVIEWS

Comprehensive review of hemolysis in ventricular assist devices

Christos A Papanastasiou, Konstantinos G Kyriakoulis, Christina A Theochari, Damianos G Kokkinidis, Theodoros D Karamitsos, Leonidas Palaiodimos

ORCID number: Christos A Papanastasiou 0000-0001-5581-2362; Konstantinos G Kyriakoulis 0000-0001-8986-2704; Christina A Theochari 0000-0002-7865-6187; Damianos G Kokkinidis 0000-0002-1381-4754; Theodoros D Karamitsos 0000-0002-4658-5273; Leonidas Palaiodimos 0000-0003-4682-5991.

Author contributions: All authors contributed equally to this manuscript.

Conflict-of-interest statement: There is no conflict of interest associated with the contributions of the senior author or other coauthors to this manuscript.

Manuscript source: Invited manuscript

Christos A Papanastasiou, Theodoros D Karamitsos, 1st Department of Cardiology, AHEPA Hospital, Aristotle University of Thessaloniki, Thessaloniki 54621, Greece

Konstantinos G Kyriakoulis, 3rd Department of Medicine, Sotiria Hospital, National and Kapodistrian University of Athens, Athens 11527, Greece

Christina A Theochari, Department of Internal Medicine, Messinia General Hospital, Kalamata 24100, Greece

Damianos G Kokkinidis, Department of Medicine, Jacobi Medical Center, Albert Einstein College of Medicine, Bronx, NY 10461, United States

Leonidas Palaiodimos, Department of Medicine, Montefiore Medical Center, Albert Einstein College of Medicine, Bronx, NY 10461, United States

Corresponding author: Leonidas Palaiodimos, MD, MSc, Assistant Professor, Department of Medicine, Montefiore Medical Center, Albert Einstein College of Medicine, 111 East 210th Street, Bronx, NY 10461, United States. palaiodimosmd@gmail.com

Abstract

Ventricular assist devices (VADs) have played an important role in altering the natural history of end-stage heart failure. Low-grade hemolysis has been traditionally described in patients with VADs, indicating effective device functionality. However, clinically significant hemolysis could be crucial in terms of prognosis, calling for prompt therapeutic actions. The absence of solid and widely approved diagnostic criteria for clinically significant hemolysis, render the utilization of hemolysis laboratory markers challenging. Hemolysis incidence varies (5%-18%) depending on definition and among different VAD generations, being slightly higher in continuous-flow devices than in pulsatile devices. Increased shear stress of red blood cells and underlying device thrombosis appear to be the main pathogenetic pathways. No certain algorithm is available for the management of hemolysis in patients with VADs, while close clinical and laboratory monitoring remains the cornerstone of management. Imaging examinations such as echocardiography ramp test or computed tomography scan could play a role in revealing the underlying cause. Treatment should be strictly personalized, including either pharmacological (antithrombotic treatment) or surgical interventions.

Key words: Ventricular assist device; Hemolysis; Thrombosis

Received: February 4, 2020
Peer-review started: February 4, 2020
First decision: March 24, 2020
Revised: May 2, 2020
Accepted: May 27, 2020
Article in press: May 27, 2020
Published online: July 26, 2020

P-Reviewer: Barik R, Kharlamov AN, Vermeersch P
S-Editor: Zhang L
L-Editor: Webster JR
E-Editor: Zhang YL

Core tip: Ventricular assist devices are essential in end-stage heart failure management. Severe hemolysis can be a significant complication, leading to increased mortality and worse outcomes. The incidence of hemolysis varies (5%-18%) depending on different definitions of hemolysis and among different ventricular assist device generations. The main pathogenetic mechanisms include increased red blood cell shear stress or underlying device thrombosis. A personalized approach is crucial in the absence of certain algorithms for the management of this complication. Close clinical and laboratory monitoring in combination with imaging examinations could play a role in revealing the underlying cause. Treatment includes pharmacological (antithrombotic treatment) or surgical interventions.

Citation: Papanastasiou CA, Kyriakoulis KG, Theochari CA, Kokkinidis DG, Karamitsos TD, Palaiodimos L. Comprehensive review of hemolysis in ventricular assist devices. *World J Cardiol* 2020; 12(7): 334-341
URL: https://www.wjgnet.com/1949-8462/full/v12/i7/334.htm
DOI: https://dx.doi.org/10.4330/wjc.v12.i7.334

INTRODUCTION

Ventricular assist devices (VADs) have evolved into an essential therapeutic option for patients with end-stage heart failure as they are used as a bridge to transplant, a bridge to recovery or as a destination therapy[1-3]. Despite their substantial benefits in this vulnerable group of patients, VADs have been associated with a great variety of adverse events, including but not limited to infection, bleeding and pump thrombosis[4]. Recently, hemolysis has gained attention in the field of mechanical circulatory support as a side-effect that is associated with important clinical and prognostic information[5].

Although a low level of hemolysis exists by default in patients supported with VADs and may indicate that the device works well, clinically significant hemolysis constitutes a major complication associated with deleterious consequences and an eminent need for aggressive management[5]. Unfortunately, the absence of unanimous criteria on the definition of clinically significant hemolysis remains its Achilles heel, blurring important epidemiological aspects of this clinical entity. In this review we discuss critical issues with regard to hemolysis from the perspective of long-term (durable) VADs, covering the entire clinical spectrum of this expected but potentially life-threatening complication.

DEFINITION

The laboratory markers lactate dehydrogenase (LDH), plasma free hemoglobin (pfHgb), haptoglobin, and bilirubin are traditionally used to detect hemolysis. However, most studies adopted different sets of "preferred" diagnostic criteria for hemolysis detection with dissimilar parameters and varying cut-off values for each biomarker. This inconsistency in the definition is also reflected in the contents of the Interagency Registry for Mechanically Assisted Circulatory Support (INTERMACS). The most recent INTERMACS definition allows the distinction of major from minor hemolysis by the presence of clinical signs, while cut-off values for LDH (2.5 times the upper limit of the normal range) and pfHgb (20 mg/dL) have been employed to indicate a hemolytic event[6].

INCIDENCE

By moving from the first to newer-generation devices, a significant reduction in the rates of most adverse events has been observed[7]. The reported hemolysis rates were slightly higher in continuous-flow devices than in pulsatile devices[7]. Even among

newer-generation devices, there are considerable differences in hemolysis incidence associated mainly with mechanical factors (Table 1)[8].

Frictional heat generated at the contacting parts of most axial-flow VADs and shear stress created by the device impeller result in increased rates of hemolysis, ranging from less than 5% up to 18% for the landmark device Heartmate II (HMII), depending on the definition of hemolysis used across the studies[9,10]. Pagani *et al*[9] defining hemolysis as two consecutive pfHgb values greater than 40 mg/dL and a LDH value greater than 1000 mg/dL, reported an incidence of 4% over a 6-mo period of support[9]. The study by Slaughter *et al*[11], which evaluated HMII as destination therapy reported a similar hemolysis incidence[11]. Another study by Ravichandran *et al*[10] used completely different parameters to define hemolysis (Hgb < 10 g/dL, haptoglobin < 8 g/dL and LDH > 250 IU/L) and demonstrated a four to five-fold higher incidence (18%)[10]. Along these lines, a recent study from Japan showed that hemolysis was the most frequent adverse event among HeartMate II receivers, of whom 14% developed a major hemolytic event[12].

The employment of non-contact bearings, which allows for rotation without wear, has significantly reduced the hemolysis rates in the third generation VADs[13]. Slaughter *et al*[14] used laboratory markers (pfHgb > 40 mg/dL) in combination with pertinent clinical signs to determine hemolysis rates for the centrifugal, continuous-flow HeartWare device and reported lower hemolysis incidence (1.2% over a 36-mo period)[14]. More impressive were the results of two small-sized studies for the Heartmate 3 LVAS, where no cases of hemolysis were observed[15,16].

ETIOLOGY

Several mechanisms have been proposed to account for hemolysis related to mechanical circulatory support[8,17]. The commonly held hypothesis is that red blood cells undergo increased shear stress as they pass through the mechanical components of the device and become fragmented, a process ultimately resulting in hemolysis. This hypothesis was also supported by Yasuda *et al*[18] who performed *in vitro* tests in order to define the factors that contribute to hemolysis during blood flow through artificial organs. According to their results, shear stress and flow acceleration were the major factors responsible for the lysis of erythrocytes[18]. These parameters are strongly associated with the hyperdynamic circulation, which can be caused by a variety of reasons, such as dehydration, aortic regurgitation, and increased pump speed. Of note, the restoration of blood flow into the ascending aorta post LVAD implantation, may affect the function of the aortic valve due to an increase in afterload creating a local circuit where blood leaks backward into the pump[19]. As a consequence, red blood cells are exposed to high mechanical shear forces caused by the blood-pump interface and hemolysis becomes an unavoidable complication.

Additionally, the presence of hemolysis may be the reason behind pump thrombus, or malpositioning of the LVAD inflow cannula[17]. Pump thrombosis and hemolysis are two complications linked in a bidirectional way. Virchow's triad, modified and applied to the context of the VAD microenvironment (bioreactive surfaces, activated platelets, abnormal flow patterns) remains the key to understanding the fundamental principles of thrombogenesis in mechanical circulatory support[20]. Bioreactive materials used in VADs set the stage for thrombus formation *via* two pathways: (1) By activating the intrinsic cascade of coagulation, when plasma proteins interact with the non-hemocompatible surface of a circulatory pump, and (2) By promoting platelet adhesion to the pump surface through adhesion proteins found on the metallic surface (*e.g.*, fibrinogen, von Willebrand factor)[21]. When platelets adhere to the surface, the secretion of their granule-stored mediators (*e.g.*, adenosine diphosphate) further fuels the self-perpetuating processes of platelet aggregation and activation. The third component of Virchow's triad plays a central role in platelet activation, as well. Shear forces have been implicated in triggering von Willebrand – platelet glycoprotein Ib interaction, leading to the formation of loose aggregates and activation of integrin aIIbβ_3, hence allowing fibrinogen to bind to platelet membranes[22]. Beyond these adhesion signaling pathways, Slepian *et al*[23] introduced mechanically-related aspects of shear-mediated platelet activation, according to which platelet porogenisity could be increased by membrane damage and shear-sensitive channels, allowing the influx of activating mediators[23].

The smaller size of newer VADs predispose them to thrombosis of the entire pump, facilitating the process of hemolysis through erythrocyte membrane injury[24]. Consequently, byproducts released by lysed erythrocytes exert pro-thrombotic actions

Table 1 Basic characteristics of different types of left ventricular assist devices

Type of LVAD	Example	Pump design	Characteristics	Hemolysis
First-generation	HeartMate I	Pulsatile flow	Larger blood contacting surfaces, multiple moving parts	Increase
Second-generation	HeartMate II	Continuous – axial flow	Smaller size	Increase
Third-generation	HeartWare	Continuous – centrifugal flow	Noncontact bearing (magnetic levitation)	Increase

LVAD: Left ventricular assist device.

through various pathways. Cell-free hemoglobin scavenges circulating nitric oxide (NO) and erythrocyte arginase depletes L-arginine, the substrate for NO synthesis, limiting the ability of endothelial NO synthase to produce NO[25]. Thus, NO bioavailability is reduced and its inhibitory actions on platelet adhesion and activation are abolished[26]. Moreover, heme catabolism *via* heme oxygenase-1 releases carbon monoxide and iron, two end-products with hypercoagulable and hypofibrinolytic features[27]. Of note, iron overload has been associated with activation of blood coagulation and formation of fibrin-like dense matted deposits, which are more resistant to degradation, compared to thrombin-induced fibrin clots[28]. Finally, a recent study demonstrated a direct relationship between hemolysis and VAD thrombosis, indicating that free hemoglobin inhibited ADAMTS-13, thus protecting active von Willebrand factor from degradation[30].

Despite significant breakthroughs in understanding the pathophysiological mechanisms of hemolysis and thrombosis in the setting of mechanical circulatory support, it is still unknown whether hemolysis or thrombosis is the first step on the cascade. It seems that these two inextricably related complications establish a new hematologic status, which is characterized by hemolytic and clotting diathesis, resulting in device dysfunction, heart failure or even death.

RISK FACTORS

Although the complications of mechanical circulatory support are well-described, there are few data on the risk factors that predispose patients to hemolysis. Three studies explored the differences in baseline characteristics between patients with and without hemolysis as a complication due to VAD[5,10,30]. Katz *et al*[5] retrieved data from the INTERMACS registry and demonstrated that patients who received a continuous-flow LVAD and suffered a hemolytic event were more likely to be younger and female[5]. In another study, younger age, smoking and female sex were also found to have a significant association with the development of hemolysis in patients who were supported with the HMII device[10]. Contrary to these findings, Cowger *et al*[30] did not detect significant differences in any of the aforementioned risk factors[30]. From a biomarker standpoint, higher LDH at the time of VAD implantation and lower INR were reported to be associated with higher rates of hemolysis[10,30].

MANAGEMENT

Although hemolysis is a potentially life-threatening complication of mechanical circulatory support, there is no consensus to date regarding the management of this clinical entity. Hemodynamic stability, surgical candidacy and the underlying cause of hemolysis should be carefully considered before initiating any treatment. The first step in the evaluation of an acute hemolytic event or worsening of pre-existing anemia should be the close monitoring of hemolysis-related biomarkers[24]. Apart from hemoglobin/hematocrit and total/indirect bilirubin, emphasis should be given to serial changes in LDH[24]. A non-significant and stable increase in LDH levels may be associated with a hyperdynamic circulation, caused by dehydration or increased pump speed. If a marked elevation in LDH levels is detected, further diagnostic studies may be necessary to specify the underlying cause of hemolysis. An echocardiography ramp test, in which left ventricular dimensions are recorded at increasing pump speeds, is suggested to detect device malfunction[31]. Although pump thrombosis is the predominant reason for defective unloading of the left ventricular, in

terms of increased pump speeds, graft malpositioning is an alternative possibility. In this case, a computed tomography scan can be used to reveal potential mechanical impairment, which should be corrected surgically.

Antithrombotic treatment should be immediately intensified, irrespective of the cause of hemolysis. Specific medication treatment strategies for device thrombosis include initiation of unfractionated heparin, either alone or in combination with antiplatelet agents or direct thrombin inhibitors, and thrombolytics[32]. Although the optimal medical approach is not well established, a recent meta-analysis sought to shed light on this topic by evaluating the efficacy and complications associated with the aforementioned agents[33]. No significant difference in thrombus resolution was found between thrombolytic and non-thrombolytic treatment, while the risk of major bleeding was higher in the thrombolysis group. Surgical therapy with device exchange has shown higher success rates in resolving pump thrombus, compared to medical treatment but is limited by its invasive nature and decreased long-term survival[34]. As a result, indications are limited to patients with hemodynamic instability, persistence of hemolysis or progressive heart failure despite the initial medical treatment[35,36].

PROGNOSIS

Although limited, observational data exist regarding the prognostic role of hemolysis after VAD implantation, it seems that the development of a serious hemolytic event is associated with poor outcomes (Table 2). Katz *et al*[5] showed that survival was significantly attenuated in patients who suffered a hemolytic episode, compared to those who did not. Similarly, in another study, 1-year survival was markedly decreased in the hemolysis group as compared to the non-hemolysis group of patients (38.9% *vs* 89.3%, $P < 0.001$)[10]. Finally, Cowger *et al*[30] demonstrated that the hazard of death was four times greater in hemolytic patients than that observed in non-hemolytic patients (HR: 4.3, 95%CI: 2.1-8.9)[30]. However, it should be highlighted that in these studies, only crude analyses were performed. Interestingly, in a recent study by Xia *et al*[37], hemolysis or pump thrombosis were found to be significant predictors of poor long-term survival, even after adjusting for potential confounders[37]. Whether hemolysis is associated with adverse outcomes in patients supported by VADs should be further investigated.

CONCLUSION

Hemolysis appears to be a relatively common complication of mechanical circulatory support that may serve as an early indicator of adverse events. Given the low specificity of the hemolysis-related biomarkers, patients supported with a VAD should be closely monitored for both clinical and laboratory signs of hemolysis. Future research studies should attempt to approach this interesting topic in a more standardized way, adopting a reliable and consistent hemolysis definition in order to elucidate further the risk factors and prognostic significance of this complication. The destruction of red blood cells may be just the tip of the iceberg of a disrupted hematologic profile in the setting of mechanical circulatory support.

Table 2 Baseline characteristics, demographics and results of studies investigating hemolysis in left ventricular assist devices

Ref.	Study design	Device	No of patients	Definition of hemolysis	Outcome	Result[a]
Xia *et al*[37], 2019	Retrospective (data obtained from the INTERMACS registry 2012-2013)	Continuous flow LVADs	1116	NA	Short-term survival (< 3 yr)	aOR: 3.57 (1.84-6.93)
Katz *et al*[5], 2015	Retrospective (data obtained from the INTERMACS registry 2006-2012)	Continuous flow LVADs	4850	PfHg > 40 mg/dL and clinical signs of hemolysis	Mortality (mean of follow-up: 11.1 mo)	OR: 1.19 (1.146-2.52)
Ravichandran *et al*[10], 2014	Retrospective	HeartMate II	100	Hgb < 10 g/dL, haptoglobin < 8 g/dL and LDH > 250 U/L	1-yr mortality	OR: 11.3 (3.56-35.93)
Cowger *et al*[30], 2014	Retrospective	HeartMate II	182	SfHg > 40 mg/dL and clinical signs of hemolysis	1-yr mortality	HR: 4.3 (2.1-8.9)

[a]The numbers in parentheses indicate 95% confidence interval. aOR: Adjusted odds ratio; LVAD: Left ventricular assist device; HMII: HeartMate II; PsHg: Plasma-free hemoglobin; sfHg: Serum-free hemoglobin.

REFERENCES

1 **Frazier OH**, Rose EA, McCarthy P, Burton NA, Tector A, Levin H, Kayne HL, Poirier VL, Dasse KA. Improved mortality and rehabilitation of transplant candidates treated with a long-term implantable left ventricular assist system. *Ann Surg* 1995; **222**: 327-336; discussion 336-338 [PMID: 7677462 DOI: 10.1097/00000658-199509000-00010]

2 **Miller LW**, Pagani FD, Russell SD, John R, Boyle AJ, Aaronson KD, Conte JV, Naka Y, Mancini D, Delgado RM, MacGillivray TE, Farrar DJ, Frazier OH; HeartMate II Clinical Investigators. Use of a continuous-flow device in patients awaiting heart transplantation. *N Engl J Med* 2007; **357**: 885-896 [PMID: 17761592 DOI: 10.1056/NEJMoa067758]

3 **Rose EA**, Gelijns AC, Moskowitz AJ, Heitjan DF, Stevenson LW, Dembitsky W, Long JW, Ascheim DD, Tierney AR, Levitan RG, Watson JT, Meier P, Ronan NS, Shapiro PA, Lazar RM, Miller LW, Gupta L, Frazier OH, Desvigne-Nickens P, Oz MC, Poirier VL; Randomized Evaluation of Mechanical Assistance for the Treatment of Congestive Heart Failure (REMATCH) Study Group. Long-term use of a left ventricular assist device for end-stage heart failure. *N Engl J Med* 2001; **345**: 1435-1443 [PMID: 11794191 DOI: 10.1056/NEJMoa012175]

4 **Yuan N**, Arnaoutakis GJ, George TJ, Allen JG, Ju DG, Schaffer JM, Russell SD, Shah AS, Conte JV. The spectrum of complications following left ventricular assist device placement. *J Card Surg* 2012; **27**: 630-638 [PMID: 22978843 DOI: 10.1111/j.1540-8191.2012.01504.x]

5 **Katz JN**, Jensen BC, Chang PP, Myers SL, Pagani FD, Kirklin JK. A multicenter analysis of clinical hemolysis in patients supported with durable, long-term left ventricular assist device therapy. *J Heart Lung Transplant* 2015; **34**: 701-709 [PMID: 25582036 DOI: 10.1016/j.healun.2014.10.002]

6 **Valle-Muñoz A**, Estornell-Erill J, Soriano-Navarro CJ, Nadal-Barange M, Martinez-Alzamora N, Pomar-Domingo F, Corbí-Pascual M, Payá-Serrano R, Ridocci-Soriano F. Late gadolinium enhancement-cardiovascular magnetic resonance identifies coronary artery disease as the aetiology of left ventricular dysfunction in acute new-onset congestive heart failure. *Eur J Echocardiogr* 2009; **10**: 968-974 [PMID: 19755468 DOI: 10.1093/ejechocard/jep115]

7 **Kirklin JK**, Naftel DC, Kormos RL, Stevenson LW, Pagani FD, Miller MA, Baldwin JT, Young JB. Fifth INTERMACS annual report: risk factor analysis from more than 6,000 mechanical circulatory support patients. *J Heart Lung Transplant* 2013; **32**: 141-156 [PMID: 23352390 DOI: 10.1016/j.healun.2012.12.004]

8 **Fraser KH**, Zhang T, Taskin ME, Griffith BP, Wu ZJ. A quantitative comparison of mechanical blood damage parameters in rotary ventricular assist devices: shear stress, exposure time and hemolysis index. *J Biomech Eng* 2012; **134**: 081002 [PMID: 22938355 DOI: 10.1115/1.4007092]

9 **Pagani FD**, Miller LW, Russell SD, Aaronson KD, John R, Boyle AJ, Conte JV, Bogaev RC, MacGillivray TE, Naka Y, Mancini D, Massey HT, Chen L, Klodell CT, Aranda JM, Moazami N, Ewald GA, Farrar DJ, Frazier OH; HeartMate II Investigators. Extended mechanical circulatory support with a continuous-flow rotary left ventricular assist device. *J Am Coll Cardiol* 2009; **54**: 312-321 [PMID: 19608028 DOI: 10.1016/j.jacc.2009.03.055]

10 **Ravichandran AK**, Parker J, Novak E, Joseph SM, Schilling JD, Ewald GA, Silvestry S. Hemolysis in left ventricular assist device: a retrospective analysis of outcomes. *J Heart Lung Transplant* 2014; **33**: 44-50 [PMID: 24418733 DOI: 10.1016/j.healun.2013.08.019]

11 **Slaughter MS**, Rogers JG, Milano CA, Russell SD, Conte JV, Feldman D, Sun B, Tatooles AJ, Delgado RM 3rd, Long JW, Wozniak TC, Ghumman W, Farrar DJ, Frazier OH; HeartMate II Investigators. Advanced heart failure treated with continuous-flow left ventricular assist device. *N Engl J Med* 2009; **361**: 2241-2251 [PMID: 19920051 DOI: 10.1056/NEJMoa0909938]

12 **Seguchi O**, Kuroda K, Kumai Y, Nakajima S, Yanase M, Wada K, Matsumoto Y, Fukushima S, Fujita T, Kobayashi J, Fukushima N. Clinical Outcomes of Patients With the HeartMate II Left Ventricular Assist Device: A Single-center Experience From Japan. *Transplant Proc* 2018; **50**: 2726-2732 [PMID: 30401385 DOI: 10.1016/j.transproceed.2018.03.091]

13 **Rodriguez LE**, Suarez EE, Loebe M, Bruckner BA. Ventricular assist devices (VAD) therapy: new

technology, new hope? *Methodist Debakey Cardiovasc J* 2013; **9**: 32-37 [PMID: 23519193 DOI: 10.14797/mdcj-9-1-32]

14 **Slaughter MS**, Pagani FD, McGee EC, Birks EJ, Cotts WG, Gregoric I, Howard Frazier O, Icenogle T, Najjar SS, Boyce SW, Acker MA, John R, Hathaway DR, Najarian KB, Aaronson KD; HeartWare Bridge to Transplant ADVANCE Trial Investigators. HeartWare ventricular assist system for bridge to transplant: combined results of the bridge to transplant and continued access protocol trial. *J Heart Lung Transplant* 2013; **32**: 675-683 [PMID: 23796152 DOI: 10.1016/j.healun.2013.04.004]

15 **Krabatsch T**, Netuka I, Schmitto JD, Zimpfer D, Garbade J, Rao V, Morshuis M, Beyersdorf F, Marasco S, Damme L, Pya Y. Heartmate 3 fully magnetically levitated left ventricular assist device for the treatment of advanced heart failure -1 year results from the Ce mark trial. *J Cardiothorac Surg* 2017; **12**: 23 [PMID: 28376837 DOI: 10.1186/s13019-017-0587-3]

16 **Nowacka A**, Hullin R, Tozzi P, Barras N, Regamey J, Yerly P, Rosner L, Marcucci C, Rusca M, Liaudet L, Kirsch M. Short-term single-centre experience with the HeartMate 3 left ventricular assist device for advanced heart failure. *Eur J Cardiothorac Surg* 2020 [PMID: 32236472 DOI: 10.1093/ejcts/ezaa075]

17 **Akin S**, Soliman OI, Constantinescu AA, Akca F, Birim O, van Domburg RT, Manintveld O, Caliskan K. Haemolysis as a first sign of thromboembolic event and acute pump thrombosis in patients with the continuous-flow left ventricular assist device HeartMate II. *Neth Heart J* 2016; **24**: 134-142 [PMID: 26689927 DOI: 10.1007/s12471-015-0786-2]

18 **Yasuda T**, Shimokasa K, Funakubo A, Higami T, Kawamura T, Fukui Y. An investigation of blood flow behavior and hemolysis in artificial organs. *ASAIO J* 2000; **46**: 527-531 [PMID: 11016500 DOI: 10.1097/00002480-200009000-00003]

19 **Gopalan RS**, Arabia FA, Noel P, Chandrasekaran K. Hemolysis from aortic regurgitation mimicking pump thrombosis in a patient with a HeartMate II left ventricular assist device: a case report. *ASAIO J* 2012; **58**: 278-280 [PMID: 22285976 DOI: 10.1097/MAT.0b013e31824708a8]

20 **de Biasi AR**, Manning KB, Salemi A. Science for surgeons: understanding pump thrombogenesis in continuous-flow left ventricular assist devices. *J Thorac Cardiovasc Surg* 2015; **149**: 667-673 [PMID: 25534307 DOI: 10.1016/j.jtcvs.2014.11.041]

21 **Koliopoulou A**, McKellar SH, Rondina M, Selzman CH. Bleeding and thrombosis in chronic ventricular assist device therapy: focus on platelets. *Curr Opin Cardiol* 2016; **31**: 299-307 [PMID: 27054505 DOI: 10.1097/HCO.0000000000000284]

22 **Chow TW**, Hellums JD, Moake JL, Kroll MH. Shear stress-induced von Willebrand factor binding to platelet glycoprotein Ib initiates calcium influx associated with aggregation. *Blood* 1992; **80**: 113-120 [PMID: 1611079 DOI: 10.1182/blood.v80.1.113.bloodjournal801113]

23 **Slepian MJ**, Sheriff J, Hutchinson M, Tran P, Bajaj N, Garcia JGN, Scott Saavedra S, Bluestein D. Shear-mediated platelet activation in the free flow: Perspectives on the emerging spectrum of cell mechanobiological mechanisms mediating cardiovascular implant thrombosis. *J Biomech* 2017; **50**: 20-25 [PMID: 27887727 DOI: 10.1016/j.jbiomech.2016.11.016]

24 **Tchantchaleishvili V**, Sagebin F, Ross RE, Hallinan W, Schwarz KQ, Massey HT. Evaluation and treatment of pump thrombosis and hemolysis. *Ann Cardiothorac Surg* 2014; **3**: 490-495 [PMID: 25452909 DOI: 10.3978/j.issn.2225-319X.2014.09.01]

25 **Ataga KI**. Hypercoagulability and thrombotic complications in hemolytic anemias. *Haematologica* 2009; **94**: 1481-1484 [PMID: 19880774 DOI: 10.3324/haematol.2009.013672]

26 **Tziros C**, Freedman JE. The many antithrombotic actions of nitric oxide. *Curr Drug Targets* 2006; **7**: 1243-1251 [PMID: 17073585 DOI: 10.2174/138945006778559111]

27 **Nielsen VG**, Pretorius E. Iron and carbon monoxide enhance coagulation and attenuate fibrinolysis by different mechanisms. *Blood Coagul Fibrinolysis* 2014; **25**: 695-702 [PMID: 24732176 DOI: 10.1097/MBC.0000000000000128]

28 **Pretorius E**, Lipinski B. Differences in morphology of fibrin clots induced with thrombin and ferric ions and its pathophysiological consequences. *Heart Lung Circ* 2013; **22**: 447-449 [PMID: 23219312 DOI: 10.1016/j.hlc.2012.10.010]

29 **Bartoli CR**, Zhang D, Kang J, Hennessy-Strahs S, Restle D, Howard J, Redline G, Bermudez C, Atluri P, Acker MA. Clinical and In Vitro Evidence That Subclinical Hemolysis Contributes to LVAD Thrombosis. *Ann Thorac Surg* 2018; **105**: 807-814 [PMID: 28942075 DOI: 10.1016/j.athoracsur.2017.05.060]

30 **Cowger JA**, Romano MA, Shah P, Shah N, Mehta V, Haft JW, Aaronson KD, Pagani FD. Hemolysis: a harbinger of adverse outcome after left ventricular assist device implant. *J Heart Lung Transplant* 2014; **33**: 35-43 [PMID: 24418732 DOI: 10.1016/j.healun.2013.08.021]

31 **Uriel N**, Morrison KA, Garan AR, Kato TS, Yuzefpolskaya M, Latif F, Restaino SW, Mancini DM, Flannery M, Takayama H, John R, Colombo PC, Naka Y, Jorde UP. Development of a novel echocardiography ramp test for speed optimization and diagnosis of device thrombosis in continuous-flow left ventricular assist devices: the Columbia ramp study. *J Am Coll Cardiol* 2012; **60**: 1764-1775 [PMID: 23040584 DOI: 10.1016/j.jacc.2012.07.052]

32 **Hohner E**, Crow J, Moranville MP. Medication management for left ventricular assist device thrombosis. *Am J Health Syst Pharm* 2015; **72**: 1104-1113 [PMID: 26092961 DOI: 10.2146/ajhp140538]

33 **Dang G**, Epperla N, Muppidi V, Sahr N, Pan A, Simpson P, Baumann Kreuziger L. Medical Management of Pump-Related Thrombosis in Patients with Continuous-Flow Left Ventricular Assist Devices: A Systematic Review and Meta-Analysis. *ASAIO J* 2017; **63**: 373-385 [PMID: 27984314 DOI: 10.1097/MAT.0000000000000497]

34 **Najjar SS**, Slaughter MS, Pagani FD, Starling RC, McGee EC, Eckman P, Tatooles AJ, Moazami N, Kormos RL, Hathaway DR, Najarian KB, Bhat G, Aaronson KD, Boyce SW; HVAD Bridge to Transplant ADVANCE Trial Investigators. An analysis of pump thrombus events in patients in the HeartWare ADVANCE bridge to transplant and continued access protocol trial. *J Heart Lung Transplant* 2014; **33**: 23-34 [PMID: 24418731 DOI: 10.1016/j.healun.2013.12.001]

35 **Bistola V**, Parissis JT, Lekakis J, Filippatos G. Non-obstructive left ventricular assist device outflow thrombus: What is the appropriate management? *Int J Cardiol* 2016; **214**: 33-34 [PMID: 27057969 DOI: 10.1016/j.ijcard.2016.03.164]

36 **Goldstein DJ**, John R, Salerno C, Silvestry S, Moazami N, Horstmanshof D, Adamson R, Boyle A, Zucker M, Rogers J, Russell S, Long J, Pagani F, Jorde U. Algorithm for the diagnosis and management of suspected pump thrombus. *J Heart Lung Transplant* 2013; **32**: 667-670 [PMID: 23796150 DOI: 10.1016/j.healun.2013.05.002]

37 **Xia Y**, Forest S, Friedmann P, Chou LC, Patel S, Jorde U, Goldstein D. Factors Associated With Prolonged Survival in Left Ventricular Assist Device Recipients. *Ann Thorac Surg* 2019; **107**: 519-526 [PMID: 30316851 DOI: 10.1016/j.athoracsur.2018.08.054]

World Journal of Cardiology

Submit a Manuscript: https://www.f6publishing.com

World J Cardiol 2020 July 26; 12(7): 342-350

DOI: 10.4330/wjc.v12.i7.342

ISSN 1949-8462 (online)

ORIGINAL ARTICLE

Retrospective Study

Mortality and morbidity in patients with atrial fibrillation and liver cirrhosis

Yousef H Darrat, Aiman Smer, Claude-Samy Elayi, Gustavo X Morales, Fahad Alqahtani, Mohamad Alkhouli, John Catanzaro, Jignesh Shah, Mohsin Salih

ORCID number: Yousef H Darrat 0000-0003-1226-1227; Aiman Smer 0000-0002-1584-9934; Claude-Samy Elayi 0000-0002-2196-8788; Gustavo X Morales 0000-0002-4032-3184; Fahad Alqahtani 0000-0001-7524-4243; Mohamad Alkhouli 0000-0001-9531-1204; John Catanzaro 0000-0001-5671-1125; Jignesh Shah 0000-0001-5551-2562; Mohsin Salih 0000-0002-7598-5882.

Author contributions: Salih M designed the research; Darrat YH, Elayi CS, and Morales GX wrote the paper; Smer A, Catanzaro J, and Shah J performed research; Alqahtani F and Alkhouli M analyzed the data; all authors contributed to this paper.

Institutional review board statement: The National (Nationwide) Inpatient Sample is a large publicly available all-payer inpatient care database in the United States. Since it is publicly available and patient data is de-identified, an institutional review board approval was not required.

Informed consent statement: The National (Nationwide) Inpatient Sample is a large publicly available all-payer inpatient care database in the United States. Since it is publicly available and there was no patient interaction, informed

Yousef H Darrat, Department of Internal Medicine, Veterans Affairs Medical Center, Lexington, KY 40515, United States

Aiman Smer, Department of Internal Medicine, Creighton University, Omaha, NE 68178, United States

Claude-Samy Elayi, John Catanzaro, Department of Internal Medicine, University of Florida, Jacksonville, FL 32211, United States

Gustavo X Morales, Cardiac Electrophysiology, Grandview Medical Center, Birmingham, AL 35243, United States

Fahad Alqahtani, Department of Internal Medicine, University of Kentucky, Lexington, KY 40536, United States

Mohamad Alkhouli, Department of Internal Medicine, West Virginia University, Morgantown, WV 26506, United States

Jignesh Shah, Cardiac Electrophysiology, Boulder Heart, Boulder, CO 80303, United States

Mohsin Salih, Department of Internal Medicine, University of Southern Illinois, Springfield, IL 62702, United States

Corresponding author: Yousef H Darrat, MD, Attending Physician, Department of Internal Medicine, Veterans Affairs Medical Center, 1101 Veterans Drive, Lexington, KY 40502, United States. ydarat@hotmail.com

Abstract

BACKGROUND

Atrial fibrillation (AF) is the most common cardiac arrhythmia encountered in clinical practice. However, the outcomes associated with AF in hospitalized patients with liver cirrhosis are unknown.

AIM

To determine the outcomes of hospitalized patients with liver cirrhosis and AF.

METHODS

In this study, we examined morbidity and mortality of patients with concomitant AF and liver cirrhosis from the National Inpatient Sample database, the largest publicly available inpatient healthcare database in the United States.

RESULTS

A total of 696937 patients with liver cirrhosis were included, 45745 of whom had concomitant AF (6.6%). Liver cirrhosis patients with AF had higher rates of in-hospital mortality (12.6% *vs* 10.3%, $P < 0.001$), clinical stroke (1.6% *vs* 1.1%, $P < 0.001$), and acute kidney injury (28.2% *vs* 25.1%, $P < 0.001$), and less gastrointestinal bleeding (4.4% *vs* 5.1%, $P < 0.001$) and blood transfusion (22.5% *vs* 23.8%, $P < 0.001$) compared with those who did not have the arrhythmia. In addition, they had a longer length of stay (8 ± 10 d *vs* 7 ± 8 d, $P < 0.001$) and higher hospitalization costs (20720 ± 33210 $ *vs* 16272 ± 24166 $, $P < 0.001$).

CONCLUSION

In subjects with liver cirrhosis, AF is associated with higher rates of inpatient mortality, stroke, and acute kidney injury compared to those who do not have the cardiac arrhythmia.

Key words: Atrial fibrillation; Liver cirrhosis; Mortality; Stroke; Acute kidney injury; Prolonged hospitalization

Core tip: Atrial fibrillation is an adverse prognostic indicator in patients with liver cirrhosis. It is associated with increased inpatient mortality and a higher risk of cerebrovascular attack and renal failure. Furthermore, it leads to a longer hospital stay and admission to an acute care or a rehabilitation facility in this patient population.

Citation: Darrat YH, Smer A, Elayi CS, Morales GX, Alqahtani F, Alkhouli M, Catanzaro J, Shah J, Salih M. Mortality and morbidity in patients with atrial fibrillation and liver cirrhosis. *World J Cardiol* 2020; 12(7): 342-350
URL: https://www.wjgnet.com/1949-8462/full/v12/i7/342.htm
DOI: https://dx.doi.org/10.4330/wjc.v12.i7.342

INTRODUCTION

Atrial fibrillation (AF) is the most common cardiac rhythm disorder in the general population. It is estimated that 3 million adults in the United States have been diagnosed with the arrhythmia and the prevalence is estimated to rise to 12.1 million in 2030[1]. However, the prevalence and outcomes of AF in patients with liver cirrhosis is not well described. There are only a few relatively small-scale studies that measured its impact in patients with liver cirrhosis, and these show discordant results[2-5]. Furthermore, the mortality rate associated with AF in patients with liver cirrhosis remains not well defined[5,6]. Therefore, conflicting data exist about the prevalence and prognosis of patients with both conditions.

The National Inpatient Sample (NIS) database is the largest publicly available inpatient healthcare database in the United States and provides an opportunity for such a comparison. It is representative of the United States population admitted to the hospital, and also reflects daily practice. Using this data set, we aimed to compare the differences in morbidity, mortality, length of stay (LOS), and trends in patients with liver cirrhosis with and without AF.

MATERIALS AND METHODS

The NIS database was used to derive patient-relevant information between January 2003 and December 2014. It is an all-payer administrative claims-based database and contains information about patient discharges from approximately 1000 nonfederal hospitals in 45 states. It contains clinical and resource utilization information on 5 to 8

consent was not obtained.

Conflict-of-interest statement: The authors declare that they have no conflict of interest.

Manuscript source: Invited manuscript

Received: January 30, 2020
Peer-review started: January 30, 2020
First decision: March 24, 2020
Revised: May 10, 2020
Accepted: May 29, 2020
Article in press: May 29, 2020
Published online: July 26, 2020

P-Reviewer: Fedeli U, Gulel O, Vidal-Perez R
S-Editor: Ma YJ
L-Editor: Wang TQ
E-Editor: Wu YXJ

million discharges annually, with safeguards to protect the privacy of individual patients, physicians, and hospitals. These data are stratified to represent approximately 20% of United States in-patient hospitalizations across different hospitals and geographic regions (random sample). National estimates of the entire United States hospitalized population were calculated using the Agency for Healthcare Research and Quality sampling and weighting method.

Patients with a discharge diagnosis of hepatic cirrhosis [International Classification of Diseases-Ninth Revision-Clinical Modification (ICD-9-CM) codes 571.2, 571.3, 571, and 572.4] and diagnosis of AF (ICD-9-CM codes 427.31 and 427.32) during the study period were identified. Advanced liver cirrhosis was determined by the presence of hepatic cirrhosis and one or more of the following: Portal hypertension, ascites, hepatic encephalopathy, and hepatorenal syndrome (ICD-9-CM codes 572.3, 789.59, 572.2, and 572.4, respectively). The study flowsheet is presented in Figure 1.

The trends of AF in patients with hepatic cirrhosis during the 12-year study period were assessed using the Cochran–Armitage test for trend. Baseline patient co-morbidities and hospital characteristics were described. In-hospital morbidity, in-hospital outcomes including disposition, and cost of care of AF were assessed. We aimed to perform a comparative analysis based on the presence of AF in patients with liver cirrhosis. We anticipated significant heterogeneity regarding demographic and comorbid characteristics. To account for potential confounding factors and reduce the effect of selection bias, a propensity score matching model was developed using logistic regression to derive two matched groups for comparative outcome analysis using a nearest neighbor 1:1 variable ratio, parallel, balanced propensity matching model using a caliper of 0.01. Propensity scores were derived from multiple clinical and demographic covariates including the Elixhauser comorbidity index (Supplementary Table 1).

The primary endpoint was in-hospital death. Secondary outcomes included cerebral vascular accidents, transient ischemic attack, acute kidney injury, blood transfusion, gastrointestinal bleeding, LOS, hospital charges, and discharge disposition.

Statistical analysis

Patient-relevant descriptive statistics are presented as frequencies with percentages for categorical variables and as the mean ± SD for continuous variables. Baseline characteristics were compared between the groups using a Pearson chi-square test for categorical variables and an independent- samples *t*-test for continuous variables. We performed multiple imputations to impute missing values for the race (missing in 13.2% of observations) using the fully conditional specification method (an iterative Markov Chain Monte Carlo algorithm) in SPSS Statistics 24 (IBM Corporation, Armonk, NY, United States). A Cochran-Armitage test was used to evaluate trends of AF in patients with cirrhosis. Matched categorical variables are presented as frequencies with percentages and were compared using the McNemar test. Matched continuous variables are presented as the mean ± SD and were compared using a paired-samples *t*-test. All statistical analyses were performed using SPSS Statistics 24 and R version 3.3.1 (Bell Laboratories, New Jersey, NJ, United States), and the statistical review of the study was performed by a biomedical statistician.

RESULTS

We identified 696937 patients with a primary diagnosis of hepatic cirrhosis, 45745 of whom had a concomitant diagnosis of AF (6.6%). Patients with AF were older and had more co-morbidities including hypertension, diabetes mellitus, coronary artery disease, chronic pulmonary disease, chronic kidney disease, and peripheral vascular disease. The baseline characteristics of patients with liver cirrhosis categorized by the presence of AF are presented in Table 1.

After accounting for covariates using propensity score matching to patients without AF (Table 2), we found that patients with AF had higher rates of in-hospital mortality (12.6% *vs* 10.3%, $P < 0.001$), clinical stroke (1.6% *vs* 1.1%, $P < 0.001$), and acute kidney injury (28.2% *vs* 25.1%, $P < 0.001$), and less gastrointestinal bleeding (4.4% *vs* 5.1%, $P < 0.001$) and blood transfusion (22.5% *vs* 23.8%, $P < 0.001$). The outcomes of propensity matched hepatic cirrhosis patients categorized by presence of AF are presented in Table 3.

We performed a regression analysis excluding stroke and acute kidney injury and found that predictors of in-hospital mortality in patients with liver cirrhosis and AF included older age (66-85 years, odds ratio [OR] = 2.014; above 86 years, OR = 2.449),

Table 1 Characteristics of hepatic cirrhosis patients stratified by presence of atrial fibrillation among 2003-2014

Characteristic	Non-AF (*n* = 651192)	AF (*n* = 45745)	*P* value
Age (mean ± SD, yr)	54 ± 11	65 ± 11	< 0.001
Female, *n* (%)	171592 (28.3)	9244 (20.2)	< 0.001
Race, *n* (%)			< 0.001
Caucasian	343516 (65.8)	30624 (76.2)	
African American	57718 (11.1)	3674 (9.1)	
Hispanic	91439 (17.5)	4130 (10.3)	
Medical comorbidity, *n* (%)			
Hypertension	215381 (35.7)	23136 (50.7)	< 0.001
Diabetes mellitus	126047 (20.8)	12282 (26.8)	< 0.001
Prior sternotomy	8602 (1.4)	2926 (6.4)	< 0.001
Chronic pulmonary disease	106826 (17.6)	14176 (31)	< 0.001
Chronic renal failure	62065 (10.3)	9884 (21.6)	< 0.001
Anemia	186205 (30.8)	13771 (30.1)	0.004
Chronic alcohol use	418372 (69.1)	29194 (63.8)	< 0.001
Hypothyroidism	35221 (5.8)	4662 (10.2)	< 0.001
Peripheral vascular disease	16026 (2.6)	3518 (7.7)	< 0.001
Smoking	159957 (26.4)	8420 (18.4)	< 0.001
Coronary artery disease	31636 (5.2)	6994 (15.3)	< 0.001
Hospital characteristic, *n* (%)			
Teaching hospital	303751 (50.4)	22069 (48.4)	< 0.001
Rural area	57619 (9.6)	4378 (9.6)	0.761
Hospital bed-size			< 0.001
Small	72730 (12.1)	5903 (13)	
Medium	156654 (26)	11616 (25.5)	
Large	373165 (61.9)	28057 (61.6)	
Primary payer, *n* (%)			< 0.001
Medicare/Medicaid	350547 (57.9)	33371 (73)	
Private including HMO	140515 (23.2)	8278 (18.1)	
Self-pay	72366 (12)	2287 (5)	

AF: Atrial fibrillation; HMO: Health maintenance organization.

congestive heart failure (CHF; OR = 1.587), and vascular disease (OR = 1.218). In AF patients with a CHA_2DS_2-VASc score of 2 or higher, there were more with clinical stroke ($P < 0.001$) and need for blood transfusion ($P = 0.018$).

Patients with AF had a longer LOS (8 ± 10 d *vs* 7 ± 8 d, $P < 0.001$) and higher hospitalization costs (20720 ± 33210 $ *vs* 16272 ± 24166 $, $P < 0.001$) compared to those without. They were also less likely to be discharged home and more likely to go to a rehabilitation or acute care facility. The prevalence of AF according to different age groups and gender for in-patients with liver cirrhosis compared to national estimates are presented in Table 4.

DISCUSSION

The main finding of this study is that patients with hepatic cirrhosis and concomitant

Table 2 Characteristics of propensity matched hepatic cirrhosis patients stratified by presence of atrial fibrillation among 2003-2014

Characteristic	Non-AF (*n* = 45504)	AF (*n* = 45504)	*P* value
Age (mean ± SD, yr)	65 ± 11	65 ± 11	0.827
Female, *n* (%)	9174 (20.2)	9221 (20.3)	0.703
Race, *n* (%)			0.561
Caucasian	34548 (75.9)	34633 (76.1)	
African American	4314 (9.5)	4179 (9.2)	
Hispanic	4644 (10.2)	4692 (10.3)	
Medical comorbidity, *n* (%)			
Hypertension	23142 (50.9)	22972 (50.5)	0.251
Diabetes mellitus	12456 (27.4)	12229 (26.9)	0.091
Prior sternotomy	2610 (5.7)	2843 (6.2)	0.07
Chronic pulmonary disease	14165 (31.1)	14051 (30.9)	0.404
Chronic renal failure	9595 (21.1)	9751 (21.4)	0.192
Anemia	13623 (29.9)	13690 (30.1)	0.634
Chronic alcohol use	29054 (63.8)	29060 (63.9)	0.972
Hypothyroidism	4456 (9.8)	4603 (10.1)	0.103
Peripheral vascular disease	3420 (7.5)	3463 (7.6)	0.592
Smoking	8264 (18.2)	8405 (18.5)	0.222
Coronary artery disease	6893 (15.1)	6898 (15.2)	0.969
Hospital characteristic, *n* (%)			
Teaching hospital	22061 (48.5)	22129 (48.6)	0.567
Rural area	41154 (90.4)	41141 (90.4)	0.893
Hospital bed-size			0.253
Small	6062 (13.3)	5871 (12.9)	
Medium	11469 (25.2)	11569 (25.4)	
Large	27973 (61.5)	28064 (61.7)	
Primary payer, *n* (%)			0.052
Medicare/ Medicaid	33277 (73.1)	33138 (72.8)	
Private including HMO	8389 (18.4)	8270 (18.2)	
Self-pay	2101 (4.6)	2287 (5)	

AF: Atrial fibrillation; HMO: Health maintenance organization.

AF are at an increased risk of in-hospital mortality, stroke, and acute kidney injury compared to their counterparts without the arrhythmia. Furthermore, the LOS and cost are higher in this group of patients.

Liver cirrhosis and the development of AF

Liver cirrhosis is the eighth leading cause of death in the United States[7] and its prevalence is increasing due to non-alcoholic steatohepatitis[8]. The prevalence of AF in the general population varies based on age as well as the geographic location[9]. This is also true among patients with liver cirrhosis, with an estimated prevalence of AF varying geographically from 0.15% to 10.9%[2-4]. The reported prevalence seems even higher in patients presenting for liver transplant with significant model for end-stage liver disease scores at 42.1%[5]. However, the latest group is sicker and may not be well representative of the overall population. In our study, the prevalence of AF in patients with liver cirrhosis was 6.6%, which is very similar to that based on estimates in the general population according to age and gender as shown in Table 4. This indicates

Table 3 In-hospital outcomes of propensity matched hepatic cirrhosis patients stratified by presence of atrial fibrillation among 2003-2014

	Non-AF (*n* = 45504)	AF (*n* = 45504)	*P* value
Clinical outcome, *n* (%)			
In-hospital death	4697 (10.3)	5755 (12.6)	< 0.001
Gastrointestinal bleeding	2329 (5.1)	1995 (4.4)	< 0.001
Blood transfusion	10841 (23.8)	10219 (22.5)	< 0.001
Transient ischemic attack	124 (0.3)	134 (0.3)	0.575
Clinical stroke	496 (1.1)	722 (1.6)	< 0.001
Acute kidney injury	11433 (25.1)	12810 (28.2)	< 0.001
Discharge status, *n* (%)			< 0.001
Discharged home	27646 (60.8)	25705 (56.5)	
Discharged SNF/NH/IC	12242 (26.9)	13114 (28.8)	
Length of stay (mean ± SD, d)	7 ± 8	8 ± 10	< 0.001
Hospital cost (mean ± SD, $)	16272 ± 24166	20720 ± 33210	< 0.001

AF: Atrial fibrillation; SNF: Skilled nursing facility; NH: Nursing home; IC: Intermediate care.

Table 4 The prevalence of atrial fibrillation according to age and gender for in-patients with liver cirrhosis compared to the general in-patient population

Age (yr)	Gender	AF in liver cirrhosis (%)	AF national estimate (%)
< 45	Male	1.70	1.76
	Female	0.90	0.88
46-65	Male	5.90	5.91
	Female	3.20	3.16
66-85	Male	20.00	20.03
	Female	16.00	15.99
> 86	Male	34.10	34.18
	Female	33.50	33.60

AF: Atrial fibrillation.

that liver cirrhosis *per se* is not associated with an increased risk of AF.

Furthermore, in a prospective study that included patients with liver cirrhosis followed for 24 mo, AF occurred in 6.2% and was found to be related to age[10]. Similarly, Gundling *et al*[3] demonstrated that AF occurred in 16.4% of a sample of patients with liver cirrhosis and correlated with advanced age and co-morbidities including atherosclerotic disease, hyperlipidemia, and diabetes mellitus. Likewise, in our study, patients with hepatic cirrhosis and associated AF had the known risk factors for developing atrial dysrhythmia, including age, hypertension, and diabetes mellitus.

Mortality and morbidity in patients with AF and liver cirrhosis

In some previous studies, mortality was not found to be increased in liver cirrhosis patients with AF compared to controls[6,10]. However, the 30-d and 1-year survival rates were found to be lower in patients with a preoperative diagnosis of AF undergoing liver transplant[5]. Besides, a meta-analysis that included 385866 patients with liver cirrhosis showed that AF was associated with a significantly increased mortality risk in cirrhotic patients with the pooled odds ratio of 1.44 (95%CI: 1.36–1.53, I^2 = 0%)[11]. Our study has almost double the number of subjects and has shown increased

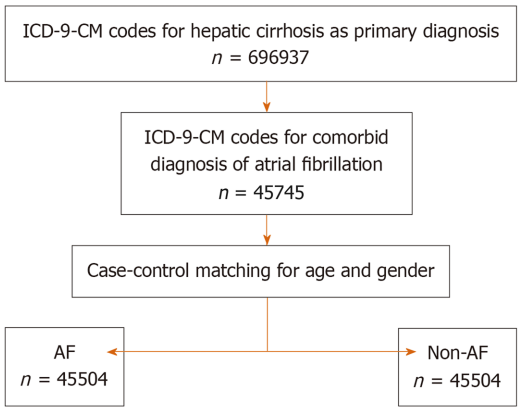

Figure 1 Study flowsheet. AF: Atrial fibrillation.

mortality, specifically in hospitalized patients. Furthermore, they were more likely to be admitted to a rehabilitation or an acute care facility, indicating that they tend to be sicker. As seen in other studies[12], we found that CHA_2DS_2-VASc of 2 or more was associated with a higher risk of stroke. The reasons that AF is linked to higher mortality and morbidity are likely higher rates of stroke and acute kidney injury (AKI). Also, long QT is commonly seen in advanced liver disease and is a strong predictor of increased death[13].

In our study, the risk of gastrointestinal bleeding and blood transfusion is higher in the non-AF group. This finding can be possibly explained using β-blockers in patients with AF, which can be protective in esophageal varices. However, this cannot be inferred from this study since medication use was not captured. The higher rate of AKI may also deter from prescribing anticoagulants and thereby this may lead to less hemorrhage. Also, the use of oral anticoagulants is associated with a higher risk of bleeding in liver cirrhosis due to the presence of thrombocytopenia or increased INR[14]. Therefore, anticoagulants are under-utilized in this population[15], which may explain the higher stroke rate but at the same time a lower bleeding risk.

Limitations

This study comes with limitations inherent to retrospective analysis[16-19]. Mainly, the NIS database consists of time-limited administrative data that is related to a specific hospitalization. The possibility of incomplete or misclassified diagnoses and procedures, or omitted documentation might have existed. Specifically, important patient-level information could not be retrieved, such as how AF was documented, and the list of medications used (including β-blockers and anticoagulants). We may have also missed patients who were not correctly labeled as having AF or liver cirrhosis, likewise, they may have been misdiagnosed as having either condition. However, the NIS database is the largest administrative United States data set with admission and discharge level information. Therefore, NIS analysis provides the opportunity to compare and reveal patients' characteristics, diagnoses, and outcomes with a strong statistical power. Even if there might be some coding errors or omissions, these should be minimized by the large number of patients analyzed.

In our investigation, we have included certain medical comorbidities (hypertension, diabetes mellitus, renal failure, chronic obstructive pulmonary disease, anemia, alcohol use, hypothyroidism, peripheral vascular disease, smoking, and coronary artery disease), but other variables that could be associated with measured outcomes were not available, additionally due to the lack of randomization. Therefore, there might have been unmeasured clinical variables related to the outcomes that were not considered. Furthermore, the database does not provide any data after hospital discharge; therefore, long-term outcomes beyond hospital discharge cannot be assessed. However, the data represents real-life inpatient practice and reflects actual hospital outcomes in patients with liver cirrhosis and AF that can guide clinical management as well as policy-making strategies.

AF is a predictor of increased in-hospital-mortality in patients with liver cirrhosis and is associated with a higher risk of stroke and AKI but interestingly less gastrointestinal bleeding and need for blood transfusion. Besides, patients with liver cirrhosis and AF have a longer length of stay and higher cost of hospitalization compared to those who do not have the arrhythmia. It is essential to recognize AF as

an adverse prognostic indicator in this population to provide them with an appropriate management strategy and to reduce associated hospitalization costs.

ARTICLE HIGHLIGHTS

Research background

Atrial fibrillation (AF) is the most common arrhythmia encountered in medical practice and is associated with adverse outcomes. However, the outcomes of AF in the special population of patients with liver cirrhosis have not been well studied and the results of several studies are conflicting.

Research motivation

Mortality rate and clinical outcomes of patients with concomitant AF and liver cirrhosis are an integral aspect of clinical decision and policymaking. Realizing the clinical impact of such disorders in a patient paves the path to design prospective studies.

Research objectives

We aimed to investigate if death is higher in patients with liver cirrhosis who have AF and to also assess outcomes during hospitalization. Understanding the outcomes will assist future research in designing prospective studies and randomized trials to improve morbidity and mortality.

Research methods

In this study, we examined outcomes of patients with concomitant AF and liver cirrhosis from the National Inpatient Sample database, the largest publicly available inpatient healthcare resource in the United States. We investigated inpatient mortality rate as a primary outcome. Secondary outcomes included cerebral vascular accidents, transient ischemic attack, acute kidney injury, blood transfusion, gastrointestinal bleeding, length of stay, hospital charges, and discharge disposition.

Research results

Inpatient mortality was found to be higher in patients with concomitant AF and liver cirrhosis compared to patients without the arrhythmia. We also found that it was associated with higher rates of stroke and acute kidney injury, and prolonged hospitalization.

Research conclusions

AF is an adverse prognostic indicator in inpatients with liver cirrhosis. It is associated with increased rates of death, stroke, and acute kidney injury but interestingly less gastrointestinal bleeding and need for blood transfusion. Also, it is associated with prolonged hospitalization and increased cost.

Research perspectives

Future studies are needed to prospectively investigate the impact of the arrhythmia in liver cirrhosis.

REFERENCES

1 **Colilla S**, Crow A, Petkun W, Singer DE, Simon T, Liu X. Estimates of current and future incidence and prevalence of atrial fibrillation in the U.S. adult population. *Am J Cardiol* 2013; **112**: 1142-1147 [PMID: 23831166 DOI: 10.1016/j.amjcard.2013.05.063]

2 **Zamirian M**, Sarmadi T, Aghasadeghi K, Kazemi MB. Liver cirrhosis prevents atrial fibrillation: A reality or just an illusion? *J Cardiovasc Dis Res* 2012; **3**: 109-112 [PMID: 22629027 DOI: 10.4103/0975-3583.95363]

3 **Gundling F**, Schmidtler F, Zelihic E, Seidl H, Haller B, Ronel J, Löffler N, Schepp W. [Frequency of cardiac arrhythmia in patients with liver cirrhoses and evaluation of associated factors]. *Z Gastroenterol* 2012; **50**: 1149-1155 [PMID: 23150106 DOI: 10.1055/s-0032-1313182]

4 **Bargehr J**, Trejo-Gutierrez JF, Patel T, Rosser B, Aranda-Michel J, Yataco ML, Taner CB. Preexisting atrial fibrillation and cardiac complications after liver transplantation. *Liver Transpl* 2015; **21**: 314-320 [PMID: 25488693 DOI: 10.1002/lt.24060]

5 **Vannucci A**, Rathor R, Vachharajani N, Chapman W, Kangrga I. Atrial fibrillation in patients undergoing liver transplantation-a single-center experience. *Transplant Proc* 2014; **46**: 1432-1437 [PMID: 24935310

DOI: 10.1016/j.transproceed.2014.02.020]
6 **Lee H**, Choi EK, Rhee TM, Lee SR, Lim WH, Kang SH, Han KD, Cha MJ, Oh S. Cirrhosis is a risk factor for atrial fibrillation: A nationwide, population-based study. *Liver Int* 2017; **37**: 1660-1667 [PMID: 28432810 DOI: 10.1111/liv.13459]
7 **Murray CJ**, Atkinson C, Bhalla K, Birbeck G, Burstein R, Chou D, Dellavalle R, Danaei G, Ezzati M, Fahimi A, Flaxman D, Foreman, Gabriel S, Gakidou E, Kassebaum N, Khatibzadeh S, Lim S, Lipshultz SE, London S, Lopez, MacIntyre MF, Mokdad AH, Moran A, Moran AE, Mozaffarian D, Murphy T, Naghavi M, Pope C, Roberts T, Salomon J, Schwebel DC, Shahraz S, Sleet DA, Murray, Abraham J, Ali MK, Atkinson C, Bartels DH, Bhalla K, Birbeck G, Burstein R, Chen H, Criqui MH, Dahodwala, Jarlais, Ding EL, Dorsey ER, Ebel BE, Ezzati M, Fahami, Flaxman S, Flaxman AD, Gonzalez-Medina D, Grant B, Hagan H, Hoffman H, Kassebaum N, Khatibzadeh S, Leasher JL, Lin J, Lipshultz SE, Lozano R, Lu Y, Mallinger L, McDermott MM, Micha R, Miller TR, Mokdad AA, Mokdad AH, Mozaffarian D, Naghavi M, Narayan KM, Omer SB, Pelizzari PM, Phillips D, Ranganathan D, Rivara FP, Roberts T, Sampson U, Sanman E, Sapkota A, Schwebel DC, Sharaz S, Shivakoti R, Singh GM, Singh D, Tavakkoli M, Towbin JA, Wilkinson JD, Zabetian A, Murray, Abraham J, Ali MK, Alvardo M, Atkinson C, Baddour LM, Benjamin EJ, Bhalla K, Birbeck G, Bolliger I, Burstein R, Carnahan E, Chou D, Chugh SS, Cohen A, Colson KE, Cooper LT, Couser W, Criqui MH, Dabhadkar KC, Dellavalle RP, Jarlais, Dicker D, Dorsey ER, Duber H, Ebel BE, Engell RE, Ezzati M, Felson DT, Finucane MM, Flaxman S, Flaxman AD, Fleming T, Foreman, Forouzanfar MH, Freedman G, Freeman MK, Gakidou E, Gillum RF, Gonzalez-Medina D, Gosselin R, Gutierrez HR, Hagan H, Havmoeller R, Hoffman H, Jacobsen KH, James SL, Jasrasaria R, Jayarman S, Johns N, Kassebaum N, Khatibzadeh S, Lan Q, Leasher JL, Lim S, Lipshultz SE, London S, Lopez, Lozano R, Lu Y, Mallinger L, Meltzer M, Mensah GA, Michaud C, Miller TR, Mock C, Moffitt TE, Mokdad AA, Mokdad AH, Moran A, Naghavi M, Narayan KM, Nelson RG, Olives C, Omer SB, Ortblad K, Ostro B, Pelizzari PM, Phillips D, Raju M, Razavi H, Ritz B, Roberts T, Sacco RL, Salomon J, Sampson U, Schwebel DC, Shahraz S, Shibuya K, Silberberg D, Singh JA, Steenland K, Taylor JA, Thurston GD, Vavilala MS, Vos T, Wagner GR, Weinstock MA, Weisskopf MG, Wulf S, Murray; U. S. Burden of Disease Collaborators. The state of US health, 1990-2010: burden of diseases, injuries, and risk factors. *JAMA* 2013; **310**: 591-608 [PMID: 23842577 DOI: 10.1001/jama.2013.13805]
8 **Kabbany MN**, Conjeevaram Selvakumar PK, Watt K, Lopez R, Akras Z, Zein N, Carey W, Alkhouri N. Prevalence of Nonalcoholic Steatohepatitis-Associated Cirrhosis in the United States: An Analysis of National Health and Nutrition Examination Survey Data. *Am J Gastroenterol* 2017; **112**: 581-587 [PMID: 28195177 DOI: 10.1038/ajg.2017.5]
9 **Darrat YH**, Shah J, Elayi CS, Morales GX, Naditch-Brûlé L, Brette S, Taniou C, Kowey PR, Schwartz PJ. Regional Lack of Consistency in the Management of Atrial Fibrillation (from the RECORD-AF Trial). *Am J Cardiol* 2017; **119**: 47-51 [PMID: 27816112 DOI: 10.1016/j.amjcard.2016.09.009]
10 **Mwalitsa JP**, Maimone S, Filomia R, Alibrandi A, Saitta C, Caccamo G, Cacciola I, Spinella R, Oliva G, Lembo T, Vadalà D, Gambino G, Raimondo G, Squadrito G. Atrial fibrillation in patients with cirrhosis. *Liver Int* 2016; **36**: 395-400 [PMID: 26235424 DOI: 10.1111/liv.12928]
11 **Chokesuwattanaskul R**, Thongprayoon C, Bathini T, O'Corragain OA, Sharma K, Preechawat S, Wijarnpreecha K, Kröner PT, Ungprasert P, Cheungpasitporn W. Epidemiology of atrial fibrillation in patients with cirrhosis and clinical significance: a meta-analysis. *Eur J Gastroenterol Hepatol* 2019; **31**: 514-519 [PMID: 30451705 DOI: 10.1097/MEG.0000000000001315]
12 **Cho MS**, Lee CH, Kim J, Ahn JM, Han M, Nam GB, Choi KJ, Kim YH. Clinical Implications of Preoperative Nonvalvular Atrial Fibrillation with Respect to Postoperative Cardiovascular Outcomes in Patients Undergoing Non-Cardiac Surgery. *Korean Circ J* 2020; **50**: 148-159 [PMID: 31845556 DOI: 10.4070/kcj.2019.0219]
13 **Kim SM**, George B, Alcivar-Franco D, Campbell CL, Charnigo R, Delisle B, Hundley J, Darrat Y, Morales G, Elayi SC, Bailey AL. QT prolongation is associated with increased mortality in end stage liver disease. *World J Cardiol* 2017; **9**: 347-354 [PMID: 28515853 DOI: 10.4330/wjc.v9.i4.347]
14 **Niizuma H**, Suzuki J, Yonemitsu T, Otsuki T. Spontaneous intracerebral hemorrhage and liver dysfunction. *Stroke* 1988; **19**: 852-856 [PMID: 2455366 DOI: 10.1161/01.str.19.7.852]
15 **Kuo L**, Chao TF, Liu CJ, Lin YJ, Chang SL, Lo LW, Hu YF, Tuan TC, Liao JN, Chung FP, Chen TJ, Lip GYH, Chen SA. Liver Cirrhosis in Patients With Atrial Fibrillation: Would Oral Anticoagulation Have a Net Clinical Benefit for Stroke Prevention? *J Am Heart Assoc* 2017; **6** [PMID: 28645935 DOI: 10.1161/JAHA.116.005307]
16 **Ogunbayo GO**, Charnigo R, Darrat Y, Shah J, Patel R, Suffredini J, Wilson W, Parrott K, Kusterer N, Biase LD, Natale A, Morales G, Elayi CS. Comparison of Complications of Catheter Ablation for Ventricular Arrhythmias in Adults With Versus Without Structural Heart Disease. *Am J Cardiol* 2018; **122**: 1345-1351 [PMID: 30115423 DOI: 10.1016/j.amjcard.2018.07.001]
17 **Elayi CS**, Darrat Y, Suffredini JM, Misumida N, Shah J, Morales G, Wilson W, Bidwell K, Czarapata M, Parrott K, Di Biase L, Natale A, Ogunbayo GO. Sex differences in complications of catheter ablation for atrial fibrillation: results on 85,977 patients. *J Interv Card Electrophysiol* 2018; **53**: 333-339 [PMID: 30062452 DOI: 10.1007/s10840-018-0416-1]
18 **Ogunbayo GO**, Charnigo R, Darrat Y, Morales G, Kotter J, Olorunfemi O, Elbadawi A, Sorrell VL, Smyth SS, Elayi CS. Incidence, predictors, and outcomes associated with pneumothorax during cardiac electronic device implantation: A 16-year review in over 3.7 million patients. *Heart Rhythm* 2017; **14**: 1764-1770 [PMID: 28735733 DOI: 10.1016/j.hrthm.2017.07.024]
19 **Romero J**, Ogunbayo G, Elayi SC, Darrat Y, Rios SA, Diaz JC, Alviz I, Cerna L, Gabr M, Chernobelsky E, Mohanty S, Trivedi CG, Della Rocca DG, Natale A, Di Biase L. Safety of catheter ablation for atrial fibrillation in the octogenarian population. *J Cardiovasc Electrophysiol* 2019; **30**: 2686-2693 [PMID: 31506996 DOI: 10.1111/jce.14165]

World Journal of Cardiology

Submit a Manuscript: https://www.f6publishing.com

World J Cardiol 2020 July 26; 12(7): 351-361

DOI: 10.4330/wjc.v12.i7.351

ISSN 1949-8462 (online)

ORIGINAL ARTICLE

Observational Study

Sonographic muscle mass assessment in patients after cardiac surgery

Stavros Dimopoulos, Vasiliki Raidou, Dimitrios Elaiopoulos, Foteini Chatzivasiloglou, Despoina Markantonaki, Efterpi Lyberopoulou, Ioannis Vasileiadis, Katerina Marathias, Serafeim Nanas, Andreas Karabinis

ORCID number: Stavros Dimopoulos 0000-0003-2199-3788; Vasiliki Raidou 0000-0001-8964-8783; Dimitrios Elaiopoulos 0000-0002-6368-2817; Foteini Chatzivasiloglou 0000-0002-4698-3458; Despoina Markantonaki 0000-0003-2841-8110; Efterpi Lyberopoulou 0000-0002-0614-5740; Ioannis Vasileiadis 0000-0002-9529-9361; Katerina Marathias 0000-0003-2114-4700; Serafeim Nanas 0000-0001-9359-815X; Andreas Karabinis 0000-0002-5666-7221.

Author contributions: Dimopoulos S conceptualized and designed the study; Karabinis A supervised the study; Dimopoulos S, Raidou V, Markantonaki D, Marathias K, Vasileiadis I and Nanas S were involved in the data curation and analysis, projet administration and provided scientific review; Dimopoulos S, Raidou V, Elaiopoulos D, Chatzivasiloglou F and Lyberopoulou E performed the research and collected the data; Dimopoulos S and Raidou V wrote the paper, reviewed, edited and revised the final version of the manuscript; all authors have read and approved the final manuscript.

Institutional review board statement: The study was reviewed and approved by Ethics Committee of the Onassis Cardiac

Stavros Dimopoulos, Dimitrios Elaiopoulos, Despoina Markantonaki, Efterpi Lyberopoulou, Katerina Marathias, Andreas Karabinis, Department of Cardiac Surgery ICU, Onassis Cardiac Surgery Center, Athens 17674, Greece

Stavros Dimopoulos, Vasiliki Raidou, Foteini Chatzivasiloglou, Ioannis Vasileiadis, Serafeim Nanas, Clinical Ergospirometry, Exercise and Rehabilitation Laboratory, National and Kapodistrian University of Athens, Athens 10676, Greece

Corresponding author: Stavros Dimopoulos, PhD, Doctor, Postdoc, Research Scientist, Senior Researcher, Staff Physician, Department of Cardiac Surgery ICU, Onassis Cardiac Surgery Center, No. 356 L. Syggrou, Athens 17674, Greece. stdimop@gmail.com

Abstract

BACKGROUND

Patients undergoing cardiac surgery particularly those with comorbidities and frailty, experience frequently higher rates of post-operative morbidity, mortality and prolonged hospital length of stay. Muscle mass wasting seems to play important role in prolonged mechanical ventilation (MV) and consequently in intensive care unit (ICU) and hospital stay.

AIM

To investigate the clinical value of skeletal muscle mass assessed by ultrasound early after cardiac surgery in terms of duration of MV and ICU length of stay.

METHODS

In this observational study, we enrolled consecutively all patients, following their admission in the Cardiac Surgery ICU within 24 h of cardiac surgery. Bedside ultrasound scans, for the assessment of quadriceps muscle thickness, were performed at baseline and every 48 h for seven days or until ICU discharge. Muscle strength was also evaluated in parallel, using the Medical Research Council (MRC) scale.

RESULTS

Of the total 221 patients enrolled, ultrasound scans and muscle strength assessment were finally performed in 165 patients (patients excluded if ICU stay < 24 h). The muscle thickness of rectus femoris (RF), was slightly decreased by 2.2%

Surgery Center, Athens, Greece, No. 607/17.11.17.

Informed consent statement: Patients were not required to give informed consent to the study because the analysis used anonymous data that were obtained after each patient agreed to treatment by written consent.

Conflict-of-interest statement: There are no conflicts of interest to report.

Data sharing statement: No additional data are available.

STROBE statement: The authors have read the STROBE Statement—checklist of items, and the manuscript was prepared and revised according to the STROBE Statement—checklist of items.

Manuscript source: Invited manuscript

Received: February 29, 2020
Peer-review started: February 29, 2020
First decision: April 7, 2020
Revised: May 11, 2020
Accepted: June 17, 2020
Article in press: June 17, 2020
Published online: July 26, 2020

P-Reviewer: El Amrousy D, Sicari R
S-Editor: Liu M
L-Editor: A
E-Editor: Zhang YL

[(95% confidence interval (CI): - 0.21 to 0.15), n = 9; P = 0.729] and the combined muscle thickness of the vastus intermedius (VI) and RF decreased by 3.5% [(95%CI: - 0.4 to 0.22), n = 9; P = 0.530]. Patients whose combined VI and RF muscle thickness was below the recorded median values (2.5 cm) on day 1 (n = 80), stayed longer in the ICU (47 ± 74 h *vs* 28 ± 45 h, P = 0.02) and remained mechanically ventilated more (17 ± 9 h *vs* 14 ± 9 h, P = 0.05). Moreover, patients with MRC score ≤ 48 on day 3 (n = 7), required prolonged MV support compared to patients with MRC score ≥ 49 (n = 33), (44 ± 14 h *vs* 19 ± 9 h, P = 0.006) and had a longer duration of extracorporeal circulation was (159 ± 91 min *vs* 112 ± 71 min, P = 0.025).

CONCLUSION

Skeletal quadriceps muscle thickness assessed by ultrasound shows a trend to a decrease in patients after cardiac surgery post-ICU admission and is associated with prolonged duration of MV and ICU length of stay.

Key words: Intensive care unit-acquired weakness; Cardiac surgery; Skeletal muscle wasting; Muscle ultrasound; Quadriceps femoris; Muscle mass

Core tip: Muscle mass wasting may occur in post-cardiac surgery patients affecting outcome. We assessed the clinical significance of muscle mass in post-cardiac surgery after intensive care unit (ICU) admission. Sonographic assessment of quadriceps muscle thickness was performed to 165 post-cardiac surgery patients for 7 d or until ICU discharge. The results of the study showed a trend to a decreased muscle mass in post-cardiac surgery patients. There was also an association between muscle mass andduration of mechanical ventilation support and ICU length of stay. Sonographic assessment seems to be a valid method to quantify quadriceps muscle mass in patients after cardiac surgery.

Citation: Dimopoulos S, Raidou V, Elaiopoulos D, Chatzivasiloglou F, Markantonaki D, Lyberopoulou E, Vasileiadis I, Marathias K, Nanas S, Karabinis A. Sonographic muscle mass assessment in patients after cardiac surgery. *World J Cardiol* 2020; 12(7): 351-361
URL: https://www.wjgnet.com/1949-8462/full/v12/i7/351.htm
DOI: https://dx.doi.org/10.4330/wjc.v12.i7.351

INTRODUCTION

Factors such as immobilization, prolonged mechanical ventilation (MV) and sedation elicit the development of neuromuscular complications to patients admitted in the intensive care unit (ICU)[1]. These functional and structural alterations of muscle and nerve fibers contribute to muscle weakness and atrophy[2]. Muscle mass wasting is detected mainly to lower limbs in critically ill ventilated patients early after their admission in ICU[3]. Low skeletal muscle area is a risk factor for mortality[4] and has been linked to long term disability[5,6] and prolonged hospitalization[7].

Previous studies have also described that patients after cardiothoracic surgery exhibit muscle mass loss[7-9], as assessed by computed tomography scanning[10,11]. This muscle weakness is associated with frailty, morbidity, prolonged hospital length of stay and low quality of life after hospital discharge. In addition, low skeletal muscle density before cardiac surgery is related to decreased muscle function post-operatively and increased mortality[11].

Muscle ultrasound is a reliable and noninvasive diagnostic tool in evaluating muscle architecture changes. It has been used widely in the ICU during the last few years. It can be performed at the bedside providing real-time quantitative and qualitative data for muscle tissue[12,13]. Recent systematic reviews have confirmed its clinical and prognostic value to the measurement of peripheral skeletal muscle alterations[14] and to the early detection of intensive care unit acquired weakness (ICUAW)[15]. However, its clinical and prognostic value in patients after cardiac surgery has not been thoroughly investigated yet.

We hypothesized that cardiac surgery patients would present a decrease in

sonographically quantified quadriceps muscle mass during their ICU stay and that decreased quadriceps muscle mass would be associated with prolonged MV support and ICU stay.

Aim of the present study is to evaluate sonographically quadriceps muscle mass in cardiac surgery patients during their ICU stay and assess its clinical and prognostic value.

MATERIALS AND METHODS

Study population

This observational study was conducted at the Cardiac Surgery ICU of Onassis Cardiac Surgery Center from February 1, 2018 to May 15, 2018. The research was approved by Ethics Committee of the Onassis Cardiac Surgery Center (No. 607/17.11.17) with obtained patients' informed consent and carried out in accordance with the ethical standards set by the Declaration of Helsinki.

Inclusion criteria were consecutive patients, over 18 years old, following their admission in the Cardiac Surgery ICU within 24 h of cardiac surgery.

Participants who were unable to get a muscle ultrasound assessment within 24 h of admission in the ICU were excluded from the study. Other exclusion criteria were severe obesity [body mass index (BMI) > 35kg/m^2], patients with open chest-sternotomy, lobectomy or Central Extracorporeal Membrane Oxygenation, extensive peripheral thigh edema and preexisting neuromuscular disease. Moreover, patients who were re-admitted to the ICU were excluded from the study.

Study design

This was a prospective observational study conducted in a single center Cardiac Surgery ICU. All patients enrolled to the study were subjected to ultrasound measurement of quadriceps muscle mass thickness and muscle strength evaluation using the Medical Research Council (MRC) scale. Ultrasound scans and MRC scale assessment were performed, every 48 h for seven days or until ICU discharge, by previously experienced ICU staff and study researchers in muscle ultrasound. Routine physiotherapy intervention was also recorded in parallel.

The duration of MV, ICU stay and the ICU outcome of enrolled patients were also recorded.

The primary outcome of the present study was the prognostic assessment of quadriceps muscle mass thickness after cardiac surgery with regards to the duration of MV, ICU stay and the ICU outcome

The secondary outcomes were: (1) The quadriceps muscle mass thickness difference after cardiac surgery from baseline to 7th day of ICU stay or discharge; and (2) The muscle strength assessment using the MRC scale from baseline to 7th day of ICU stay or discharge.

Sonographic imaging procedure

A portable GE Healthcare Vivid-I; Wauwatosa, Wisconsin, United States. Device was used with a 7.5-MHz linear transducer to obtain scans on days 1 (within 24 h from admission), 3, 5 and 7 subjects were positioned in supine position with their right thigh in neutral position, knee extended and muscles relaxed. Transducer was placed perpendicular to the thigh, at a standardized anatomical point, in the middle distance between anterior lower iliac crest and the upper pole of the patella of the thigh. Prior to the assessment, the located point was marked to enable repeated measurements on the subjects' limb. To avoid muscle compression, a water-soluble transmission gel was applied to the ultrasound transducer. All underlying tissues as scanned with the ultrasound, were displayed in "B" mode and saved to the ultrasound hard drive for further analysis to a computer using an ultrasound imaging software.

Two sonographic images were acquired in each measurement illustrating the subcutaneous tissue, rectus femoris muscle, muscle fascia, vastus intermedius muscle and femur (Figure 1). Analyses performed on each image included measurements of rectus femoris muscle thickness (RF mass) in centimeters (cm) and combined muscle thickness of rectus femoris and vastus intermedius (RF_VI mass) in cm and averaged values were calculated. Sonographic assessment and image acquisition analyses were performed by an experienced operator and intra-rater variability was tested.

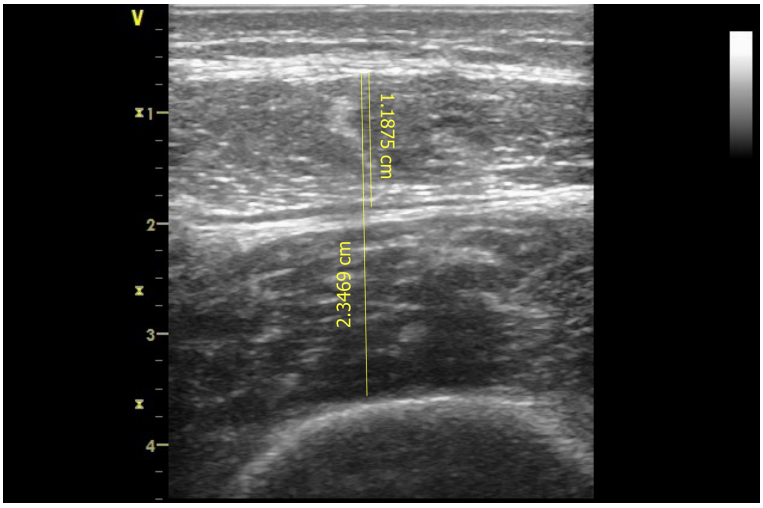

Figure 1 Illustration of sonographic imaging of rectus femoris and rectus femoris and vastus intermedius muscle thickness (1.19 cm and 2.35 cm, respectively).

Muscle strength testing

The MRC scale was used to evaluate muscle strength. Patients proceeded to assessment as soon as were awake and cooperative. Evaluation included the measurement of six muscle groups bilaterally: Shoulder abductors, elbow flexors and wrist dorsiflexors for the upper limbs as well as hip flexors, knee extensors and ankle dorsiflexors for the lower limbs. Test was performed in the same order each time. Each muscle group scored from 0 indicating no contraction to 5 indicating normal power. Total maximum score was 60 whilst MRC score ≤ 48 defined as ICUAW.

Statistical analysis

Descriptive statistics analysis was performed to describe the baseline data. Distribution's normality was checked with Kolmogorov-Smirnov test. Normally distributed continuous variables were expressed as mean ± SD and non-normally distributed variables as median with interquartile range, and categorical variables as proportions with percentages and absolute numbers. The sample size was estimated based on feasibility for a predefined certain period. Differences between the same patients were analyzed with the Paired *t* test for continuous variables and χ^2 test for categorical variables. To analyze continuous variables between patient groups, Mann Whitney test was used for those with non-normal distribution and *t* test for those with normal distribution. Reliability analysis was performed and intra-class correlation coefficient (ICC) was calculated for intra-rater variability of quadriceps muscle mass thickness measured by ultrasound. Level of significance was set at *P* value < 0.05. All statistical analyses were performed with SPSS v.25 software.

RESULTS

Clinical characteristics

In this study, we included 221 consecutive patients (148 men and 73 women) post-Cardiac Surgery ICU admission. Fifty-six patients were excluded from the study; 48 patients due to missing ultrasound scan within 24 h from admission, 5 patients due to high BMI (> 35 kg/m^2), 2 patients due to open chest-sternotomy or lobectomy, and one patient due to missing data. Study population consisted of 165 patients, 107 males (64.8) and 58 females (35.2), median age 71 (64-77) years (Figure 2). All patients underwent ultrasound scans of quadriceps muscle mass and muscle strength evaluation. Baseline clinical characteristics of the 165 included subjects are summarized in Table 1. ICU length of stay was 41 (24-77) h, duration of sedation until awakening was 672 (553-896) min and duration of MV was 15 (12-21) h (Table 2).

Sonographic muscle mass assessment

Assessment of ultrasound measurements has shown excellent reliability results with a high ICC calculated for intra-rater variability of quadriceps muscle mass thickness

Table 1 Baseline characteristics of patients enrolled in the study, *n* (%)

Characteristics	Values
Demographic data	
Sex (male, female)	107 (65)/58 (35)
Age (yr)	71 (64-77)
Weight (kg)	77 ± 11.84
Height (m)	1.67 ± 0.09
Body mass index (kg/m^2)	27.55 ± 3.69
Clinical characteristics	
Hypertension	126 (76)
Diabetes	57 (34)
Dyslipidemia	97 (59)
Smoker	34 (21)
Former smoker	38 (23)
Coronary heart disease	89 (54)
Chronic heart Failure	10 (6)
Chronic pulmonary disease	22 (13)
Chronic kidney failure	13 (8)
Thoracic aortic aneurysm	11 (7)
Valve disease	10 (6)
Other disease	65 (39.4)
Apache II score	2 (1.2)
SOFA score	5 (3-6)

Categorical variables are continuous as median (Q1-Q3) or mean ± SD, $^aP < 0.05$.

[ICC: 0.99, 95% confidence interval (CI): 0.97-0.99, $P < 0.001$].

Muscle ultrasound assessment showed that RF mass was 1.34 cm (1.15-1.65) within the first 24 h post admission ($n = 165$), 1.2 ± 0.5 cm on day 3 ($n = 15$), and 1.25 ± 0.52 cm on day 5 ($n = 10$). RF_VI mass within the first 24 h was 2.52 cm (2.16-3.12), ($n = 165$), on day 3 was 2.41 ± 0.94 cm ($n = 15$), and on day 5 was 2.37 ± 0.8 cm ($n = 10$). During the first five days, RF mass presented a trend to decrease by 2.2% [(95%CI: - 0.21 to 0.15), $n = 9$; $P = 0.729$] and RF_VI mass by 3.5% [(95%CI: - 0.4 to 0.22), $n = 9$; $P = 0.530$].

Patients remained more in the ICU (47 ± 74 h *vs* 28 ± 46 h, $P = 0.02$), (Figure 3) and greater time on ventilator (17 ± 9 h *vs* 14 ± 9 h, $P = 0.05$), (Figure 4), if presented a combined RF_VI mass below the median value (2.5 cm) on day 1 ($n = 80$).

Patients with ICUAW on day 3 ($n = 7$), stayed more intubated on ventilator compared to patients with no ICUAW ($n = 33$), (44 ± 14 h *vs* 19 ± 9 h, $P = 0.006$), (Figure 5) and had also greater duration of extracorporeal circulation, (159 ± 91 min *vs* 112 ± 71 min, $P = 0.025$), (Figure 6).

DISCUSSION

This study investigated quadriceps muscle mass, as assessed by ultrasound, in patients who underwent cardiac surgery as well as factors associated with their ICU length of stay. The main results of the study demonstrated a trend to a decrease of quadriceps muscle mass thickness over the first wk post-admission in the ICU and that quadriceps muscle mass was associated with prolonged MV support and ICU stay.

The quadriceps muscle mass has shown a trend to decrease in the present study which reflects acute muscle mass wasting occurring early in cardiac surgery patients, post-ICU admission. Our results are in line with a recent observational study[3] and

Table 2 Peri-operative study characteristics of patients enrolled in the study, *n* (%)

Characteristics	Values
Type of surgery	
Coronary artery bypass grafting	86 (52)
Heart valve repair or replacement surgery	79 (48)
Other cardiac surgery	6 (4)
Medication	
Propofol	111 (67)
Dobutamine	103 (62)
Noradrenaline	40 (24)
Morphine	13 (8)
Adrenaline	11 (7)
Other characteristics	
Duration of extracorporeal circulation (min)	104 (81-135)
Duration of aortic cross-clamp (min)	75 (56-99)
Duration of mechanical ventilation (h)	15 (12-21)
Duration of surgery anesthesia (min)	246 (202-292)
Duration of sedation (min)	672 (553-896)
Duration of intensive care unit stay (h)	41 (24-77)

Categorical variables are continuous as median (Q1-Q3), $^{a}P < 0.05$.

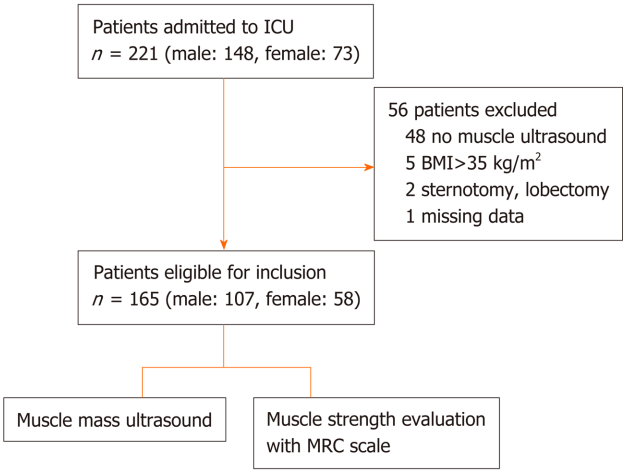

Figure 2 Flowchart of the intensive care unit patients enrolled for the study. ICU: Intensive care unit; BMI: Body mass index; MRC: Medical Research Council.

another pilot study[16] which reported a significant muscle loss of lower limbs within the first week of ICU hospitalization. A previous study[17] has shown similar results and it is notable that the largest muscle wasting is on average 10% and occurs during the first week of hospitalization[18].

The results of these studies confirm our finding that muscle mass wasting occurs during the first week of hospitalization. However, we reported a low rate of muscle mass loss in our study without statistical significance. Main explanation for these differentiate results is possibly due to our study population characteristics compared to general ICU patients. Cardiac surgery ICU patients mostly have a short ICU stay with less severity scores as shown from our study, making the ICUAW syndrome less pronounced. Interestingly, in a small subgroup of patients we observed a relative

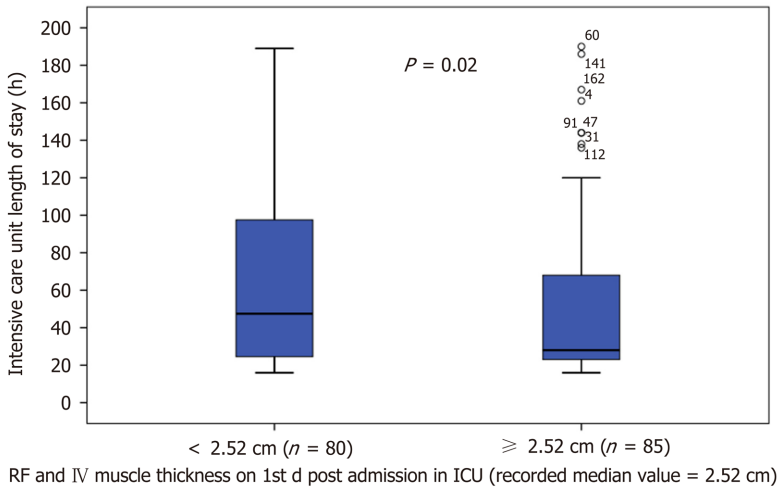

Figure 3 Intensive care unit length of stay of patients in which rectus femoris and vastus intermedius mass was below and above the recorded median values on day 1 post intensive care unit admission. ICU: Intensive care unit; RF: Rectus femoris; VI: Vastus intermedius.

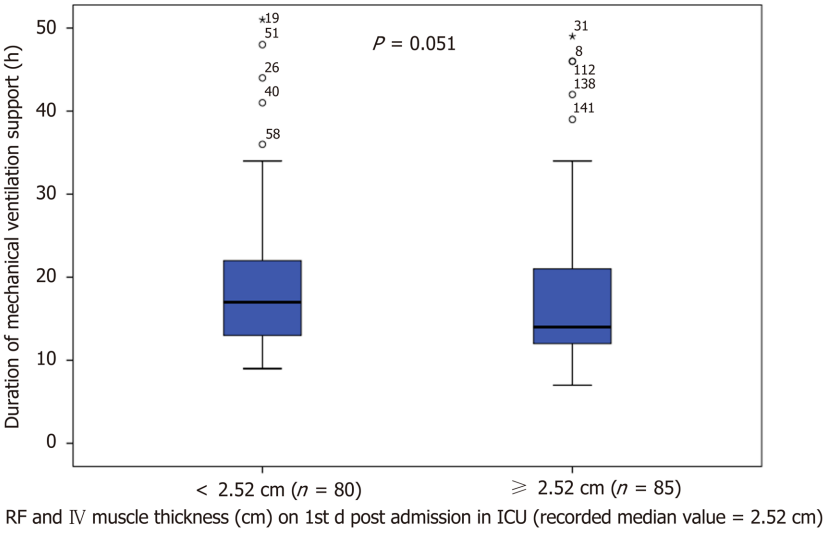

Figure 4 Duration of mechanical ventilation of patients' rectus femoris and vastus intermedius mass was below and above the recorded median values on day 1 post ICU admission. ICU: Intensive care unit; RF: Rectus femoris; VI: Vastus intermedius.

"increase" of muscle mass thickness during the first week, reflecting possibly muscle mass edema. We believe that this finding occurs probably due to the fluid overload necessary to preserve hemodynamic stability of post-operative cardiac surgery patients. However further studies are needed to elucidate this possible mechanism.

Another significant finding from the present study was that the size of muscle mass affected the length of ICU stay and the duration of MV. The prolonged hospitalization of patients with reduced muscle mass thickness on the first day post-cardiac ICU admission emphasizes the prognostic and clinical value of quadriceps muscle mass. Muscle mass wasting of psoas muscle has been previously associated with prolonged ICU stay in patients after cardiac surgery[7]. A recent study[19] stated that the muscle mass is an independent factor of mortality and serious morbidity in patients undergoing heart transplantation. Similar results have been reported by Yamashita *et al*[11], where skeletal muscle density seems to affect muscle function and mortality after cardiovascular surgery. However not all studies are in concordance; in a retrospective cohort study[10] they found that low psoas muscle mass is not related to the survival outcome of patients with asymptomatic abdominal aortic aneurysm.

A secondary finding in our study was that patients who developed ICU acquired weakness post-cardiac surgery had also greater duration of extracorporeal circulation and prolonged MV support. Kraft *et al*[20] reported that extracorporeal circulation is

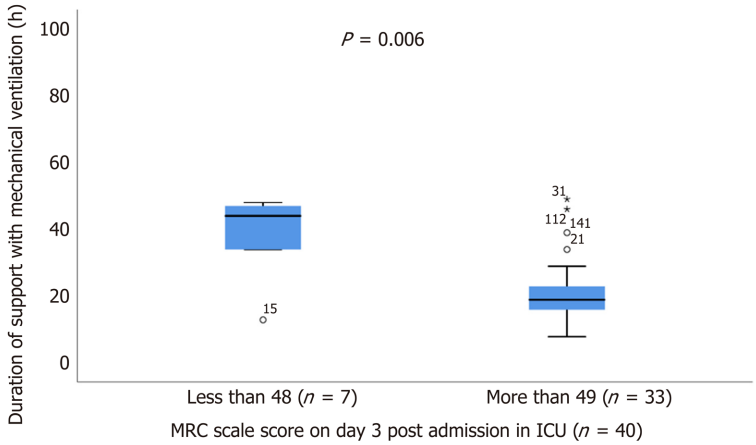

Figure 5 Duration of mechanical ventilation of patients with Medical Research Council scale score below and above 48 on day 3 post admission in intensive care unit. MRC: Medical Research Council; ICU: Intensive care unit.

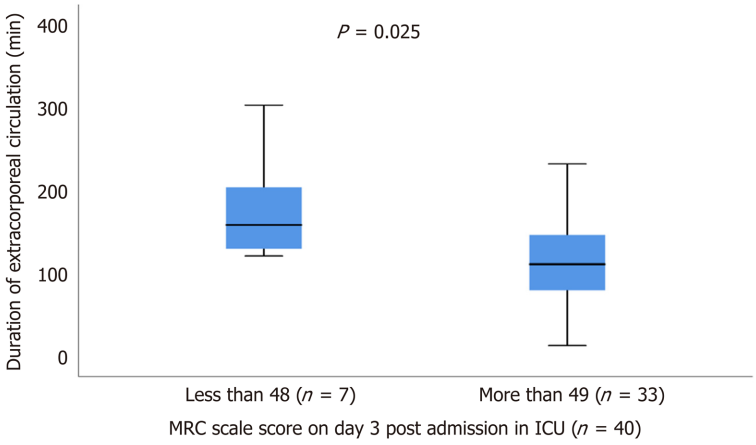

Figure 6 Duration of extracorporeal circulation of patients with Medical Research Council scale score below and above 48 on day 3 post admission in intensive care unit. MRC: Medical Research Council; ICU: Intensive care unit.

related to the development of systematic inflammatory response to patients undergoing cardiac surgery. However, a single-centre prospective randomized study[21], has shown that minimally invasive extracorporeal circulation in patients undergoing coronary artery bypass grafting improves postoperative health-related quality of life compared to conventional cardiopulmonary bypass. According to our findings, patients with muscle weakness had longer duration of mechanical ventilation support. Other previous studies[5,22] confirm our finding showing also that muscle weakness is associated with weaning failure and ICU mortality[23].

Assessing quadriceps muscle mass by ultrasound might help identify those patients at high risk of developing ICU acquired weakness post-cardiac surgery, but also patients that would stay longer in MV and in ICU. Frailty is an independent predictor of hospital mortality, prolonged ICU stay and mid-term survival for patients undergoing cardiac interventions[24]. Early mobilization and rehabilitation on the first postoperative days are beneficial in terms of increasing muscle strength and functional capacity even after ICU discharge and reducing ICU length of stay[25]. In particular those ICU patients with decreased quadriceps muscle thickness would possibly require earlier passive mobilization and intensified rehabilitation and if possibly, pre-habilitation prior to cardiac surgery to avoid ICUAW and post-cardiac surgery worse outcome. Previous studies have shown that neuromuscular electrical stimulation has local and systemic effects in critical ill patients[26,27] and might prevent muscle atrophy and reduce mechanical MV and ICU stay[28,29].

Limitations

This observational study represents one of the first prospective studies investigating the clinical value of sonographically muscle mass assessment of patients after cardiac surgery and consists of the first study from a Greek cardiac surgery ICU. However, the present study has several limitations. This is an explorative study and the sample size was estimated based mainly on feasibility for a predefined certain period. For this reason, the study might have been underpowered to demonstrate quadriceps muscle thickness changes during ICU and association with ICU outcome. Although the number of patients enrolled to the study was large, the sample size for the observed effect size was small. Most patients remained in the ICU for a short time period, which did not allow the assessment of a sufficient number of patients until the seventh day post admission. However, results from the present study will allow future studies to perform power analysis and calculate sample size. The presence of muscle edema during the first postoperative days might have affected the ultrasound measurements too. Ultrasound scans are operator-dependent that may limit accuracy of results. In our study ultrasound measurements analyses were done by an experienced researcher with excellent intra-rater reproducibility results. This is consistent with previous intra- and inter-rater variability studies that have demonstrated high diagnostic accuracy results[30,31]. We were not be able to associate the grade of muscle mass decrease with long-term outcome after cardiac surgery due to short-term follow-up period of the present study; however, we did found an important association with duration of MV and ICU length of stay.

In conclusion, quadriceps muscle mass assessed by ultrasound presented with a trend to decrease during the first week post-ICU admission in patients after cardiac surgery. Quadriceps muscle mass is associated with the duration of MV support and ICU length of stay. Quadriceps muscle mass sonography seems to be a valid tool to assess preventive and therapeutic measures efficacy.

ARTICLE HIGHLIGHTS

Research background

Intensive care unit (ICU) acquired weakness (ICUAW) remains a major cause of mortality and morbidity in critically ill patients. Ultrasonography is a valid diagnostic tool in critical ill patients who present muscle weakness. Muscle wasting may occur in cardiac surgery patients' post-ICU admission affecting outcome. Early detection of muscle wasting may benefit interventions to decrease the duration of mechanical ventilation, increase muscle strength and improve their quality of life.

Research motivation

Sonography is a diagnostic method that allows the assessment of muscle mass in bedridden. It has been introduced recently as a valid and reliable to measure quantity and quality of skeletal muscle. It's a non-invasive, low-cost method offering real-time imaging without radiation exposure.

Research objectives

The clinical value of ultrasound-assessed muscle mass in patients post-cardiac surgery ICU admission.

Research methods

An observational study was conducted to 221 consecutive patients after cardiac surgery at the Cardiac Surgery ICU of Onassis Cardiac Surgery Center from February 1, 2018 to May 15, 2018. Sonographic assessment of quadriceps muscle thickness and evaluation of muscle strength using the Medical Research Council (MRC) scale were performed until 7th day post-ICU admission or ICU discharge.

Research results

Among the 165 patients finally included in the analysis [median age: 71 (64-77) years], there was a decrease of femoris muscle thickness by 2.2% [(95% confidence interval (CI): - 0.21 to 0.15), n = 9; P = 0.729] and vastus intermedius mass (RF_VI mass) decreased by 3.5% [(95%CI: - 0.4 to 0.22), n = 9; P = 0.530]. Patients with RF_VI mass below the recorded median values (2.5 cm) on day 1 (n = 80) had a longer ICU length of stay compared to those patients with RF_VI mass above than 2.5 cm (n = 85), (47 ± 74 h *vs* 28 ± 45 h, P = 0.02) and remained to MV more time, (17 ± 9 h *vs* 14 ± 9 h, P =

0.05). Patients with ICUAW on day 3 (n = 7) had prolonged ventilation (44 ± 14 h *vs* 19 ± 9 h, P = 0.006) compared to patients with no ICUAW (n = 33). Moreover, the duration of extracorporeal circulation was greater for patients with low MRC scale score on day 3 (n = 7) compared with patients with higher MRC scale score (n = 33), (159 ± 91 min *vs* 112 ± 71 min, P = 0.025).

Research conclusions

The results of the study have shown that there is a trend to a decreased muscle mass in patients after cardiac surgery post-ICU admission. Patients with decreased muscle mass remained more on ventilator and stayed longer in ICU. Sonographic assessment seems to be a valid method to quantify quadriceps muscle mass in patients after cardiac surgery.

Research perspectives

We advocate further research to investigate muscle wasting in patients after cardiac surgery in order to implement preventive measures for ICU acquired weakness. Furthermore, it is recommended to identify a standardized protocol for sonographic muscle mass assessment to be implemented in research studies and intervention protocols.

ACKNOWLEDGEMENTS

We would like to thank Aggeliki Dorkofiti, professional English translator and editor for her contribution editing our manuscript and all ICU staff of Cardiac Surgery ICU of Onassis Cardiac Surgery Center for their continuous support throughout the whole study period.

REFERENCES

1 **Hermans G**, Van den Berghe G. Clinical review: intensive care unit acquired weakness. *Crit Care* 2015; **19**: 274 [PMID: 26242743 DOI: 10.1186/s13054-015-0993-7]
2 **Friedrich O**, Reid MB, Van den Berghe G, Vanhorebeek I, Hermans G, Rich MM, Larsson L. The Sick and the Weak: Neuropathies/Myopathies in the Critically Ill. *Physiol Rev* 2015; **95**: 1025-1109 [PMID: 26133937 DOI: 10.1152/physrev.00028.2014]
3 **Turton P**, Hay R, Taylor J, McPhee J, Welters I. Human limb skeletal muscle wasting and architectural remodeling during five to ten days intubation and ventilation in critical care - an observational study using ultrasound. *BMC Anesthesiol* 2016; **16**: 119 [PMID: 27894277 DOI: 10.1186/s12871-016-0269-z]
4 **Sekine H**. [An immunohistochemical study of various breast tissues using CA15-3 (MAb 115D8 and MAb DF3)]. *Gan No Rinsho* 1987; **33**: 913-919 [PMID: 2441086 DOI: 10.1186/cc13189]
5 **Matthews EK**, Petersen OH, Williams JA. Analysis of tissue amylase output by an automated method. *Anal Biochem* 1974; **58**: 155-160 [PMID: 4825371 DOI: 10.1164/rccm.201312-2257OC]
6 **Moisey LL**, Mourtzakis M, Cotton BA, Premji T, Heyland DK, Wade CE, Bulger E, Kozar RA; Nutrition and Rehabilitation Investigators Consortium (NUTRIC). Skeletal muscle predicts ventilator-free days, ICU-free days, and mortality in elderly ICU patients. *Crit Care* 2013; **17**: R206 [PMID: 24050662 DOI: 10.1186/cc12901]
7 **Zuckerman J**, Ades M, Mullie L, Trnkus A, Morin JF, Langlois Y, Ma F, Levental M, Morais JA, Afilalo J. Psoas Muscle Area and Length of Stay in Older Adults Undergoing Cardiac Operations. *Ann Thorac Surg* 2017; **103**: 1498-1504 [PMID: 27863730 DOI: 10.1016/j.athoracsur.2016.09.005]
8 **Hansen D**, Linsen L, Verboven K, Hendrikx M, Rummens JL, van Erum M, Eijnde BO, Dendale P. Magnitude of muscle wasting early after on-pump coronary artery bypass graft surgery and exploration of aetiology. *Exp Physiol* 2015; **100**: 818-828 [PMID: 25963928 DOI: 10.1113/EP085053]
9 **van Venrooij LM**, Verberne HJ, de Vos R, Borgmeijer-Hoelen MM, van Leeuwen PA, de Mol BA. Postoperative loss of skeletal muscle mass, complications and quality of life in patients undergoing cardiac surgery. *Nutrition* 2012; **28**: 40-45 [PMID: 21621393 DOI: 10.1016/j.nut.2011.02.007]
10 **Indrakusuma R**, Zijlmans JL, Jalalzadeh H, Planken RN, Balm R, Koelemay MJW. Psoas Muscle Area as a Prognostic Factor for Survival in Patients with an Asymptomatic Infrarenal Abdominal Aortic Aneurysm: A Retrospective Cohort Study. *Eur J Vasc Endovasc Surg* 2018; **55**: 83-91 [PMID: 29158067 DOI: 10.1016/j.ejvs.2017.10.007]
11 **Yamashita M**, Kamiya K, Matsunaga A, Kitamura T, Hamazaki N, Matsuzawa R, Nozaki K, Tanaka S, Nakamura T, Maekawa E, Masuda T, Ako J, Miyaji K. Prognostic Value of Psoas Muscle Area and Density in Patients Who Undergo Cardiovascular Surgery. *Can J Cardiol* 2017; **33**: 1652-1659 [PMID: 29173605 DOI: 10.1016/j.cjca.2017.10.009]
12 **Mourtzakis M**, Parry S, Connolly B, Puthucheary Z. Skeletal Muscle Ultrasound in Critical Care: A Tool in Need of Translation. *Ann Am Thorac Soc* 2017; **14**: 1495-1503 [PMID: 28820608 DOI: 10.1513/AnnalsATS.201612-967PS]
13 **Paris MT**, Mourtzakis M, Day A, Leung R, Watharkar S, Kozar R, Earthman C, Kuchnia A, Dhaliwal R, Moisey L, Compher C, Martin N, Nicolo M, White T, Roosevelt H, Peterson S, Heyland DK. Validation of

Bedside Ultrasound of Muscle Layer Thickness of the Quadriceps in the Critically Ill Patient (VALIDUM Study). *JPEN J Parenter Enteral Nutr* 2017; **41**: 171-180 [PMID: 26962061 DOI: 10.1177/0148607116637852]

14 **Connolly B**, MacBean V, Crowley C, Lunt A, Moxham J, Rafferty GF, Hart N. Ultrasound for the assessment of peripheral skeletal muscle architecture in critical illness: a systematic review. *Crit Care Med* 2015; **43**: 897-905 [PMID: 25559437 DOI: 10.1097/CCM.0000000000000821]

15 **Bunnell A**, Ney J, Gellhorn A, Hough CL. Quantitative neuromuscular ultrasound in intensive care unit-acquired weakness: A systematic review. *Muscle Nerve* 2015; **52**: 701-708 [PMID: 26044880 DOI: 10.1002/mus.24728]

16 **Ten Haaf D**, Hemmen B, van de Meent H, Bovend'Eerdt TJH. The Magnitude and Time Course of Muscle Cross-section Decrease in Intensive Care Unit Patients. *Am J Phys Med Rehabil* 2017; **96**: 634-638 [PMID: 28151763 DOI: 10.1097/PHM.0000000000000711]

17 **Puthucheary ZA**, Rawal J, McPhail M, Connolly B, Ratnayake G, Chan P, Hopkinson NS, Phadke R, Dew T, Sidhu PS, Velloso C, Seymour J, Agley CC, Selby A, Limb M, Edwards LM, Smith K, Rowlerson A, Rennie MJ, Moxham J, Harridge SD, Hart N, Montgomery HE. Acute skeletal muscle wasting in critical illness. *JAMA* 2013; **310**: 1591-1600 [PMID: 24108501 DOI: 10.1001/jama.2013.278481]

18 **Joskova V**, Patkova A, Havel E, Najpaverova S, Uramova D, Kovarik M, Zadak Z, Hronek M. Critical evaluation of muscle mass loss as a prognostic marker of morbidity in critically ill patients and methods for its determination. *J Rehabil Med* 2018; **50**: 696-704 [PMID: 30080234 DOI: 10.2340/16501977-2368].]

19 **Bibas L**, Saleh E, Al-Kharji S, Chetrit J, Mullie L, Cantarovich M, Cecere R, Giannetti N, Afilalo J. Muscle Mass and Mortality After Cardiac Transplantation. *Transplantation* 2018; **102**: 2101-2107 [PMID: 29877924 DOI: 10.1097/TP.0000000000002311]

20 **Kraft F**, Schmidt C, Van Aken H, Zarbock A. Inflammatory response and extracorporeal circulation. *Best Pract Res Clin Anaesthesiol* 2015; **29**: 113-123 [PMID: 26060024 DOI: 10.1016/j.bpa.2015.03.001]

21 **Anastasiadis K**, Antonitsis P, Kostarellou G, Kleontas A, Deliopoulos A, Grosomanidis V, Argiriadou H. Minimally invasive extracorporeal circulation improves quality of life after coronary artery bypass grafting. *Eur J Cardiothorac Surg* 2016; **50**: 1196-1203 [PMID: 27307483 DOI: 10.1093/ejcts/ezw210]

22 **Dres M**, Dubé BP, Mayaux J, Delemazure J, Reuter D, Brochard L, Similowski T, Demoule A. Coexistence and Impact of Limb Muscle and Diaphragm Weakness at Time of Liberation from Mechanical Ventilation in Medical Intensive Care Unit Patients. *Am J Respir Crit Care Med* 2017; **195**: 57-66 [PMID: 27310484 DOI: 10.1164/rccm.201602-0367OC]

23 **Dres M**, Jung B, Molinari N, Manna F, Dubé BP, Chanques G, Similowski T, Jaber S, Demoule A. Respective contribution of intensive care unit-acquired limb muscle and severe diaphragm weakness on weaning outcome and mortality: a post hoc analysis of two cohorts. *Crit Care* 2019; **23**: 370 [PMID: 31752937 DOI: 10.1186/s13054-019-2650-z].]

24 **Reichart D**, Rosato S, Nammas W, Onorati F, Dalén M, Castro L, Gherli R, Gatti G, Franzese I, Faggian G, De Feo M, Khodabandeh S, Santarpino G, Rubino AS, Maselli D, Nardella S, Salsano A, Nicolini F, Zanobini M, Saccocci M, Bounader K, Kinnunen EM, Tauriainen T, Airaksinen J, Seccareccia F, Mariscalco G, Ruggieri VG, Perrotti A, Biancari F. Clinical frailty scale and outcome after coronary artery bypass grafting. *Eur J Cardiothorac Surg* 2018; **54**: 1102-1109 [PMID: 29897529 DOI: 10.1093/ejcts/ezy222]

25 **Tipping CJ**, Harrold M, Holland A, Romero L, Nisbet T, Hodgson CL. The effects of active mobilisation and rehabilitation in ICU on mortality and function: a systematic review. *Intensive Care Med* 2017; **43**: 171-183 [PMID: 27864615 DOI: 10.1007/s00134-016-4612-0]

26 **Angelopoulos E**, Karatzanos E, Dimopoulos S, Mitsiou G, Stefanou C, Patsaki I, Kotanidou A, Routsi C, Petrikkos G, Nanas S. Acute microcirculatory effects of medium frequency versus high frequency neuromuscular electrical stimulation in critically ill patients - a pilot study. *Ann Intensive Care* 2013; **3**: 39 [PMID: 24355422 DOI: 10.1186/2110-5820-3-39]

27 **Stefanou C**, Karatzanos E, Mitsiou G, Psarra K, Angelopoulos E, Dimopoulos S, Gerovasili V, Boviatsis E, Routsi C, Nanas S. Neuromuscular electrical stimulation acutely mobilizes endothelial progenitor cells in critically ill patients with sepsis. *Ann Intensive Care* 2016; **6**: 21 [PMID: 26969168 DOI: 10.1186/s13613-016-0123-y]

28 **Gerovasili V**, Stefanidis K, Vitzilaios K, Karatzanos E, Politis P, Koroneos A, Chatzimichail A, Routsi C, Roussos C, Nanas S. Electrical muscle stimulation preserves the muscle mass of critically ill patients: a randomized study. *Crit Care* 2009; **13**: R161 [PMID: 19814793 DOI: 10.1186/cc8123]

29 **Routsi C**, Gerovasili V, Vasileiadis I, Karatzanos E, Pitsolis T, Tripodaki E, Markaki V, Zervakis D, Nanas S. Electrical muscle stimulation prevents critical illness polyneuromyopathy: a randomized parallel intervention trial. *Crit Care* 2010; **14**: R74 [PMID: 20426834 DOI: 10.1186/cc8987]

30 **Pardo E**, El Behi H, Boizeau P, Verdonk F, Alberti C, Lescot T. Reliability of ultrasound measurements of quadriceps muscle thickness in critically ill patients. *BMC Anesthesiol* 2018; **18**: 205 [PMID: 30591032 DOI: 10.1186/s12871-018-0647-9]

31 **Kumar R**, Shah TH, Hadda V, Tiwari P, Mittal S, Madan K, Khan MA, Mohan A. Assessment of quadriceps muscle thickness using bedside ultrasonography by nurses and physicians in the intensive care unit: Intra- and inter-operator agreement. *World J Crit Care Med* 2019; **8**: 127-134 [PMID: 31853448 DOI: 10.5492/wjccm.v8.i7.127]

Published by **Baishideng Publishing Group Inc**
7041 Koll Center Parkway, Suite 160, Pleasanton, CA 94566, USA
Telephone: +1-925-3991568
E-mail: bpgoffice@wjgnet.com
Help Desk: https://www.f6publishing.com/helpdesk
https://www.wjgnet.com